UNCLASSIFIED

SECURITY CLASSIFICATION OF THIS PAGE *(When Data Entered)*

REPORT DOCUMENTATION PAGE		READ INSTRUCTIONS BEFORE COMPLETING FORM
1. REPORT NUMBER RADC-TR-76-101, Vol III (of seven)	2. GOVT ACCESSION NO.	3. RECIPIENT'S CATALOG NUMBER
4. TITLE *(and Subtitle)* APPLICATIONS OF MULTICONDUCTOR TRANSMISSION LINE THEORY TO THE PREDICTION OF CABLE COUPLING Prediction of Crosstalk in Random Cable Bundles		5. TYPE OF REPORT & PERIOD COVERED Final Technical Report 6. PERFORMING ORG. REPORT NUMBER N/A
7. AUTHOR(s) Clayton R. Paul		8. CONTRACT OR GRANT NUMBER(s) F30602-75-C-0118
9. PERFORMING ORGANIZATION NAME AND ADDRESS University of Kentucky Department of Electrical Engineering Lexington KY 40506		10. PROGRAM ELEMENT, PROJECT, TASK AREA & WORK UNIT NUMBERS 62702F 45400130
11. CONTROLLING OFFICE NAME AND ADDRESS Rome Air Development Center (RBCT) Griffiss AFB NY 13441		12. REPORT DATE February 1977 13. NUMBER OF PAGES 86
14. MONITORING AGENCY NAME & ADDRESS*(if different from Controlling Office)* Same		15. SECURITY CLASS. *(of this report)* UNCLASSIFIED 15a. DECLASSIFICATION/DOWNGRADING SCHEDULE N/A

16. DISTRIBUTION STATEMENT *(of this Report)*

Approved for public release; distribution unlimited.

17. DISTRIBUTION STATEMENT *(of the abstract entered in Block 20, if different from Report)*

Same

18. SUPPLEMENTARY NOTES

RADC Project Engineer:
James C. Brodock (RBCT)

19. KEY WORDS *(Continue on reverse side if necessary and identify by block number)*

Electromagnetic Compatibility
Cable Coupling
Transmission Lines
Multiconductor Transmission Lines
Wire-to-wire Coupling
Ribbon Cable
Flat Pack Cable

20. ABSTRACT *(Continue on reverse side if necessary and identify by block number)*

This report is the third volume in a seven volume series of reports documenting the Application of Multiconductor Transmission Line Theory to the Prediction of Cable Coupling. Modern avionics systems are becoming increasingly complex. These systems generally contain large numbers of the wires connecting the various electronic equipments. The majority of the wires are in very close proximity to each other in either random cable bundles (in which the relative wire positions are not known and may vary considerably along the cable) or in ribbon cables (in which the relative wire positions are carefully controlled).

DD FORM 1 JAN 73 1473 EDITION OF 1 NOV 65 IS OBSOLETE

UNCLASSIFIED

SECURITY CLASSIFICATION OF THIS PAGE *(When Data Entered)*

The prediction of wire-coupled interference in these cable bundles is of considerable importance in the prediction of overall system compatibility.

It is the purpose of this report to examine the prediction of wire-coupled interference in random cable bundles. It will be shown that the sensitivity of the cable responses to relative wire position can be extraordinarily large. Thus in certain cases, it may be impossible to obtain coupling predictions with any extreme degree of accuracy for random cable bundles. A more realistic approach for random cable bundles may be to estimate the cable responses using some simple, approximate prediction models.

The volumes in this series which are in preparation or have been published are:

Volume I	Multiconductor Transmission Line Theory
Volume II	Computation of the Capacitance Matrices for Ribbon Cables
Volume III	Prediction of Crosstalk in Random Cable Bundles
Volume IV	Prediction of Crosstalk in Ribbon Cables
Volume VII	Digital Computer Programs for the Analysis of Multiconductor Transmission Lines

PREFACE

This effort was conducted by the University of Kentucky under the sponsorship of the Rome Air Development Center Post-Doctoral Program for RADC's Compatibility Branch. Mr. Jim Brodock of RADC was the task project engineer and provided overall technical direction and guidance. The author of this report is Dr. Clayton Paul.

The RADC Post-Doctoral Program is a cooperative venture between RADC and some sixty-five universities eligible to participate in the program. Syracuse University (Department of Electrical Engineering), Purdue University (School of Electrical Engineering), Georgia Institute of Technology (School of Electrical Engineering), and State University of New York at Buffalo (Department of Electrical Engineering) act as prime contractor schools with other schools participating via sub-contracts with the prime schools. The U.S. Air Force Academy (Department of Electrical Engineering), Air Force Institute of Technology (Department of Electrical Engineering), and the Naval Post Graduate School (Department of Electrical Engineering) also participate in the program.

The Post-Doctoral Program provides an opportunity for faculty at participating universities to spend up to one year full time on exploratory development and problem-solving efforts with the post-doctorals splitting their time between the customer location and their educational institutions. The program is totally customer-funded with current projects being undertaken for Rome Air Development Center (RADC), Space and Missile Systems Organization (SAMSO), Aeronautical Systems Division (ASD), Electronics Systems Division (ESD), Air Force Avionics Laboratory (AFAL), Foreign Technology Division (FTD), Air Force Weapons Laboratory (AFWL), Armament Development and Test

Center (ADTC), Air Force Communications Service (AFCS), Aerospace Defense Command (ADC), Hq USAF, Defense Communications Agency (DCA), Navy, Army, Aerospace Medical Division (AMD), and Federal Aviation Administration (FAA).

Further information about the RADC Post-Doctoral Program can be obtained from Mr. Jacob Scherer, RADC/RBC, Griffiss AFB, NY, 13441, telephone Autovon 587-2543, commercial (315) 330-2543.

Clayton R. Paul received the BSEE degree from the Citadel (1963), the MSEE degree from Georgia Institute of Technology (1964), and the PhD degree from Purdue University (1970). He served as a graduate assistant (1963-64) and as an instructor (1964-65) on the faculty of Georgia Institute of Technology. As a graduate instructor at Purdue University (1965-70) he taught courses in linear system theory, electrical circuits and electronics. From 1970-71 he was a Post Doctoral Fellow with RADC, working in the area of Electromagnetic Compatibility. His areas of research interests are in linear multivariable systems and electrical network theory with emphasis on distributed parameter networks and multiconductor transmission lines.

TABLE OF CONTENTS

PAGE

I. INTRODUCTION ---------- 1

II. PREDICTION MODELS ---------- 3

2.1. The Multiconductor Transmission Line (MTL) Model ---------- 3

2.2. The Transmission Line Model Specialized to the Generator-Receptor Circuit Pair and the BOUND Model ----------14

III. SENSITIVITY OF CABLE RESPONSES TO VARIATIONS IN WIRE POSITION ----------31

3.1. The Multiconductor Transmission Line Model and the BOUND Model ----------34

3.2. Sensitivity of the Cable Responses to Wire Position and Effect of Parasitic Wires as a Function of Impedance Levels ----------37

IV. EXPERIMENTAL VERIFICATION OF THE SENSITIVITY OF CABLE RESPONSES TO VARIATIONS IN WIRE POSITION ----------55

4.1. Effects of Parasitic Wires ----------61

4.2. Prediction Accuracies of the MTL Model for PAIR Results ----------61

4.3. Prediction Accuracies of the MTL Model for 13 WIRE Results ----------68

4.4. Sensitivity of Cable Responses to Variations in Wire Position ----------81

V. SUMMARY AND CONCLUSIONS ----------96

REFERENCES ----------100

LIST OF ILLUSTRATIONS

FIGURE PAGE

2-1. An (n+1) conductor, uniform transmission line. Sheet 1 of 2 ---- 5
Sheet 2 of 2 ---- 6
2-2. The per-unit-length equivalent circuit. ---- 7

2-3. The termination networks. ---- 11

2-4. The generator-receptor circuit pair. ---- 18

2-5. The per-unit-length equivalent circuit of the generator-receptor circuit pair. ---- 19

2-6. A lumped model of the receptor circuit. ---- 27

3-1. A cross section of the cable. ---- 32

3-2. The load structure on the cable. ---- 33

3-3(a) ---- 39

3-3(b) ---- 40

3-4(a) ---- 41

3-4(b) ---- 42

3-5(a) ---- 43

3-5(b) ---- 44

3-6(a) ---- 45

3-6(b) ---- 46

3-7 ---- 48

3-8 ---- 49

3-9 ---- 50

3-10 ---- 51

3-11 ---- 52

3-12 ---- 53

4-1 The experimental configuration. Sheet 1 of 2 ---- 56
Sheet 2 of 2 ---- 57

4-2 The experimental configuration----------58

4-3(a)----------62

4-3(b)----------63

4-4(a)----------64

4-4(b)----------65

4-5(a)----------66

4-5(b)----------67

4-6(a)----------69

4-6(b)----------70

4-7(a)----------71

4-7(b)----------72

4-8(a)----------73

4-8(b)----------74

4-9(a)----------75

4-9(b)----------76

4-10(a)----------77

4-10(b)----------78

4-11(a)----------79

4-11(b)----------80

4-12(a)----------82

4-12(b)----------83

4-13(a)----------84

4-13(b)----------85

4-14(a)----------86

4-14(b)----------87

4-15(a)----------89

4-15(b)----------90
4-16(a)----------91
4-16(b)----------92
4-17(a)----------93
4-17(b)----------94

I. INTRODUCTION

Random cable bundles as described in this report are groups of wires (cylindrical conductors) in which the relative wire positions are unknown and vary in some uncontrolled fashion along the cable length. These cable bundles result from the need to contain wires connecting electronic equipments in compact groups. Current practice in the avionics industry is to group wires into these random bundles although the use of ribbon cables (in which wire position is carefully controlled) is increasing [1]. These random bundles can be quite large and no attempt is made to control the relative wire positions within the bundle.

Wire-coupled interference (crosstalk) in cable bundles results from the unintentional coupling of signals from one circuit into another by virtue of the electromagnetic interaction between wires in the same cable bundle. The ability to predict this crosstalk is obviously quite important in determining overall system compatibility, i.e., will the system performance be degraded to an intolerable level by this interference.

The seemingly obvious approach to this problem is the use of uniform, multiconductor transmission line (MTL) theory to model the cable bundle [1]. However, this model requires that the wires be parallel to each other along the entire cable length and their relative positions, of course, must be known and should not vary along the cable length [1]. Random cable bundles do not satisfy these criteria. Another difficulty inherent in the application of the MTL model is the computation time required to obtain the response at each frequency [1]. Determining the response of a large number of closely coupled wires at a large number of frequencies can be quite time consuming even on a modern, high-speed digital computer [1]. Furthermore, in cases

where the cable responses are sensitive to variations in relative wire position, then it may be impossible to obtain predictions with any extreme degree of accuracy in random cable bundles. A more reasonable approach would seem to be the use of simpler models which bound or at least estimate these, perhaps sensitive, cable responses.

It is with the above considerations in mind that the prediction of cable coupling in random cable bundles is investigated in this report. In Chapter II, the MTL prediction model as well as a simpler model for estimating random cable bundle responses are described. Chapter III describes an investigation of the sensitivity of the cable responses to wire position. The results are obtained by using the MTL model and varying the wire positions for a 13 wire cable above a ground plane. In Chapter IV, an experimental investigation of the 13 wire cable used in Chapter III is described and the sensitivities to wire position uncovered in Chapter III are verified.

II. PREDICTION MODELS

In this Chapter, two models for predicting cable coupling will be described. The first model is the Multiconductor Transmission Line (MTL) model. This model is exact in the sense that all interactions between the wires in the cable bundle are considered, and the distributed parameter representation (assuming the TEM mode of propagation on the line) is used. The second model (referred to as the BOUND model) is an approximation of the MTL model. The BOUND model is a specialization of the MTL model in which only the generator and receptor circuits are considered. The effects of the remaining parasitic circuits are neglected in an attempt to achieve an upper bound estimate of the cable responses.

2.1 The Multiconductor Transmission Line (MTL)Model

The MTL model is described in detail in Volume I of this series [1] and in reference [2]. In this section, a brief review of the MTL model will be given and the reader should consult Volume I [1] or reference [2] for further details.

If the line is immersed in a homogeneous medium, e.g., bare wires in free space, the fundamental mode of propagation is the TEM (Transverse Electro-Magnetic) mode. If the line is immersed in an inhomogeneous medium, e.g., wires with circular dielectric insulations surrounded by free space, the fundamental mode of propagation is assumed to be the "quasi-TEM" mode. The essential difference in these two cases is as follows. For lines in a homogeneous medium, the TEM mode assumption is legitimate. For lines in an inhomogeneous medium, the TEM mode cannot exist except in the limiting case of zero frequency (DC). However, for the inhomogeneous medium case, the assumption is made that the electric and magnetic fields are almost transverse

to the direction of propagation, i.e., the mode of propagation is almost TEM.

With the assumption of the TEM mode or "quasi-TEM" mode of propagation, line voltages and currents may be defined. Consider a general (n + 1) conductor, uniform transmission line shown in Figure 2-1.[1] The (n + 1)st or zero-th conductor is the reference conductor for the line voltages. For sinusoidal, steady-state excitation of the line, the line voltages, $\mathcal{V}_i(x,t)$, (with respect to the reference, the zero-th, conductor) and line currents, $\mathcal{I}_i(x,t)$, are

$$\mathcal{V}_i(x,t) = V_i(x)\, e^{j\omega t} \tag{2-1a}$$

$$\mathcal{I}_i(x,t) = I_i(x)\, e^{j\omega t} \tag{2-1b}$$

for i = 1, ---, n where $V_i(x)$ and $I_i(x)$ are the complex, phasor line voltages and currents. The current in the reference conductor satifies

$$\mathcal{I}_0(x,t) = -\sum_{i=1}^{n} \mathcal{I}_i(x,t) \tag{2-2a}$$

$$I_0(x) = -\sum_{i=1}^{n} I_i(x) \tag{2-2b}$$

The MTL equations can be derived from the per-unit-length equivalent circuit in Figure 2-2 and are a set of 2n, complex-valued, first order, ordinary differential equations

$$\frac{d}{dx}\begin{bmatrix}\underline{V}(x)\\ \underline{I}(x)\end{bmatrix} = -\begin{bmatrix}\underset{\sim}{0}_{n\times n} & \underset{\sim}{Z}\\ \underset{\sim}{Y} & \underset{\sim}{0}_{n\times n}\end{bmatrix}\begin{bmatrix}\underline{V}(x)\\ \underline{I}(x)\end{bmatrix} + \begin{bmatrix}\underline{V}_s(x)\\ \underline{I}_s(x)\end{bmatrix} \tag{2-3}$$

A matrix $\underset{\sim}{M}$ with m rows and p columns is said to be mχp and the element in the i-th row and j-th column is designated by $[\underset{\sim}{M}]_{ij}$ with i=1, ---, m and

---

[1] The line is considered to be uniform in the sense that all conductors are parallel to each other and there is no variation in the cross sections of the conductors or the surrounding medium along the line axis (x direction) [1].

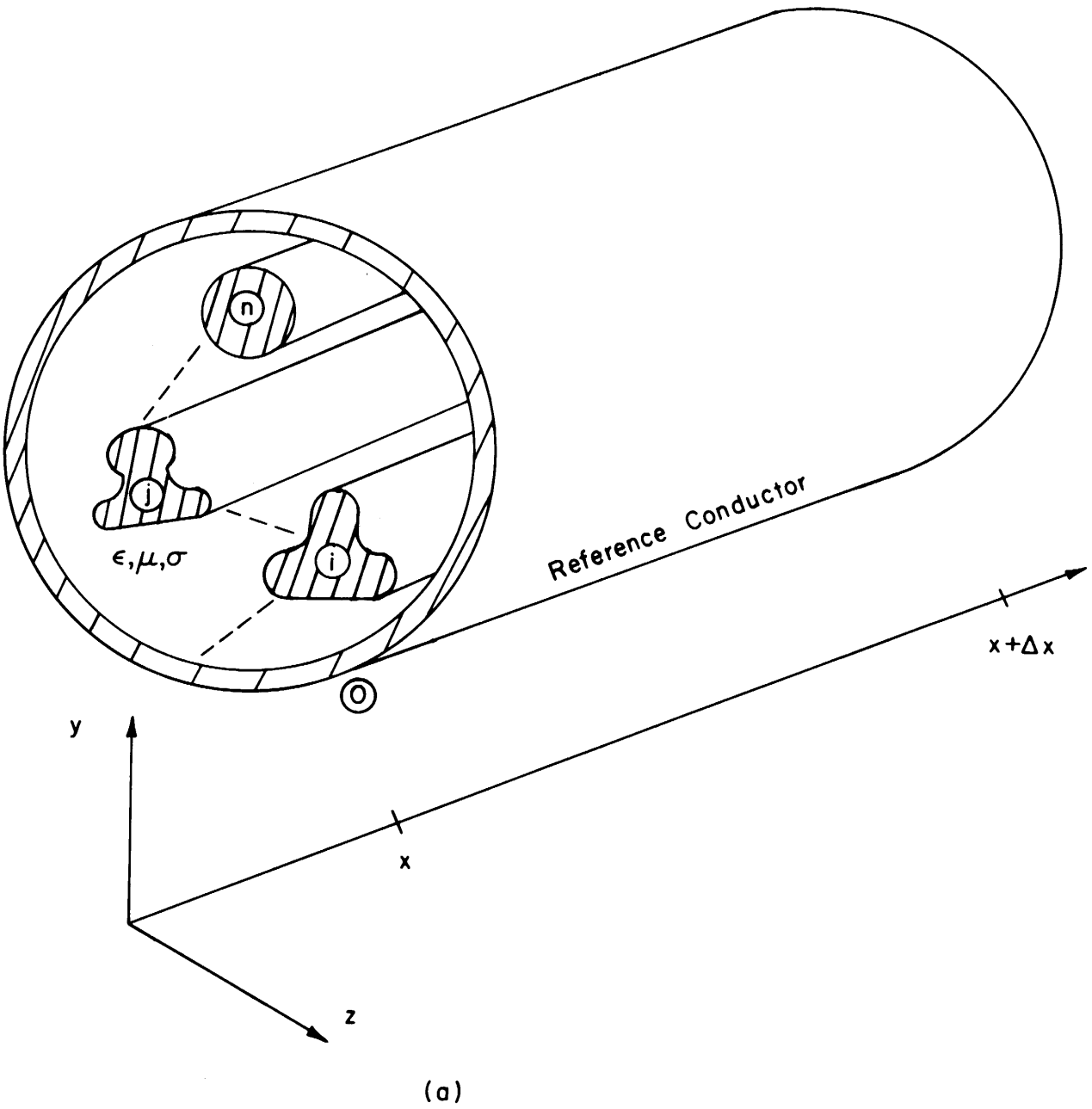

Figure 2-1. An (n+1) conductor, uniform transmission line (cont.).

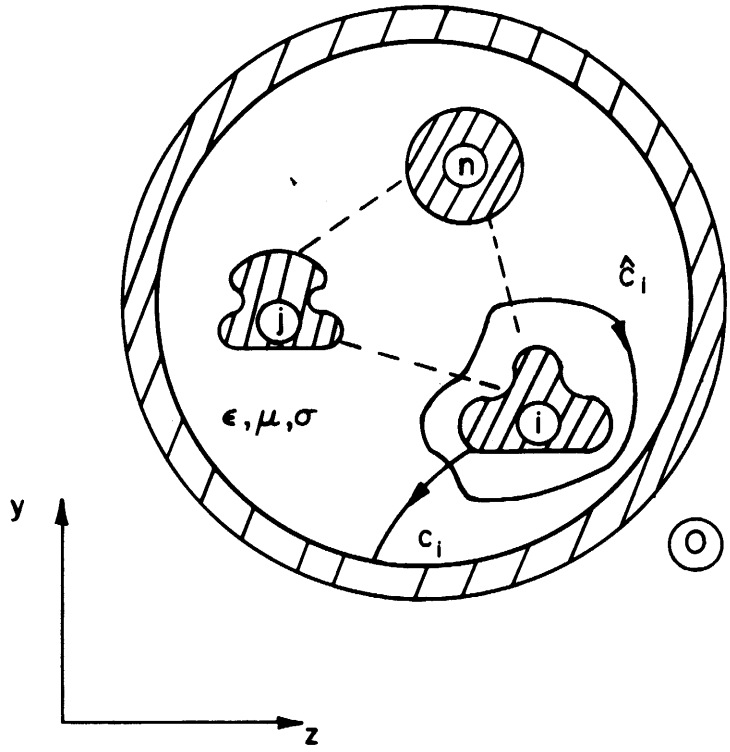

(b)

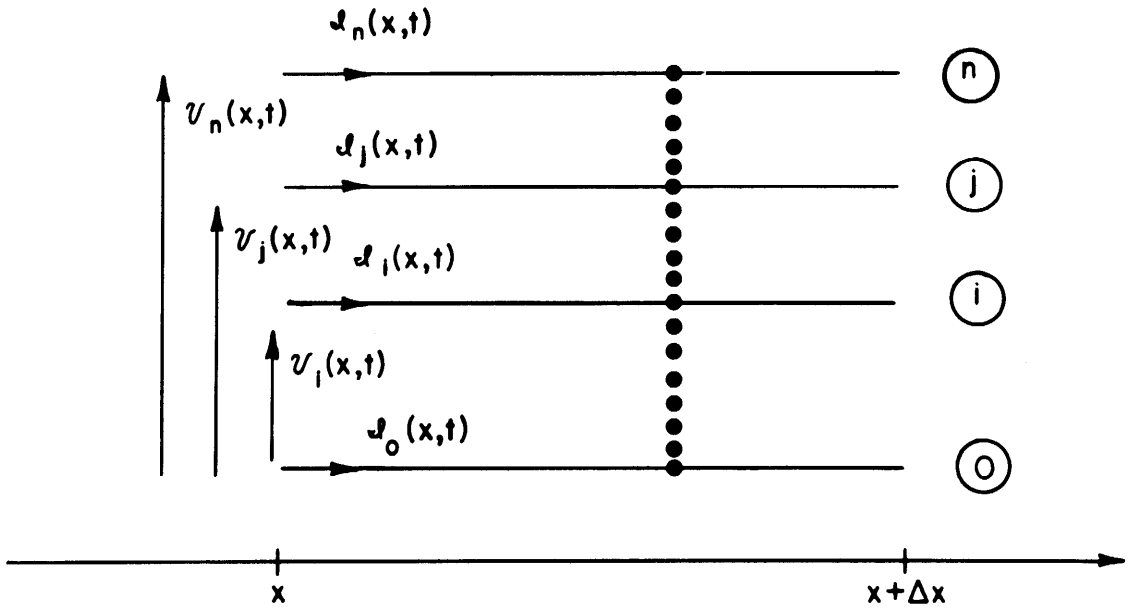

(c)

Figure 2-1. An (n+1) conductor, uniform transmission line.

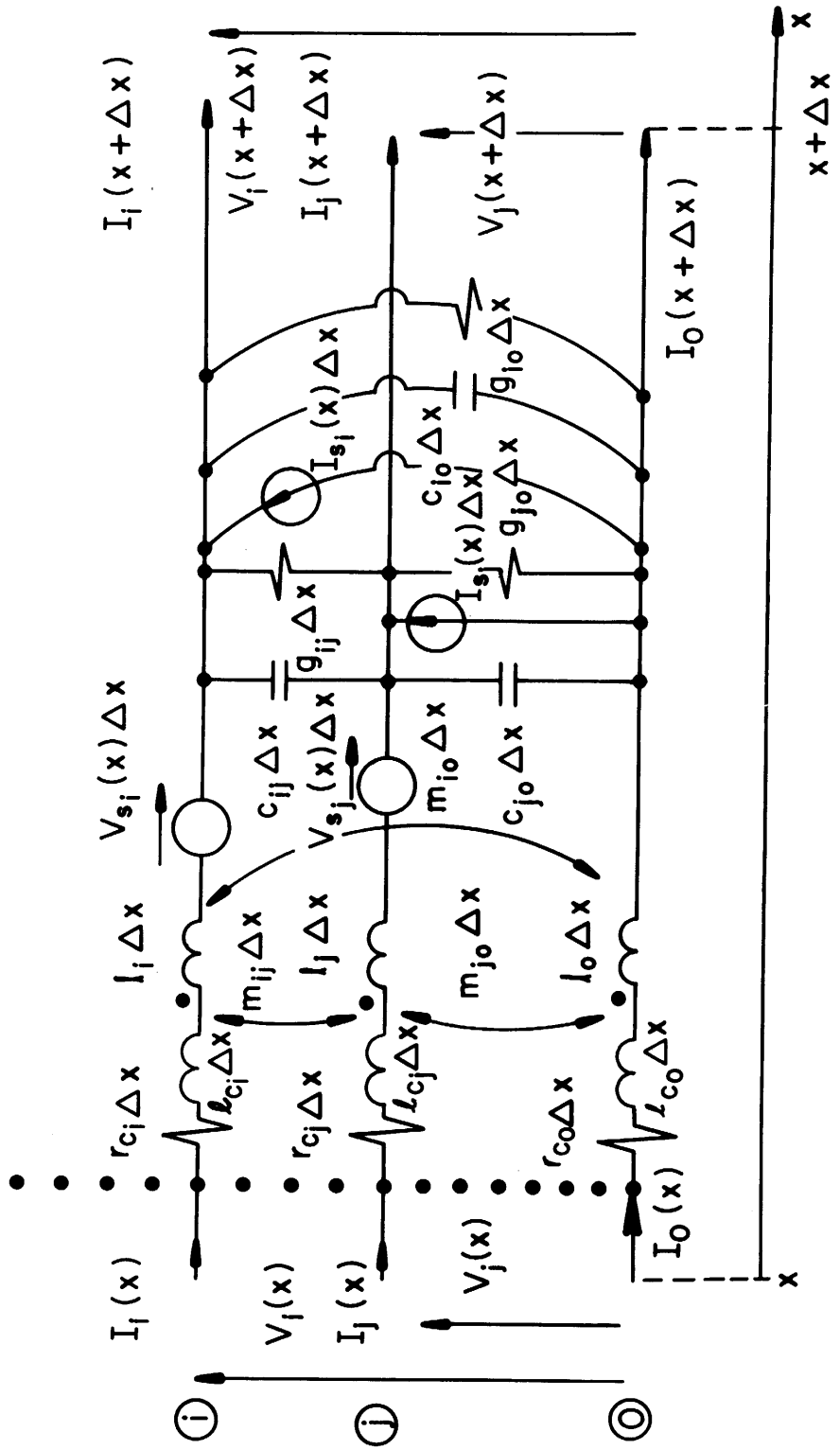

Figure 2-2. The per-unit-length equivalent circuit.

$j=1, ---, p$. The matrix $\underset{m\sim p}{0}$ is the $m\chi p$ zero matrix with zeros in every position i.e., $[\underset{m\sim p}{0}]_{ij} = 0$ for $i=1, ---, m$ and $j=1, ---, p$. The complex-valued phasor line voltages with respect to the reference conductor (the zero-th conductor), $V_i(x)$, and line currents, $I_i(x)$, are given by $[\underline{V}(x)]_i = V_i(x)$ and $[\underline{I}(x)]_i = I_i(x)$.

The $n\chi n$ complex-valued, symmetric matrices, $\underset{\sim}{Z}$ and $\underset{\sim}{Y}$, are the per-unit-length impedance and admittance matrices of the line, respectively. Since the line is assumed to be uniform, these matrices are independent of x. These per-unit-length matrices are separable as

$$\underset{\sim}{Z} = \underset{\sim c}{R} + j\omega \underset{\sim c}{L} + j\omega \underset{\sim}{L} \tag{2-4a}$$

$$\underset{\sim}{Y} = \underset{\sim}{G} + j\omega \underset{\sim}{C} \tag{2-4b}$$

where the $n\chi n$ real, symmetric matrices $\underset{\sim c}{R}$, $\underset{\sim c}{L}$, $\underset{\sim}{L}$, $\underset{\sim}{G}$, $\underset{\sim}{C}$ are the per-unit-length conductor resistance, conductor internal inductance, external inductance, conductance and capacitance matrices, respectively. The entries in these matrices may be straightforwardly obtained in terms of the elements of the per-unit-length equivalent circuit in Figure 2-2 as

$$[\underset{\sim c}{R}]_{ii} = r_{c_i} + r_{c_0}, \quad [\underset{\sim c}{R}]_{\substack{ij \\ i\neq j}} = r_{c_0} \tag{2-5a}$$

$$[\underset{\sim c}{L}]_{ii} = \ell_{c_i} + \ell_{c_0}, \quad [\underset{\sim c}{L}]_{\substack{ij \\ i\neq j}} = \ell_{c_0} \tag{2-5b}$$

$$[\underset{\sim}{L}]_{ii} = \ell_i + \ell_0 - 2m_{i0}, \quad [\underset{\sim}{L}]_{\substack{ij \\ i\neq j}} = \ell_0 + m_{ij} - m_{i0} - m_{j0} \tag{2-5c}$$

$$[\underset{\sim}{G}]_{ii} = g_{i0} + \sum_{\substack{j=1 \\ i\neq j}}^{n} g_{ij}, \quad [\underset{\sim}{G}]_{\substack{ij \\ i\neq j}} = -g_{ij} \tag{2-5d}$$

$$[\underset{\sim}{C}]_{ii} = c_{i0} + \sum_{\substack{j=1 \\ i\neq j}}^{n} c_{ij}, \quad [\underset{\sim}{C}]_{\substack{ij \\ i\neq j}} = -c_{ij}. \tag{2-5e}$$

The nχ1 column vectors, $\underline{V}_s(x)$ and $\underline{I}_s(x)$ contain per-unit-length equivalent voltage and current sources, $[\underline{V}_s(x)]_i = V_{s_i}(x)$ and $[\underline{I}_s(x)]_i = I_{s_i}(x)$, which are included to represent the effects of the spectral components of incident electromagnetic field sources which illuminate the line. These entries are complex-valued functions of frequency and position, x, along the line. In this report, no external incident fields are considered and these sources are set equal to zero, i.e., $\underline{V}_s(x) = \underset{n-1}{0}$ and $\underline{I}_s(x) = \underset{n-1}{0}$, in all computations with this model.

The solution to (2-3) is

$$\begin{bmatrix} \underline{V}(x) \\ \underline{I}(x) \end{bmatrix} = \underset{\sim}{\Phi}(x,x_0) \begin{bmatrix} \underline{V}(x_0) \\ \underline{I}(x_0) \end{bmatrix} + \int_{x_0}^{x} \underset{\sim}{\Phi}(x,\hat{x}) \begin{bmatrix} \underline{V}_s(\hat{x}) \\ \underline{I}_s(\hat{x}) \end{bmatrix} d\hat{x}$$

$$= \underset{\sim}{\Phi}(x,x_0) \begin{bmatrix} \underline{V}(x_0) \\ \underline{I}(x_0) \end{bmatrix} + \begin{bmatrix} \hat{\underline{V}}_s(x) \\ \underline{I}_s(x) \end{bmatrix} \qquad (2\text{-}6)$$

where $\underset{\sim}{\Phi}(x,x_0)$ is the 2nχ2n chain parameter matrix (or state transition matrix) and x_0 is some arbitrary position along the line $x \geq x_0$. The chain parameter matrix can be partitioned as

$$\underset{\sim}{\Phi}(x,x_0) = \begin{bmatrix} \underset{\sim}{\Phi}_{11}(x,x_0) & \underset{\sim}{\Phi}_{12}(x,x_0) \\ \underset{\sim}{\Phi}_{21}(x,x_0) & \underset{\sim}{\Phi}_{22}(x,x_0) \end{bmatrix} \qquad (2\text{-}7)$$

where $\underset{\sim}{\Phi}_{ij}(x,x_0)$ are nχn for i, j=1, 2. Thus (2-6) can be written as

$$\underline{V}(x) = \underset{\sim}{\Phi}_{11}(x,x_0)\,\underline{V}(x_0) + \underset{\sim}{\Phi}_{12}(x,x_0)\,\underline{I}(x_0) + \hat{\underline{V}}_s(x) \qquad (2\text{-}8a)$$

$$\underline{I}(x) = \underset{\sim}{\Phi}_{21}(x,x_0)\,\underline{V}(x_0) + \underset{\sim}{\Phi}_{22}(x,x_0)\,\underline{I}(x_0) + \hat{\underline{I}}_s(x) \qquad (2\text{-}8b)$$

The entries $\underset{\sim}{\Phi}_{ij}(x,x_0)$ are given by

$$\underset{\sim}{\Phi}_{11}(x,x_0) = 1/2\ \underset{\sim}{Y}^{-1}\ \underset{\sim}{T}\ (\underset{\sim}{e}^{\underset{\sim}{\gamma}(x-x_0)} + \underset{\sim}{e}^{-\underset{\sim}{\gamma}(x-x_0)})\ \underset{\sim}{T}^{-1}\ \underset{\sim}{Y} \qquad (2\text{-}9a)$$

$$\underset{\sim}{\Phi}_{12}(x,x_0) = -1/2\ \underset{\sim}{Y}^{-1}\underset{\sim}{T}\ \underset{\sim}{\gamma}(\underset{\sim}{e}^{\underset{\sim}{\gamma}(x-x_0)} - \underset{\sim}{e}^{-\underset{\sim}{\gamma}(x-x_0)})\ \underset{\sim}{T}^{-1} \qquad (2\text{-}9b)$$

$$\underset{\sim}{\Phi}_{21}(x,x_0) = -1/2\ \underset{\sim}{T}\ (\underset{\sim}{e}^{\gamma(x-x_0)} - \underset{\sim}{e}^{-\gamma(x-x_0)})\ \underset{\sim}{\gamma}^{-1}\ \underset{\sim}{T}^{-1}\ \underset{\sim}{Y} \qquad (2\text{-}9c)$$

$$\underset{\sim}{\Phi}_{22}(x,x_0) = 1/2\ \underset{\sim}{T}\ (\underset{\sim}{e}^{\gamma(x-x_0)} + \underset{\sim}{e}^{-\gamma(x-x_0)})\ \underset{\sim}{T}^{-1} \qquad (2\text{-}9d)$$

where $\underset{\sim}{e}^{\gamma(x-x_0)}$ is an nχn diagonal matrix with $[\underset{\sim}{e}^{\gamma(x-x_0)}]_{ii} = e^{\gamma_i(x-x_0)}$ and $[\underset{\sim}{e}^{\gamma(x-x_0)}]_{ij} = 0$ for i, j=1, ---, n and i$\neq$j. The matrix $\underset{\sim}{T}$ is an nχn, complex-valued matrix which diagonalizes the matrix product $\underset{\sim\sim}{YZ}$ as

$$\underset{\sim}{T}^{-1}\ \underset{\sim}{Y}\ \underset{\sim}{Z}\ \underset{\sim}{T} = \underset{\sim}{\gamma}^2 \qquad (2\text{-}10)$$

where $\underset{\sim}{\gamma}^2$ is an nχn diagonal matrix with $[\underset{\sim}{\gamma}^2]_{ii} = \gamma_i^2$ and $[\underset{\sim}{\gamma}^2]_{ij} = 0$ for i, j=1, ---, n and i$\neq$j. The nχn characteristic impedance matrix, $\underset{\sim}{Z}_C$, is given by

$$\underset{\sim}{Z}_C = \underset{\sim}{Y}^{-1}\ \underset{\sim}{T}\ \underset{\sim}{\gamma}\ \underset{\sim}{T}^{-1} = \underset{\sim}{Z}\ \underset{\sim}{T}\ \underset{\sim}{\gamma}^{-1}\ \underset{\sim}{T}^{-1} \qquad (2\text{-}11)$$

The transmission line is of length $\mathcal{L}$ with termination networks at x = 0 and at x = $\mathcal{L}$ as shown in Figure 2-3. For generality, the termination networks are considered to be in the form of linear n-ports and are characterizable by "Generalized Thevenin Equivalents" as

$$\underline{V}(0) = \underline{V}_0 - \underset{\sim}{Z}_0\ \underline{I}(0) \qquad (2\text{-}12a)$$

$$\underline{V}(\mathcal{L}) = \underline{V}_{\mathcal{L}} + \underset{\sim}{Z}_{\mathcal{L}}\ \underline{I}(\mathcal{L}) \qquad (2\text{-}12b)$$

where $\underline{V}_0$ and $\underline{V}_{\mathcal{L}}$ are nχ1 complex-valued vectors of equivalent, open-circuit, port excitation voltages (with respect to the reference conductor) and $\underset{\sim}{Z}_0$ and $\underset{\sim}{Z}_{\mathcal{L}}$ are nχn symmetric, complex-valued port impedance matrices.

As an alternate characterization, (2-12) may be written as "Generalized Norton Equivalents" by multiplying (2-12a) on the left by $\underset{\sim}{Z}_0^{-1}$ and (2-12b) on the left by $\underset{\sim}{Z}_{\mathcal{L}}^{-1}$ and rearranging as

$$\underline{I}(0) = \underline{I}_0 - \underset{\sim}{Y}_0\ \underline{V}(0) \qquad (2\text{-}13a)$$

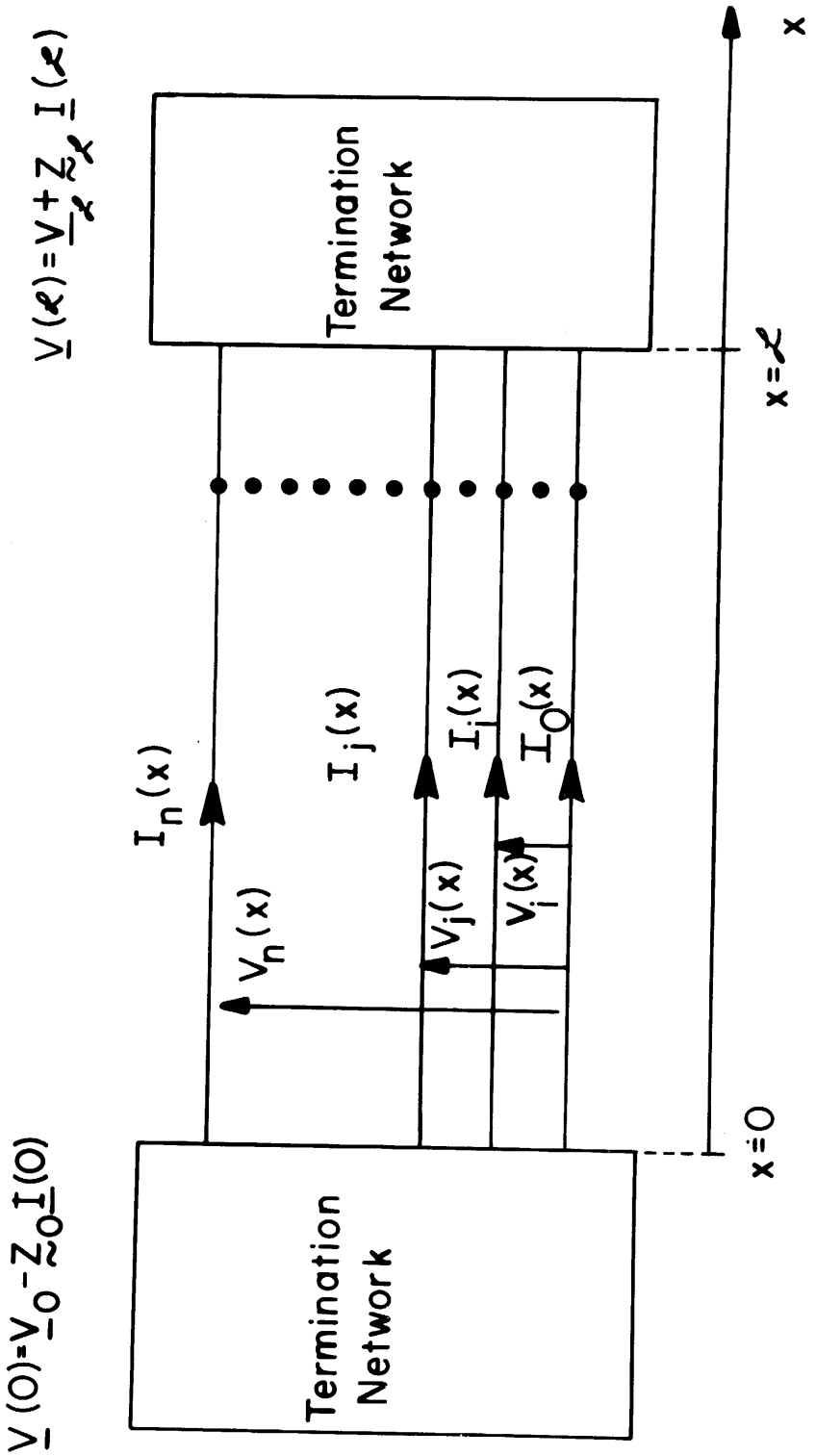

Figure 2-3. The termination networks.

$$\underline{I}(\ell) = -\underline{I}_{\ell} + \underset{\sim}{Y}_{\ell}\,\underline{V}(\ell) \qquad (2\text{-}13b)$$

where $\underline{I}_0$ and $\underline{I}_{\ell}$ are equivalent, short-circuit, port excitation current sources. The $n\chi n$ port admittance matrices $\underset{\sim}{Y}_0$ and $\underset{\sim}{Y}_{\ell}$ are given by $\underset{\sim}{Y}_0 = \underset{\sim}{Z}_0^{-1}$ and $\underset{\sim}{Y}_{\ell} = \underset{\sim}{Z}_{\ell}^{-1}$ where the inverse of an $n\chi n$ matrix $\underset{\sim}{M}$ is denoted by $\underset{\sim}{M}^{-1}$ and $\underline{I}_0 = \underset{\sim}{Y}_0\,\underline{V}_0$, $\underline{I}_{\ell} = \underset{\sim}{Y}_{\ell}\,\underline{V}_{\ell}$. These port admittance matrices can be found by treating the line currents $\underline{I}(0)$ or $\underline{I}(\ell)$ as independent sources and writing the node voltage equations for the termination networks. The transmission line voltages, $\underline{V}(0)$ or $\underline{V}(\ell)$, will comprise subsets of the node voltages of the termination networks. The additional node voltages can be eliminated from the node voltage equations describing the networks to yield (2-13). If the termination networks at $x = 0$ and $x = \ell$ consist only of admittances between the i-th and j-th wires, $Y_{0_{ij}}$ and $Y_{\ell_{ij}}$, respectively, and between the i-th wire and the reference conductor, $Y_{0_{ii}}$ and $Y_{\ell_{ii}}$, respectively, then the entries in $\underset{\sim}{Y}_{0_n}$ and $\underset{\sim}{Y}_{\ell}$ become $[\underset{\sim}{Y}_0]_{ii} = Y_{0_{ii}} + \sum_{j=1}^{n} Y_{0_{ij}}$ $[\underset{\sim}{Y}_0]_{ij} = -Y_{0_{ij}}$, $[\underset{\sim}{Y}_{\ell}]_{ii} = Y_{\ell_{ii}} + \sum_{j=1} Y_{\ell_{ij}}$, $[\underset{\sim}{Y}_{\ell}]_{ij} = -Y_{\ell_{ij}}$ for i, j=1, ---, n and $i \neq j$.

With $x = \ell$ and $x_0 = 0$ in (2-8), one can straightforwardly obtain using the "Generalized Thevenin Equivalent" characterization of the termination networks given in (2-12)[2]

$$[\underset{\sim}{Z}_{\ell}\,\underset{\sim}{\Phi}_{22}(\ell) - \underset{\sim}{Z}_{\ell}\,\underset{\sim}{\Phi}_{21}(\ell)\,\underset{\sim}{Z}_0 - \underset{\sim}{\Phi}_{12}(\ell) + \underset{\sim}{\Phi}_{11}(\ell)\,\underset{\sim}{Z}_0]\,\underline{I}(0) =$$

$$[\underset{\sim}{\Phi}_{11}(\ell) - \underset{\sim}{Z}_{\ell}\,\underset{\sim}{\Phi}_{21}(\ell)]\,\underline{V}_0 - \underline{V}_{\ell} + \hat{\underline{V}}_s(\ell) - \underset{\sim}{Z}_{\ell}\hat{\underline{I}}_s(\ell) \qquad (2\text{-}14a)$$

---

[2] In (2-8a) with $x=\ell$, $x_0=0$ substitute (2-12a) for $\underline{V}(0)$ and (2-12b) for $\underline{V}(\ell)$. Then substitute $\underline{I}(\ell)$ from (2-8b) with $x=\ell$, $x_0=0$ into the result and rearrange into the form in (2-14a). Substitute $\underline{V}(0)$ from (2-12a) into (2-8b) and rearrange to yield (2-14b).

$$\underline{I}(\ell) = \underset{\sim}{\Phi}_{21}(\ell)\,\underline{V}_0 + [\underset{\sim}{\Phi}_{22}(\ell) - \underset{\sim}{\Phi}_{21}(\ell)\,\underset{\sim}{Z}_0]\,\underline{I}(0) + \hat{\underline{I}}_s(\ell) \qquad (2\text{-}14b)$$

where $\underset{\sim}{\Phi}(\ell,0) = \underset{\sim}{\Phi}(\ell)$. $\underline{V}(x)$ and $\underline{I}(x)$ can be obtained for any x, $0 \leq x \leq \ell$, from (2-8) with $\underline{I}(0)$ from the solution of (2-14a) and $\underline{V}(0)$ determined from (2-12a). Generally, we are only interested in the terminal voltages and currents, $\underline{V}(0)$, $\underline{V}(\ell)$, $\underline{I}(0)$, $\underline{I}(\ell)$. The terminal currents, $\underline{I}(0)$ and $\underline{I}(\ell)$, can be obtained from (2-14) and the terminal voltages, $\underline{V}(0)$ and $\underline{V}(\ell)$, can be obtained from (2-12). Here one only needs to solve n equations in n unknowns (equation (2-14a)).

The $\underset{\sim}{\Phi}_{ij}$ submatrices of the chain parameter matrix in (2-7) satisfy certain fundamental identities, [1,2]. These identities can be used to formulate (2-14a) in an alternate form [1,2]:

$$[\{\underset{\sim}{\Phi}_{21}(\ell)\,\underset{\sim}{Z}_\ell - \underset{\sim}{\Phi}_{22}(\ell)\}\{\underset{\sim}{\Phi}_{21}(\ell)\,\underset{\sim}{Z}_0 - \underset{\sim}{\Phi}_{22}(\ell)\} - \underset{\sim}{1}_n]\,\underline{I}(0) =$$
$$\underset{\sim}{\Phi}_{21}(\ell)\,\underline{V}_\ell + \{\underset{\sim}{\Phi}_{21}(\ell)\,\underset{\sim}{Z}_\ell - \underset{\sim}{\Phi}_{22}(\ell)\}\,\underset{\sim}{\Phi}_{21}(\ell)\,\underline{V}_0 - \underset{\sim}{\Phi}_{21}(\ell)\,[\hat{\underline{V}}_s(\ell) - \underset{\sim}{Z}_\ell\hat{\underline{I}}_s(\ell)] \qquad (2\text{-}15)$$

where $\underset{\sim}{1}_n$ is the nχn identity matrix with $[\underset{\sim}{1}_n]_{ii} = 1$ and $[\underset{\sim}{1}_n]_{ij} = 0$ for i, j=1, ---, n and $i \neq j$. Note that the formulation in (2-15) and (2-14b) require computation of only two of the four chain parameter submatrices, $\underset{\sim}{\Phi}_{21}(\ell)$ and $\underset{\sim}{\Phi}_{22}(\ell)$.

As an alternate formulation, the above equations can be written in terms of the "Generalized Norton Equivalent" representation of the termination networks given in (2-13). Rather than rederiving the above equations. it is much simplier to note the direct similarity of the Norton equivalent representation in (2-13) and the Thevenin equivalent representation in (2-12). By noting the analogous variables in (2-13) and (2-12) and observing the form of (2-8) we may simply make certain substitutions of these analogous

variables in (2-14) and (2-15) as shown in Table I. The result is

$$[\underset{\sim}{Y}_{\ell}\,\underset{\sim}{\Phi}_{11}(\ell) - \underset{\sim}{Y}_{\ell}\,\underset{\sim}{\Phi}_{12}(\ell)\,\underset{\sim}{Y}_{0} - \underset{\sim}{\Phi}_{21}(\ell) + \underset{\sim}{\Phi}_{22}(\ell)\,\underset{\sim}{Y}_{0}]\,\underline{V}(0) =$$

$$[\underset{\sim}{\Phi}_{22}(\ell) - \underset{\sim}{Y}_{\ell}\underset{\sim}{\Phi}_{12}(\ell)]\,\underline{I}_{0} + \underline{I}_{\ell} + \hat{\underline{I}}_{s}(\ell) - \underset{\sim}{Y}_{\ell}\,\hat{\underline{V}}_{s}(\ell) \qquad (2\text{-}16a)$$

$$\underline{V}(\ell) = \underset{\sim}{\Phi}_{12}(\ell)\,\underline{I}_{0} + [\underset{\sim}{\Phi}_{11}(\ell) - \underset{\sim}{\Phi}_{12}(\ell)\,\underset{\sim}{Y}_{0}]\,\underline{V}(0) + \hat{\underline{V}}_{s}(\ell) \qquad (2\text{-}16b)$$

$$[\{\underset{\sim}{\Phi}_{12}(\ell)\,\underset{\sim}{Y}_{\ell} - \underset{\sim}{\Phi}_{11}(\ell)\}\ \{\underset{\sim}{\Phi}_{12}(\ell)\,\underset{\sim}{Y}_{0} - \underset{\sim}{\Phi}_{11}(\ell)\} - \underset{\sim}{1}_{n}]\,\underline{V}(0) =$$

$$-\underset{\sim}{\Phi}_{12}(\ell)\,\underline{I}_{\ell} + [\underset{\sim}{\Phi}_{12}(\ell)\,\underset{\sim}{Y}_{\ell} - \underset{\sim}{\Phi}_{11}(\ell)]\,\underset{\sim}{\Phi}_{12}(\ell)\,\underline{I}_{0} \qquad (2\text{-}16c)$$

$$-\underset{\sim}{\Phi}_{12}(\ell)[\hat{\underline{I}}_{s}(\ell) - \underset{\sim}{Y}_{\ell}\,\hat{\underline{V}}_{s}(\ell)]$$

2.2 The Transmission Line Model Specialized to the Generator - Receptor Circuit Pair and the BOUND Model

The general problem of interest in cable coupling predictions is as follows. One generally excites one end of a generator circuit (which consists of one wire, the "generator wire", and the reference conductor) and is then interested in determining the induced signals at each end of the receptor circuit (which consists of another wire, the "receptor wire", and the reference conductor). The remaining circuits in the cable bundle will influence this coupling to some degree and the wires in these circuits will be designated as "parasitic wires".

One might expect that an upper bound estimate of the coupling between the generator-receptor circuit pair may be obtained if the effects of the parasitic circuits are ignored. It will be shown in the computed and experimental results that the sensitivity of the cable responses to relative wire position can be extraordinarily large. Therefore a realistic approach to the prediction of cable coupling in random cable bundles (in which

TABLE I

Analogous variables in the Generalized Thevenin Equivalent (2-12) and Generalized Norton Equivalent (2-13) representation of the termination networks. The analogous variables are substituted in equations (2-14) and (2-15) to obtain equations (2-16).

Generalized Thevenin Equivalent (2-12)	Generalized Norton Equivalent (2-13)
$\underline{I}(0)$	$\underline{V}(0)$
$\underline{I}(\lambda)$	$\underline{V}(\lambda)$
$\underset{\sim}{Z}_0$	$\underset{\sim}{Y}_0$
$\underset{\sim}{Z}\lambda$	$\underset{\sim}{Y}\lambda$
$\underline{V}(0)$	$\underline{I}(0)$
$\underline{V}(\lambda)$	$-\underline{I}(\lambda)$
$\underset{\sim}{\Phi}_{11}(\lambda)$	$\underset{\sim}{\Phi}_{22}(\lambda)$
$\underset{\sim}{\Phi}_{12}(\lambda)$	$\underset{\sim}{\Phi}_{21}(\lambda)$
$\underset{\sim}{\Phi}_{21}(\lambda)$	$\underset{\sim}{\Phi}_{12}(\lambda)$
$\underset{\sim}{\Phi}_{22}(\lambda)$	$\underset{\sim}{\Phi}_{11}(\lambda)$
$\hat{\underline{V}}_s(\lambda)$	$\hat{\underline{I}}_s(\lambda)$
$\hat{\underline{I}}_s(\lambda)$	$\hat{\underline{V}}_s(\lambda)$

relative wire position is not known and may vary considerably along the cable length) would seem to be to neglect the effects of the parasitic wires in an attempt to achieve an upper bound estimate of the cable responses. This alternative to considering all circuit interactions with the MTL model will also have the effect of reducing the computation time required to obtain the receptor terminal voltages since one will not need to solve large sets of simultaneous equations as indicated in (2-14), (2-15) or (2-16). Therefore one of the prime approximations in formulating the BOUND model will be to neglect the effects of the parasitic circuits on the coupling between the generator and receptor circuits. In addition, the generator and receptor wires are assumed to be parallel to each other and the reference conductor.

The reader will,perhaps, appreciate the difficulty in making predictions of random cable bundle responses since one has virtually no information on some of the important parameters, i.e., relative wire positions. Therefore, the above approximation seems to be somewhat reasonable in this regard. Nevertheless, one will need to know or assume separation distances between the generator and receptor wires and between these wires and the reference conductor. Since it is not intended that this model provide "accurate" predictions of the random cable bundle responses and it is only intended that the model provide estimates of these responses, some reasonable approximations to these parameters may be used. For example, the heights of each wire above the reference conductor,e.g., a ground plane, may be taken to be the average height of the cable bundle above the reference conductor. The wire separations may be taken to be, for example, one-half of the bundle diameter.

If the effects of the parasitic circuits are ignored, one can obtain the solution for the receptor circuit terminal voltages in a simple form. In order to provide a simple solution, two additional approximations will be used. Wires in random cable bundles are usually insulated from each other by coating them with dielectric insulations. If the effects of the wire dielectrics on the coupling are neglected, simple approximations to the per-unit-length parameters in the transmission line equations can be obtained [1]. In addition, the solution for the receptor circuit terminal voltages will be simplified. The purpose of the BOUND model is to estimate the cable responses since accurate predictions are generally not achievable for random cable bundles. In view of this objective and the simplifications resulting from neglecting the effects of the wire insulations, it will be assumed that the generator and receptor circuits are immersed in a homogeneous medium (free space), i.e., the wire insulations are removed. Also, because of the above considerations, it will be assumed that the generator and receptor wires as well as the reference conductor are perfect conductors.

To obtain the equations for the receptor terminal voltages, consider the isolated generator-receptor circuit pair along with the line terminations shown in Figure 2-4. The transmission line equations of the generator-receptor pair can be derived in the following manner [1]. Consider an "electrically small" Δx length shown in Figure 2-5. Since the conductors and the surrounding medium are assumed to be lossless, the resistance and internal inductance of the conductors as well as the conductance of the surrounding medium in Figure 2-2 are zero. From Figure 2-5, one can obtain

$$\frac{V_G(x+\Delta x) - V_G(x)}{\Delta x} = -j\omega \ell_G I_G(x) - j\omega \ell_m I_R(x) \qquad (2\text{-}17a)$$

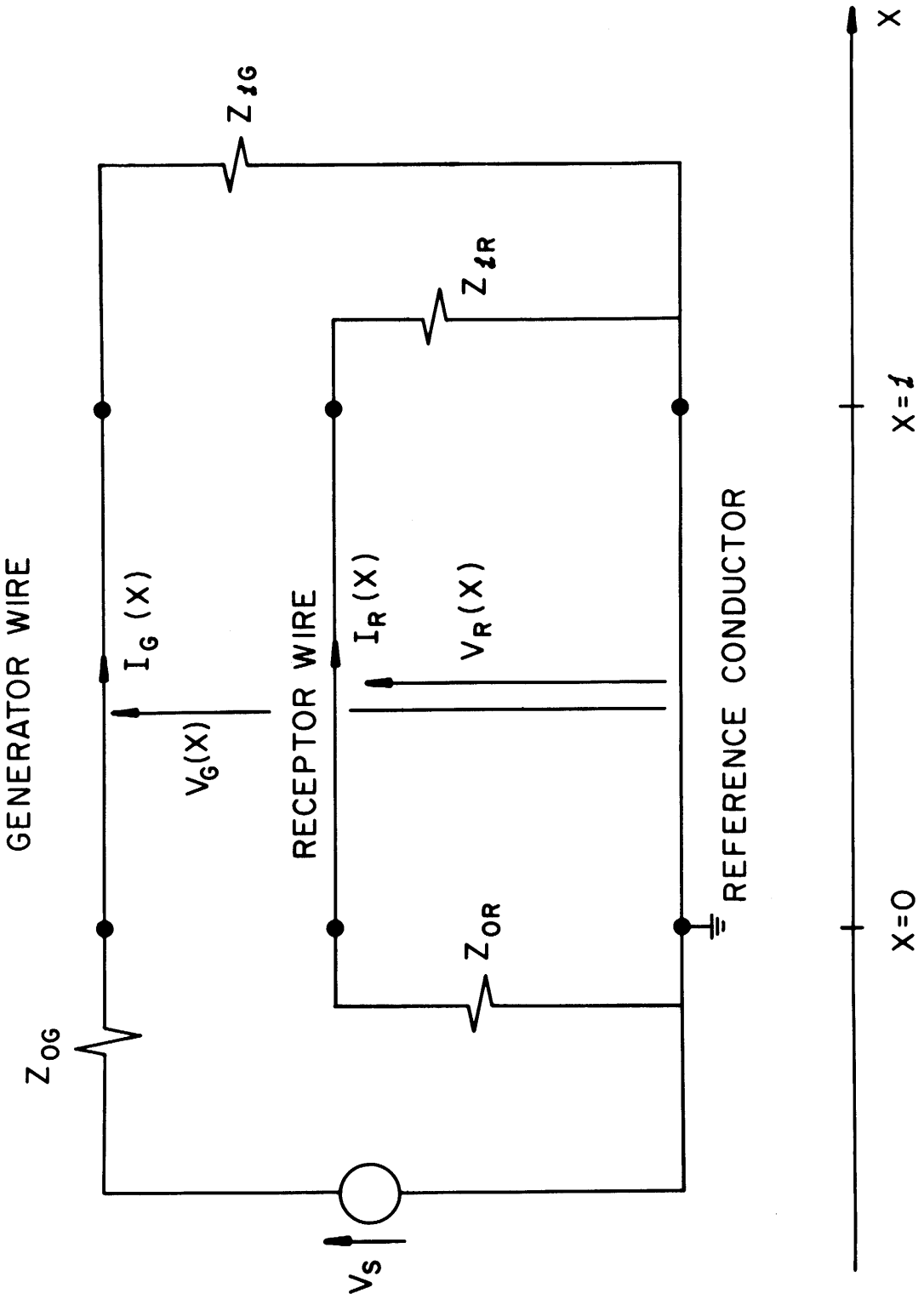

Figure 2-4. The generator-receptor circuit pair.

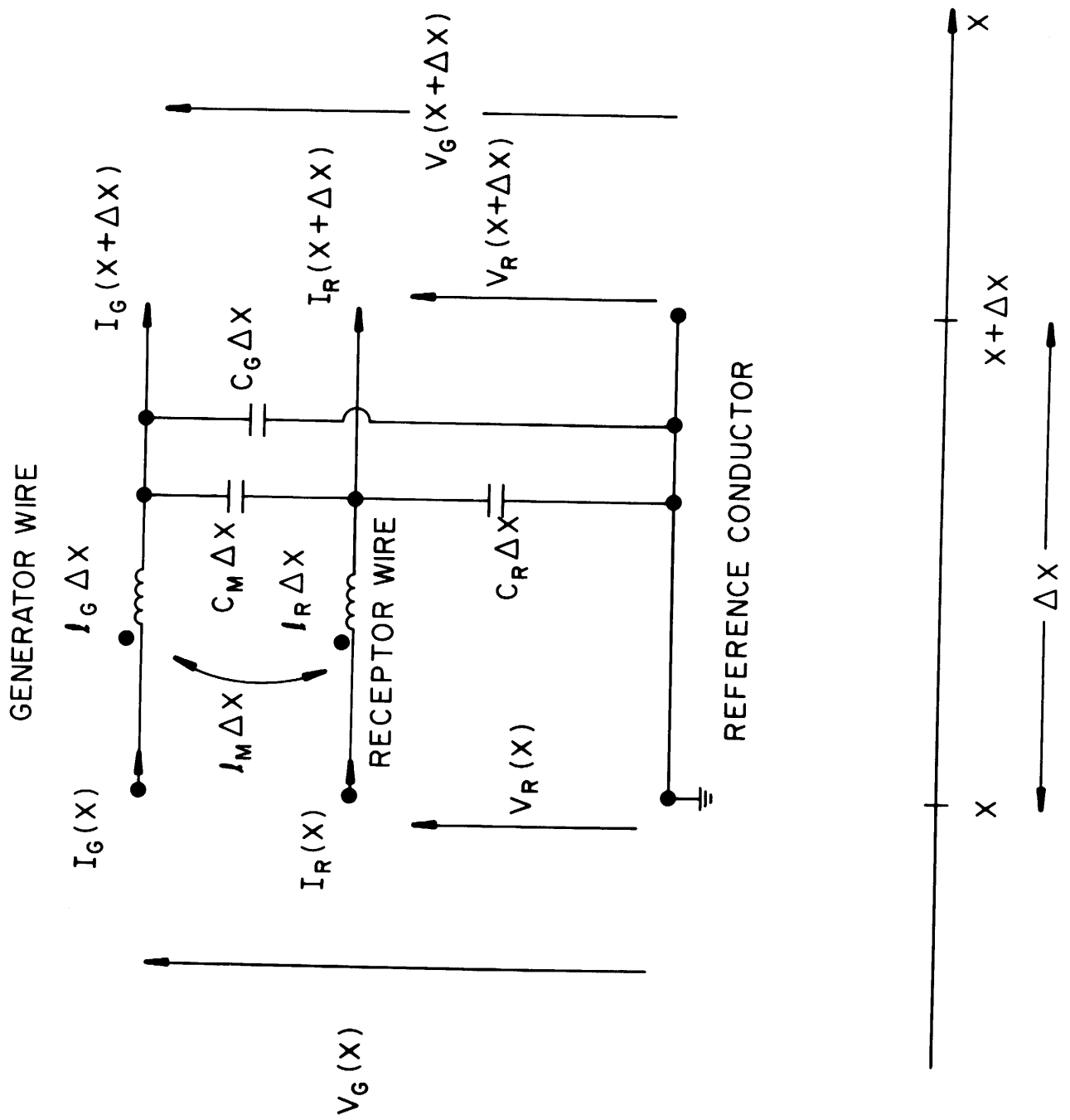

Figure 2-5. The per-unit-length equivalent circuit of the generator-receptor circuit pair.

$$\frac{V_R(x+\Delta x) - V_R(x)}{\Delta x} = -j\omega \ell_m I_G(x) - j\omega \ell_R I_R(x) \qquad (2\text{-}17b)$$

$$\frac{I_G(x+\Delta x) - I_G(x)}{\Delta x} = -j\omega(c_G+c_m)\, V_G(x+\Delta x) + j\omega c_m\, V_R(x+\Delta x) \qquad (2\text{-}17c)$$

$$\frac{I_R(x+\Delta x) - I_R(x)}{\Delta x} = j\omega c_m V_G(x+\Delta x) - j\omega(c_R+c_m)\, V_R(x+\Delta x) \qquad (2\text{-}17d)$$

In the limit as $\Delta x \to 0$ these equations become the differential equations of the line given in (2-3) specialized to the case of the isolated generator-receptor pair:

$$\frac{dV_G(x)}{dx} = -j\omega \ell_G I_G(x) - j\omega \ell_m I_R(x) \qquad (2\text{-}18a)$$

$$\frac{dV_R(x)}{dx} = -j\omega \ell_m I_G(x) - j\omega \ell_R I_R(x) \qquad (2\text{-}18b)$$

$$\frac{dI_G(x)}{dx} = -j\omega(c_G+c_m)\, V_G(x) + j\omega c_m\, V_R(x) \qquad (2\text{-}18c)$$

$$\frac{dI_R(x)}{dx} = j\omega c_m\, V_G(x) - j\omega(c_R+c_m)\, V_R(x) \qquad (2\text{-}18d)$$

The matrix chain parameters provide a solution to the transmission line equations by relating the voltages and currents at one end of the line, $V_G(\ell)$, $V_R(\ell)$, $I_G(\ell)$ and $I_R(\ell)$, to the voltages and currents at the other end of the line $V_G(0)$, $V_R(0)$, $I_G(0)$ and $I_R(0)$, as (see (2-6) - (2-8))

$$\begin{bmatrix} \underline{V}(\ell) \\ \underline{I}(\ell) \end{bmatrix} = \begin{bmatrix} \underset{\sim}{\Phi}_{11}(\ell) & \underset{\sim}{\Phi}_{12}(\ell) \\ \underset{\sim}{\Phi}_{21}(\ell) & \underset{\sim}{\Phi}_{22}(\ell) \end{bmatrix} \begin{bmatrix} \underline{V}(0) \\ \underline{I}(0) \end{bmatrix} \qquad (2\text{-}19)$$

where

$$\underline{V}(\ell) = \begin{bmatrix} V_G(\ell) \\ V_R(\ell) \end{bmatrix} \qquad \underline{V}(0) = \begin{bmatrix} V_G(0) \\ V_R(0) \end{bmatrix}$$

$$\underline{I}(\ell) = \begin{bmatrix} I_G(\ell) \\ I_R(\ell) \end{bmatrix} \qquad \underline{I}(0) = \begin{bmatrix} I_G(0) \\ I_R(0) \end{bmatrix} \tag{2-20}$$

The matrix chain parameters with the wire insulations removed and perfect conductors assumed become (see Section 3.1 of [1])

$$\underset{\sim}{\Phi}_{11}(\ell) = \cos(\beta\ell)\ \underset{\sim}{1}_2 \tag{2-21a}$$

$$\underset{\sim}{\Phi}_{12}(\ell) = -j\sin(\beta\ell)\ v\ \underset{\sim}{L} = -j\omega\underset{\sim}{L}\ell\left\{\frac{\sin(\beta\ell)}{\beta\ell}\right\} \tag{2-21b}$$

$$\underset{\sim}{\Phi}_{21}(\ell) = -j\sin(\beta\ell)\ (v\underset{\sim}{L})^{-1} = -j\omega\underset{\sim}{C}\ell\left\{\frac{\sin(\beta\ell)}{\beta\ell}\right\} \tag{2-21c}$$

$$\underset{\sim}{\Phi}_{22}(\ell) = \cos(\beta\ell)\ \underset{\sim}{1}_2 \tag{2-21d}$$

where β is the phase constant or wave number given by $\beta = \frac{\omega}{v} = 2\pi/\lambda$; λ is a wavelength at the frequency of interest, i.e., $\lambda = v/f$, and v is the velocity of propagation, $v \cong 3\times10^8$ m/sec. The per-unit-length inductance and capacitance matrices, $\underset{\sim}{L}$ and $\underset{\sim}{C}$, respectively, are given by

$$\underset{\sim}{L} = \begin{bmatrix} \ell_G & \ell_m \\ \ell_m & \ell_R \end{bmatrix} \tag{2-22a}$$

$$\underset{\sim}{C} = \begin{bmatrix} (c_G + c_m) & -c_m \\ -c_m & (c_R + c_m) \end{bmatrix} \tag{2-22b}$$

and

$$\underset{\sim}{1}_2 = \begin{bmatrix} 1 & 0 \\ 0 & 1 \end{bmatrix} \tag{2-22c}$$

where $\underset{\sim}{L}$ and $\underset{\sim}{C}$ satisfy [1]

$$\underset{\sim}{L}\,\underset{\sim}{C} = \mu\varepsilon\ \underset{\sim}{1}_2 = \frac{1}{v^2}\,\underset{\sim}{1}_2 \tag{2-23}$$

since the generator-receptor pair is assumed to be immersed in a homogeneous medium (free space).

The termination networks are described by Generalized Thevenin Equivalents in (2-12) as

$$\underline{V}(0) = \underline{V}_0 - \underset{\sim}{Z}_0\,\underline{I}(0) \tag{2-24a}$$

$$\underline{V}(\mathcal{L}) = \underline{V}_{\mathcal{L}} + \underset{\sim}{Z}_{\mathcal{L}}\,\underline{I}(\mathcal{L}) \tag{2-24b}$$

Substituting (2-24) and (2-21) into (2-19) yields (see (2-14))

$$\begin{aligned}&[\cos(\beta\mathcal{L})\ (\underset{\sim}{Z}_{\mathcal{L}} + \underset{\sim}{Z}_0) + j\sin(\beta\mathcal{L})\ (\underset{\sim}{Z}_{\mathcal{L}}\underset{\sim}{C}\ \underset{\sim}{Z}_0 + \underset{\sim}{L})]\ \underline{I}(0) = \\ &\quad [\cos(\beta\mathcal{L})\ \underset{\sim}{1}_2 + j\sin(\beta\mathcal{L})\ \underset{\sim}{Z}_{\mathcal{L}}\underset{\sim}{C}]\ \underline{V}_0 - \underline{V}_{\mathcal{L}}\end{aligned} \tag{2-25}$$

One can easily obtain a similar equation for $\underline{I}(\mathcal{L})$ without any further derivation. The matrix chain parameter solution in (2-19) may be written as [1] (This becomes fairly obvious when one redefines the x variable.)

$$\begin{bmatrix}\underline{V}(0)\\ \underline{I}(0)\end{bmatrix} = \begin{bmatrix}\underset{\sim}{\Phi}_{11}(-\mathcal{L}) & \underset{\sim}{\Phi}_{12}(-\mathcal{L})\\ \underset{\sim}{\Phi}_{21}(-\mathcal{L}) & \underset{\sim}{\Phi}_{22}(-\mathcal{L})\end{bmatrix}\begin{bmatrix}\underline{V}(\mathcal{L})\\ \underline{I}(\mathcal{L})\end{bmatrix} \tag{2-26a}$$

or [1] (also see (2-21))

$$\begin{bmatrix}\underline{V}(0)\\ -\underline{I}(0)\end{bmatrix} = \begin{bmatrix}\underset{\sim}{\Phi}_{11}(\mathcal{L}) & \underset{\sim}{\Phi}_{12}(\mathcal{L})\\ \underset{\sim}{\Phi}_{21}(\mathcal{L}) & \underset{\sim}{\Phi}_{22}(\mathcal{L})\end{bmatrix}\begin{bmatrix}\underline{V}(\mathcal{L})\\ -\underline{I}(\mathcal{L})\end{bmatrix} \tag{2-26b}$$

The terminal conditions in (2-24) can also be written as

$$\underline{V}(\mathcal{L}) = \underline{V}_{\mathcal{L}} - \underset{\sim}{Z}_{\mathcal{L}}\,(-\underline{I}(\mathcal{L})) \tag{2-27a}$$

$$\underline{V}(0) = \underline{V}_0 + \underset{\sim}{Z}_0\,(-\underline{I}(0)) \tag{2-27b}$$

Comparing (2-26b) and (2-27) to (2-19) and (2-24), one may obviously replace $\underline{I}(0)$, Z_ℓ, Z_0, $\underline{V}_0$, and $\underline{V}_\ell$ in (2-25) by $-\underline{I}(\ell)$, Z_0, Z_ℓ, $\underline{V}_\ell$, and $\underline{V}_0$, respectively, to obtain

$$[\cos(\beta\ell)\ (\underset{\sim}{Z}_0 + \underset{\sim}{Z}_\ell) + j\sin(\beta\ell)\ (\underset{\sim}{Z}_0\ \underset{\sim}{C}\ \underset{\sim}{Z}_\ell + \underset{\sim}{L})]\ \underline{I}(\ell) = \tag{2-28}$$

$$-[\cos(\beta\ell)\ \underset{\sim}{1}_2 + j\sin(\beta\ell)\ \underset{\sim}{Z}_0\ \underset{\sim}{C}]\ \underline{V}_\ell + \underline{V}_0$$

The quantities in (2-24) for the isolated generator-receptor circuit pair become (see Figure 2-4)

$$\underline{V}_0 = \begin{bmatrix} 1 \\ 0 \end{bmatrix} V_s \tag{2-29a}$$

$$\underline{V}_\ell = \begin{bmatrix} 0 \\ 0 \end{bmatrix} \tag{2-29b}$$

$$\underset{\sim}{Z}_0 = \begin{bmatrix} Z_{0G} & 0 \\ 0 & Z_{0R} \end{bmatrix} \tag{2-29c}$$

$$\underset{\sim}{Z}_\ell = \begin{bmatrix} Z_{\ell G} & 0 \\ 0 & Z_{\ell R} \end{bmatrix} \tag{2-29d}$$

Substituting (2-29) and (2-22) into (2-28) and multiplying out the result, one obtains

$$[\cos(\beta\ell)\ (Z_{0G} + Z_{\ell G}) + j\sin(\beta\ell)\ \{Z_{\ell G}\ Z_{0G}(c_G + c_m) + \ell_G\}\ ] I_G(\ell) + [j\sin(\beta\ell)\ \{\ell_m - c_m\ Z_{0G}\ Z_{\ell R}\ \}\ I_R(\ell) = V_s \tag{2-30a}$$

$$[j\sin(\beta\ell)\ \{\ell_m - c_m\ Z_{\ell G}\ Z_{0R}\}\ ]\ I_G(\ell) + [\cos(\beta\ell)\ (Z_{0R} + Z_{\ell R}) + j\sin(\beta\ell)\ \{Z_{0R}\ Z_{\ell R}\ (c_R + c_m) + \ell_R\}\ ]\ I_R(\ell) = 0 \tag{2-30b}$$

Solving for $I_R(\ell)$, and utilizing $V_R(\ell) = Z_{\ell R} I_R(\ell)$ one obtains

$$V_R(\ell) = \frac{-j\sin(\beta\ell)\ Z_{\ell R}\ \{\ell_m - c_m\ Z_{\ell G}\ Z_{0R}\}\ V_s}{\Delta} \tag{2-31}$$

where

$$\Delta = [\cos(\beta\ell)\ (Z_{0G} + Z_{\ell G}) + jv\sin(\beta\ell)\ \{Z_{\ell G}\ Z_{0G}\ (c_G + c_m) + \ell_G\}\ ] \times$$

$$[\cos\beta\ell)\ (Z_{0R} + Z_{\ell R}) + jv\sin(\beta\ell)\ \{Z_{0R}\ Z_{\ell R}\ (c_R + c_m) + \ell_R\ \}\ ] \qquad (2\text{-}32)$$

$$- [jv\sin(\beta\ell)\ \{\ell_m - c_m\ Z_{0G}\ Z_{\ell R}\}\ ] \times$$

$$[jv\sin(\beta\ell)\ \{\ell_m - c_m\ Z_{\ell G}\ Z_{0R}\}\ ]$$

After some manipulation, Δ can be written as

$$\Delta = (Z_{0G} + Z_{\ell G})\ (Z_{0R} + Z_{\ell R})\cos^2(\beta\ell)$$

$$- v^2 \sin^2(\beta\ell)\ [\{Z_{\ell G}\ Z_{0G}\ (c_G + c_m) + \ell_G\}\ \{Z_{0R}\ Z_{\ell R}(c_R + c_m) + \ell_R\}$$

$$- (\ell_m - c_m\ Z_{0G}\ Z_{\ell R})\ (\ell_m - c_m\ Z_{\ell G}\ Z_{0R})\ ] \qquad (2\text{-}33)$$

$$+ jv\sin(\beta\ell)\cos(\beta\ell)\ [(Z_{0R} + Z_{\ell R})\ \{Z_{\ell G}\ Z_{0G}\ (c_G + c_m) + \ell_G\ \}$$

$$+ (Z_{0G} + Z_{\ell G})\ \{Z_{0R}\ Z_{\ell R}\ (c_R + c_m) + \ell_R\ \}\ ]$$

Similarly from (2-25), one can derive

$$V_R(0) = \frac{jv\sin(\beta\ell)\ Z_{0R}}{\Delta} \Big\{\cos(\beta\ell)\ [Z_{\ell R}\ Z_{\ell G}\ c_m + \ell_m] \qquad (2\text{-}34)$$

$$+ jv\sin(\beta\ell)\ [Z_{\ell R}\ c_m\ \ell_G + Z_{\ell G}\ \ell_m\ (c_G + c_m)\ ]\Big\} V_s$$

where Δ is given in (2-33). From the property $\underset{\sim}{L}\ \underset{\sim}{C} = \frac{1}{v^2}\ \underset{\sim}{1}_n$ in (2-23), one can show that

$$\ell_m\ (c_G + c_m) = \ell_R\ c_m \qquad (2\text{-}35a)$$

$$\ell_m\ (c_R + c_m) = \ell_G\ c_m \qquad (2\text{-}35b)$$

Therefore, (2-34) can be written in an alternate form as

$$V_R(0) = \frac{j\sin(\beta \ell)\ Z_{0R}}{\Delta} \{ \cos(\beta \ell)\ [Z_{\ell R}\ Z_{\ell G}\ c_m + \ell_m]$$

$$+ j\sin(\beta \ell)\ [Z_{\ell R}\ \ell_m\ (c_R + c_m) + Z_{\ell G}\ \ell_R\ c_m]\}\ V_s \qquad (2\text{-}36)$$

The solutions for the receptor terminal voltages, $V_R(0)$ and $V_R(\ell)$, are therefore given by (2-31), (2-33) and (2-36) and are quite simple. However note in (2-31) that there is the possibility that $V_R(\ell)$ will be identically zero for all frequencies whereas $V_R(0)$ given by (2-36) may not be identically zero. Transmission lines are sometimes purposely designed for this condition and are called directional couplers [3]. The condition for the directional coupler effect, i.e., $V_R(\ell)$ is zero for all frequencies, is that the numerator of (2-31) be identically zero. This results in the condition

$$Z_{0R}\ Z_{\ell G} = \ell_m / c_m \qquad (2\text{-}37)$$

From (2-23), one can obtain

$$\ell_G\ (c_G + c_m) = \ell_R\ (c_R + c_m) \qquad (2\text{-}38a)$$

$$\ell_m\ (c_G + c_m) = \ell_R\ c_m \qquad (2\text{-}38b)$$

$$\ell_m\ (c_R + c_m) = \ell_G\ c_m \qquad (2\text{-}38c)$$

and (2-37) can be written as

$$Z_{0R}\ Z_{\ell G} = \sqrt{\frac{\ell_m^2}{c_m^2}}$$

$$= \sqrt{\frac{\ell_R\ \ell_G}{(c_G+c_m)\ (c_R+c_m)}} \qquad (2\text{-}39)$$

$$= \sqrt{\frac{\ell_G}{(c_G+c_m)}}\sqrt{\frac{\ell_R}{(c_R+c_m)}} = Z_{CG}\ Z_{CR}$$

where

$$Z_{CG} \triangleq \sqrt{\frac{\ell_G}{(c_G+c_m)}} \tag{2-40a}$$

$$Z_{CR} \triangleq \sqrt{\frac{\ell_R}{(c_R+c_m)}} \tag{2-40b}$$

The quantities Z_{CG} and Z_{CR} look somewhat like the characteristic impedances of the individual circuits and are sometimes referred to as being the characteristic impedances of each circuit in the presence of the other circuit [3].

Certain low frequency approximations of the solution may also be obtained. If the line is electrically short, i.e. $\beta\ell \ll 1$, then the following approximations may be used in the terminal voltage equations in (2-31), (2-33) and (2-36):

$$\cos(\beta\ell) \cong 1 \tag{2-41a}$$

$$v \sin(\beta\ell) \cong v\beta\ell = \omega\ell \tag{2-41b}$$

In addition, if the termination impedances, Z_{0G}, $Z_{\ell G}$, Z_{0R} and $Z_{\ell R}$, are frequency independent, then, for a sufficiently small frequency, one can further approximate (2-31), (2-33) and (2-36) as

$$V_R(\ell) \cong \frac{-j\omega\ell\, Z_{\ell R}\{\ell_m - c_m Z_{\ell G} Z_{0R}\}}{(Z_{0G} + Z_{\ell G})(Z_{0R} + Z_{\ell R})} V_s \tag{2-42a}$$

$$V_R(0) \cong \frac{j\omega\ell\, Z_{0R}\{\ell_m + c_m Z_{\ell G} Z_{\ell R}\}}{(Z_{0G} + Z_{\ell G})(Z_{0R} + Z_{\ell R})} V_s \tag{2-42b}$$

One can obtain the same result from a lumped circuit representation of the receptor circuit in Figure 2-6 as [3]

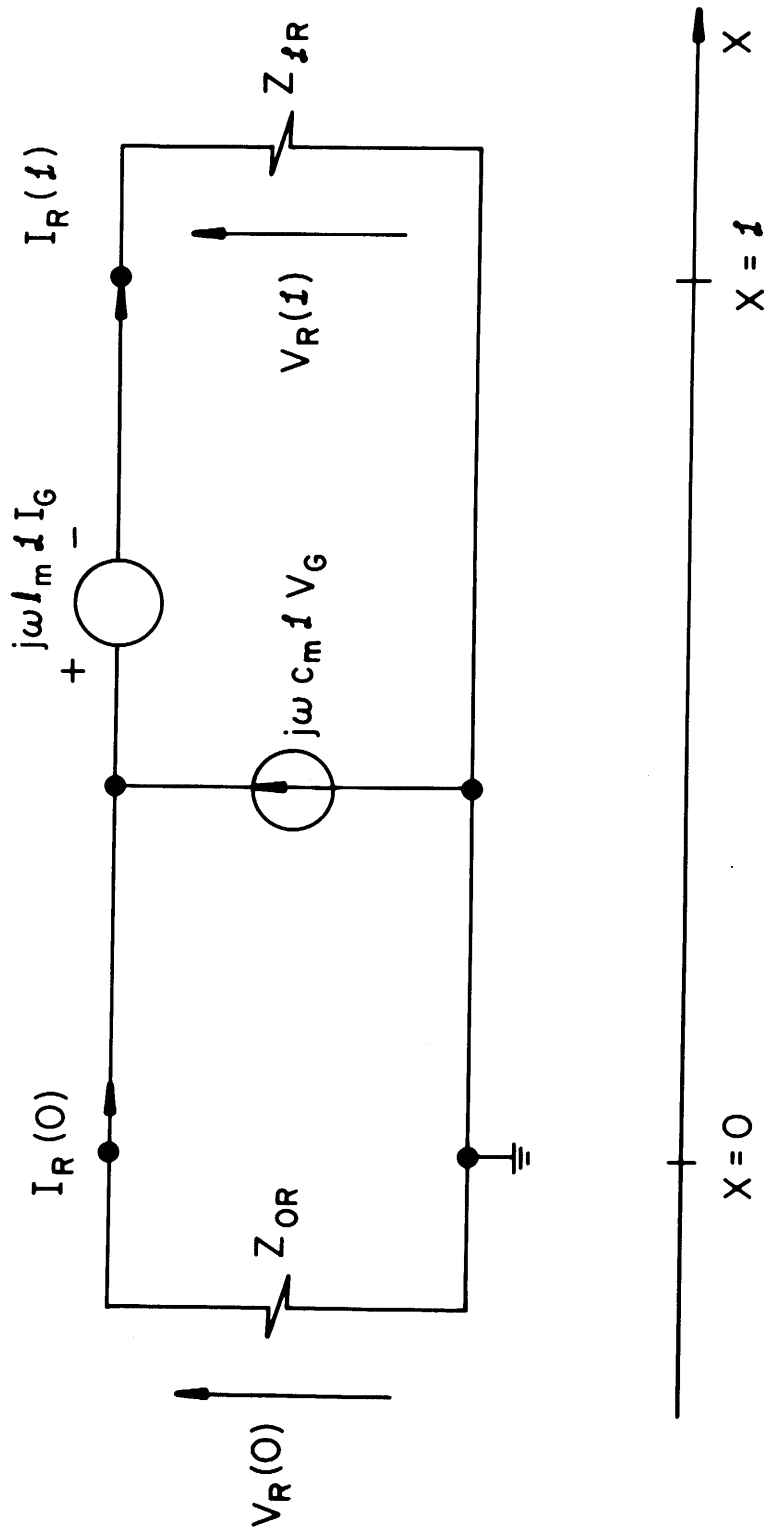

Figure 2-6. A lumped model of the receptor circuit.

$$V_R(\ell) = \frac{-j\omega \ell_m \ell \, Z_{\ell R}}{Z_{\ell R} + Z_{0R}} I_G + \frac{j\omega c_m \ell \, Z_{0R} \, Z_{\ell R}}{Z_{\ell R} + Z_{0R}} V_G \qquad (2\text{-}43a)$$

$$V_R(0) = \frac{j\omega \ell_m \ell \, Z_{0R}}{Z_{\ell R} + Z_{0R}} I_G + \frac{j\omega c_m \ell \, Z_{0R} \, Z_{\ell R}}{Z_{\ell R} + Z_{0R}} V_G \qquad (2\text{-}43b)$$

Since the line is assumed to be electrically short and the frequency is assumed to be sufficiently small, one may approximate the generator circuit voltage and current, V_G and I_G in (2-43) as

$$V_G \cong \frac{Z_{\ell G}}{Z_{0G} + Z_{\ell G}} V_s \qquad (2\text{-}44a)$$

$$I_G \cong \frac{1}{Z_{0G} + Z_{\ell G}} V_s \qquad (2\text{-}44b)$$

Substituting (2-44) into (2-43) yields the equations in (2-42).

From the low frequency approximation in (2-43), it is clear that there are two contributions to each receptor voltage; a term due to the mutual inductance, ℓ_m, which will be classified as an inductive coupling contribution and a term due to the mutual capacitance, c_m, which will be classified as a capacitive coupling contribution. The inductive and capacitive coupling contributions are in phase in $V_R(0)$ but are 180^o out of phase in $V_R(\ell)$. Clearly, the directional coupler effect will result if the inductive and capacitive coupling contributions in $V_R(\ell)$ are equal in magnitude.

Depending upon the values of $Z_{\ell G}$, Z_{0R}, $Z_{\ell R}$, ℓ_m and c_m, the inductive coupling contribution may dominate the capacitive coupling contribution and vice versa. The inductive coupling contribution dominates the capacitive coupling contribution in $V_R(\ell)$ in (2-42a) if

$$\ell_m >> c_m Z_{OR} Z_{\ell G} \tag{2-45}$$

which becomes (see(2-39) and (2-40))

$$Z_{CG} Z_{CR} >> Z_{OR} Z_{\ell G} \tag{2-46a}$$

or

$$\frac{Z_{CG}}{Z_{\ell G}} \quad \frac{Z_{CR}}{Z_{OR}} >> 1 \tag{2-46b}$$

Similarly in (2-42b), the inductive coupling dominates the capacitive coupling in $V_R(0)$ if

$$\frac{Z_{CG}}{Z_{\ell G}} \quad \frac{Z_{CR}}{Z_{\ell R}} >> 1 \tag{2-47}$$

Capacitive coupling dominates the inductive coupling when the above inequalities are reversed.

The above resolution of the receptor terminal voltages into inductive and capacitive coupling contributions is valid for a sufficiently small frequency. This concept has also been used in formulating other approximate prediction models for random cable bundles [4,5].

It may appear that (2-31), (2-33) and (2-36) would have the possibility of yielding reasonable bounds or estimates of the random cable bundle responses. However, it will be shown in Chapter III, that the presence of the parasitic wires in the cable bundle will nullify the directional coupler effect inherent in $V_R(\ell)$ in (2-31) as discussed above. In order that this model not underpredict the random cable bundle responses when the directional coupler effect is nullified by the parasitic wires, one may simply add the inductive and capacitive coupling contributions in $V_R(\ell)$ in (2-31).

The equation for $V_R(0)$ in (2-36) is unchanged. This result will be referred to as the BOUND model and the receptor terminal voltage equations become

$$V_R(\ell) = \frac{-jv\sin(\beta\ell)\ Z_{\ell R}}{\Delta} \{\ell_m + c_m\ Z_{\ell G}\ Z_{0R}\}\ V_s \qquad (2\text{-}48a)$$

$$V_R(0) = \frac{jv\sin(\beta\ell)\ Z_{0R}}{\Delta} \{\cos(\beta\ell)\ [\ell_m + c_m\ Z_{\ell R}\ Z_{\ell G}] \qquad (2\text{-}48b)$$

$$+ j\sin(\beta\ell)\ [Z_{\ell R}\ \ell_m\ (c_R + c_m) + Z_{\ell G}\ell_R\ c_m]\}\ V_s$$

where Δ is given by (2-33). The addition of the inductive and capacitive coupling contributions in $V_R(\ell)$ when they are in reality 180^o out of phase can be further justified since in many cases, the coupling is primarily due to only one of these contributions. In these cases, little error will result in the addition of the inductive and capacitive coupling contributions in $V_R(\ell)$. In cases where these contributions are of the same order of magnitude, the addition of the two contributions in $V_R(\ell)$ will yield a result which is larger than the actual result. The result for $V_R(0)$ is, of course, unchanged.

III. SENSITIVITY OF CABLE RESPONSES TO VARIATIONS IN WIRE POSITION

In order to thoroughly investigate the sensitivity of cable responses to variations in wire position, one should consider an almost unlimited number of wires in the cable and possible combinations of termination impedances, relative wire positions and wire sizes. Rather than considering some large combination, a specific cable bundle consisting of 13 wires will be investigated [6].

The cable configuration will consist of 13 identical #20 gauge wires. A cross-sectional view of the cable is shown in Figure 3-1(b).The wires are suspended above an infinite ground plane (the reference conductor for the line voltages). Wire #7 will be the generator wire and wires #1 and #13 will be the receptor wires. A one volt sinusoidal source (zero source impedance) drives the generator line at $x = 0$ as shown in Figure 3-2. The generator line is terminated at $x = \mathscr{L}$ in a resistance of R ohms. Both ends of the receptor wires (#1 and #13) are also terminated in a resistance of R ohms between the wire and the ground plane. The remaining wires, the parasitic wires, are terminated at both ends in a fixed resistance of either 50 Ω or 10K Ω.

The wires are in three layers, each layer being at a different height above the ground plane and the upper and lower layers of wires are above and below the middle layer a distance of Δh. The middle layer is at a fixed height of 1.2 cm. The wires have a horizontal separation of Δd. The wire separations will be varied by changing Δh and Δd and these cases are denoted by

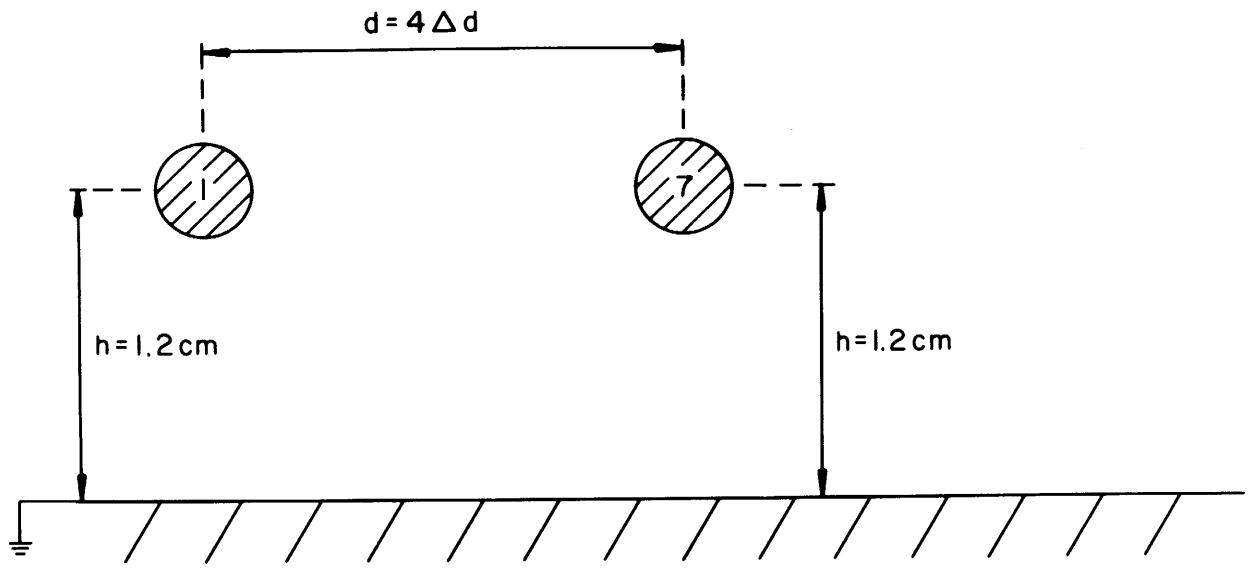

(a) Pair

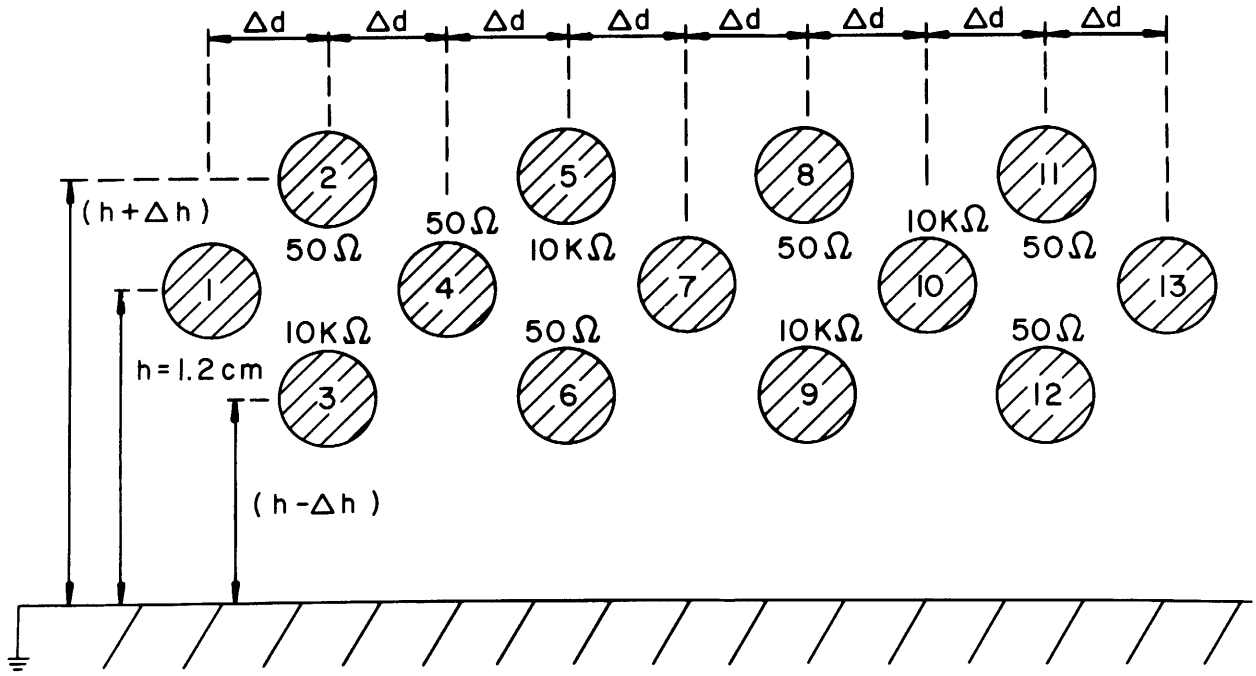

(b) 13 Wire

Figure 3-1. A cross section of the cable.

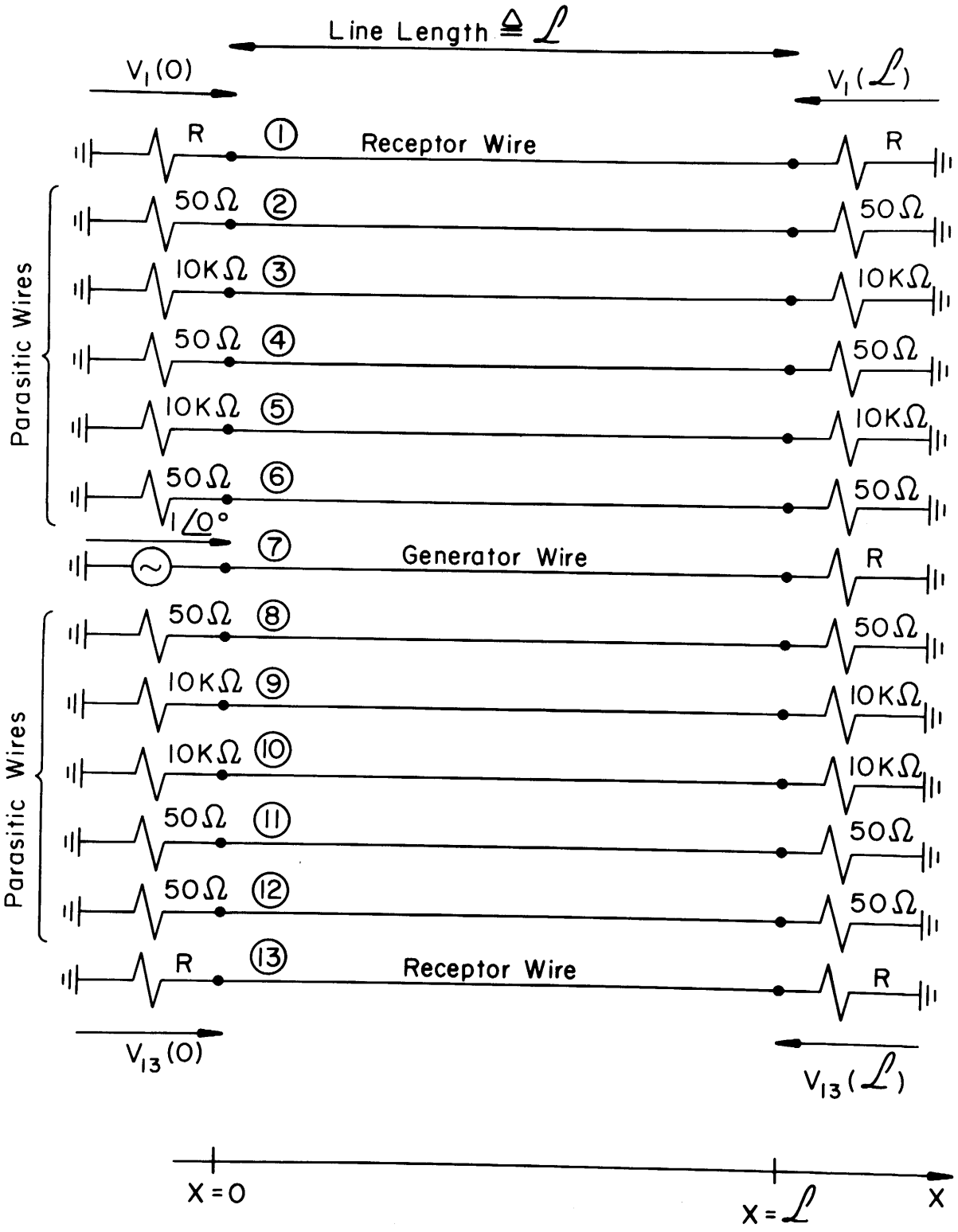

Figure 3-2. The load structure on the cable.

	Δd	Δh
Initial	.175 cm	.3 cm
30%	.1225 cm	.21 cm
40%	.105 cm	.18 cm
50%	.0875 cm	.15 cm

where, for example, 40% means that the horizontal (Δd) and vertical (Δh) wire separations have been reduced by 40% from their initial values.

The value of the resistance, R, which terminates the generator wire (#7) and both ends of the receptor wires (#1 and #13) will be varied from 10Ω to 10,000Ω for the various wire positions to determine the effect of the impedance levels on the sensitivity of the cable responses to relative wire position.

The effect of parasitic wires on the coupling between two wires in the bundle will also be investigated by comparing the coupling between wire #7 and wire #1 with the parasitic wires and wire #13 removed (designated by PAIR and shown in Figure 3-1(a)) to the coupling between wire #7 and wire #1 with all wires present (designated by 13 WIRE and shown in Figure 3-1(b)).

3.1 The Multiconductor Transmission Line Model and the BOUND Model

The multiconductor transmission line (MTL) model described in Section 2.1 will be used to investigate the cable coupling sensitivities in this Chapter. In Chapter IV, experimental results for this cable bundle will also be obtained. In this Chapter, the wires are considered to be bare (no dielectric insulations). Dielectric insulations will surround each wire in the experimental investigation of this cable bundle in Chapter IV.

Since the wires are considered to be bare, the MTL model as well as

the per-unit-length parameters become particularly simple. The MTL equations in (2-14a) and (2-14b) become, by substituting the matrix chain parameters for the homogeneous case given in Section 3.1 of reference [1][1],

$$[\cos(\beta\ell)\ \{\underset{\sim}{Z}_0 + \underset{\sim}{Z}_\ell\} + j\sin(\beta\ell)\ \{\underset{\sim}{Z}_C + \underset{\sim}{Z}_\ell \underset{\sim}{Z}_C^{-1} \underset{\sim}{Z}_0\}\ ]\ \underline{I}(0) = -\underline{V}_\ell + [j\sin(\beta\ell)\ \underset{\sim}{Z}_\ell \underset{\sim}{Z}_C^{-1} + \cos(\beta\ell)\ \underset{\sim}{1}_n]\ \underline{V}_0 \qquad (3\text{-}1a)$$

$$\underline{I}(\ell) = -j\sin(\beta\ell)\ \underset{\sim}{Z}_C^{-1} \underline{V}_0 + [\cos(\beta\ell)\ \underset{\sim}{1}_n + j\sin(\beta\ell)\ \underset{\sim}{Z}_C^{-1} \underset{\sim}{Z}_0]\ \underline{I}(0) \qquad (3\text{-}1b)$$

The wave number is given by [1]

$$\beta = \frac{2\pi}{\lambda} \qquad (3\text{-}2)$$

where a wavelength is given by $\lambda = v/f$, f is the frequency of excitation and v is the velocity of light in the surrounding medium (free space), $v \cong 3\times10^8$ m/sec.

The entries in the termination impedance matrices, $\underset{\sim}{Z}_0$ and $\underset{\sim}{Z}_\ell$, and the source voltage vectors, $\underline{V}_0$ and $\underline{V}_\ell$, are obtained from Figure 3-2. The entries in the characteristic impedance matrix, $\underset{\sim}{Z}_C$, are given by [1,6].

$$[\underset{\sim}{Z}_C]_{ii} = v[\underset{\sim}{L}]_{ii} = v\frac{\mu_v}{2\pi}\ \ell n\left(\frac{2h_i}{r_{wi}}\right) \qquad (3\text{-}3a)$$

$$[\underset{\sim}{Z}_C]_{\substack{ij \\ i\neq j}} = v[\underset{\sim}{L}]_{\substack{ij \\ i\neq j}} = v\frac{\mu_v}{2\pi}\ \ell n\left(\frac{\sqrt{d_{ij}^2 + 4h_i h_j}}{d_{ij}}\right) \qquad (3\text{-}3b)$$

---

[1] Observe that no incident electromagnetic fields illuminate the line. Therefore $\hat{\underline{V}}_s(\ell)$ and $\hat{\underline{I}}_s(\ell)$ are removed from (2-14). In addition, the wires and the ground plane are considered to be perfect conductors.

for i, j=1, ---, 13 where $\mu_v = 4\pi x10^{-7}$, v is the velocity of light in free space ($v \tilde{=} 3x10^8$ m/sec), h_i is the height of the i-th wire above ground, and d_{ij} is the center-to-center separation of the i-th and j-th wires. Equations (3-1) and (3-3) were programmed on an IBM 370/165 digital computer in double precision arithmetic. A description of the program, XTALK, a program listing and a users manual are contained in Volume VII of this series [7].

Note that equations (3-1) show that since the line is immersed in a homogeneous medium (free space), the line responses are independent of line length and are dependent only on $\beta\mathcal{L} = 2\pi\mathcal{L}/\lambda$, i.e., the responses at each frequency are dependent only upon the portion of a wavelength that the line occupies. The computed results will therefore be plotted in terms of $\mathcal{L} = k\lambda$.

The BOUND model is described in Section 2.2. It should again be noted that one of the fundamental assumptions in this model is that only the generator and receptor wires are considered and the effect of all other wires in the bundle (the parasitic wires) are not considered. For example, when computing the coupling between wire #7 and wire #1, all other wires (#2 - #6, #8 - #13) are removed from the bundle (PAIR). The self inductances of the generator and receptor circuits, ℓ_G and ℓ_R, mutual inductance, ℓ_m, self capacitances of the generator and receptor circuits, c_G and c_R, and mutual capacitance, c_m, in the BOUND model are given by [1]

$$\ell_G = \frac{\mu_v}{2\pi} \ell n\left(\frac{2h_G}{r_{wG}}\right) \qquad (3\text{-}4a)$$

$$\ell_R = \frac{\mu_v}{2\pi} \ell n\left(\frac{2h_R}{r_{wR}}\right) \qquad (3\text{-}4b)$$

$$\ell_m = \frac{\mu_v}{2\pi} \ell n\left(\frac{\sqrt{d_{GR}^2 + 4h_G h_R}}{d_{GR}}\right) \qquad (3\text{-}4c)$$

$$c_G + c_m = \mu_v \varepsilon_v \ell_R / (\ell_G \ell_R - \ell_m^2) \qquad (3\text{-}4d)$$

$$c_R + c_m = \mu_v \varepsilon_v \ell_G / (\ell_G \ell_R - \ell_m^2) \qquad (3\text{-}4e)$$

$$c_m = \mu_v \varepsilon_v \ell_m / (\ell_G \ell_R - \ell_m^2) \qquad (3\text{-}4f)$$

where h_G and h_R are the heights of the generator (#7) and receptor (#1) wires above the ground plane, respectively; r_{wG} and r_{wR} are the radii of the generator and receptor wires, respectively; d_{GR} is the center-to-center separation between the generator and receptor wires, and ε_v is the permittivity of free space ($\varepsilon_v \cong (1/36\pi) \times 10^{-9}$). The BOUND model is extremely simple to program on a digital computer.

3.2 Sensitivity of the Cable Responses to Wire Position and Effect of Parasitic Wires as a Function of Impedance Levels

In this section, we will investigate the sensitivity of the cable responses to wire position as a function of impedance level by varying the resistance, R, which terminates the generator wire(#7) and both ends of the receptor wires (#1 and #13) in Figure 3-2. The 50 Ω and 10K Ωresistances on the ends of the parasitic wires in Figure 3-2 will be unchanged. The induced signal at the ends of receptor wire #1 ($V_1(0)$ and $V_1(\ell)$) will be plotted with R varied from 10 Ω to 10K Ω. Four such results will be obtained in terms of line length as a portion of a wavelength, i.e., $\ell = 10^{-4}\lambda$, $\ell = 10^{-3}\lambda$, $\ell = 10^{-2}\lambda$, $\ell = 10^{-1}\lambda$. One might expect rather extreme sentivities to be uncovered when the cable is not electrically short, e.g., $\ell > 10^{-2}\lambda$, since standing waves occur on the line for this range of frequencies.[1] However, it is not generally known that large sensitivities can exist even when a cable is electrically short, e.g., $\ell \leq 10^{-2}\lambda$. The results

[1] Technically, standing waves are always present. However, for electrically long lines, their effects are more pronounced.

of the MTL model with all wires present (13 WIRE), the MTL model with only wires #1 and #7 present and the other wires removed (PAIR), and the BOUND model (PAIR, BOUND) will be shown.

The results are shown in Figure 3-3 through Figure 3-6. Note in Figure 3-3(b), 3-4(b), 3-5(b) and 3-6(b) that the directional coupler effects are evident in the PAIR, $V_1(\ell)$ results. $V_1(\ell)$ has a deep null at approximately R = 230 Ω. Since the wires are identical and are at the same height, the characteristic impedances of each circuit in the presence of the other given in (2-40) are identical and are equal to 232.5 Ω. Thus the condition for a directional coupler, (2-39), is satisfied. Note that for this special case, the PAIR results are not worst case, i.e., the 13 WIRE response is larger than the PAIR response. However, note that the BOUND model does provide an upper bound. This is due to the fact that in the BOUND model, the capacitive and inductive coupling contributions are added in $V_R(\ell)$.

As for the effect of the parasitic wires on the coupling between a generator wire and a receptor wire, there is a marked effect, on the order of 30dB or more, for "high impedance loads", i.e., R > 230Ω, and virtually no effect for "low impedance loads", i.e., R < 230Ω.[1]

The sensitivity to variations in wire position can be extraordinarily large for high impedance loads, R > 230 Ω. Note in Figure 3-3(a) that $\ell = 10^{-4}\lambda$, i.e., the cable is very short, electrically. However, for R ≅ 1200 Ω, increasing or decreasing the wire separations by only 10% (from 40% to 50% and from 30% to 40%) results in a change in the $V_1(0)$ response

---

[1] The ratio of two voltage quantities, V_A and V_B, will be expressed in dB as

$$(V_A/V_B)_{dB} = 20 \log_{10} (V_A/V_B)$$

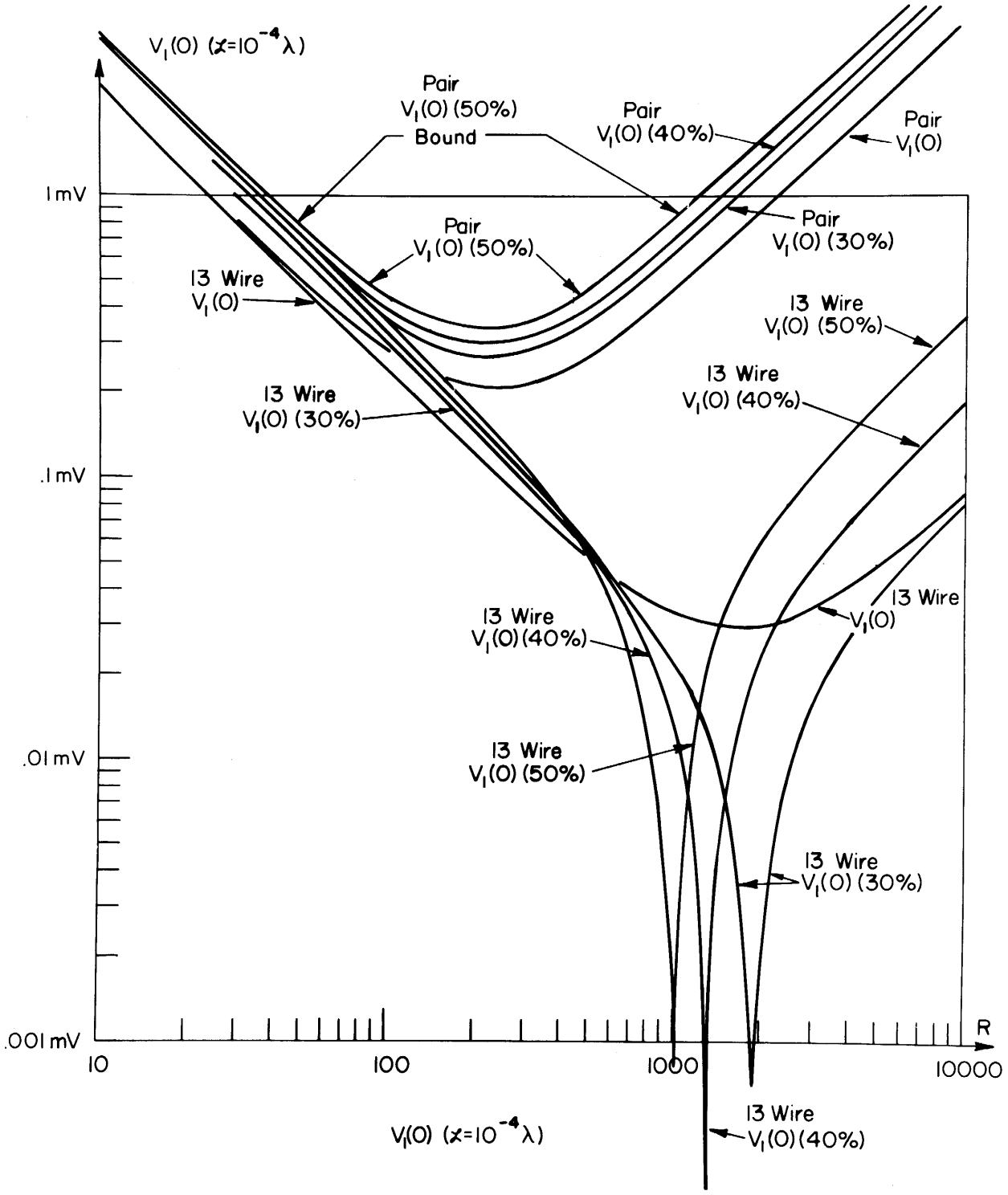
$V_1(0)$ ($x=10^{-4}\lambda$)
Pair
$V_1(0)$ (50%)
Bound
Pair
$V_1(0)$ (40%)
Pair
$V_1(0)$
1 mV
Pair
$V_1(0)$ (50%)
Pair
$V_1(0)$ (30%)
13 Wire
$V_1(0)$
13 Wire
$V_1(0)$ (50%)
13 Wire
$V_1(0)$ (40%)
13 Wire
$V_1(0)$ (30%)
.1 mV
13 Wire
$V_1(0)$
13 Wire
$V_1(0)$ (40%)
13 Wire
$V_1(0)$ (40%)
.01 mV
13 Wire
$V_1(0)$ (50%)
13 Wire
$V_1(0)$ (30%)
.001 mV
R
10
100
1000
10000
$V_1(0)$ ($x=10^{-4}\lambda$)
13 Wire
$V_1(0)$ (40%)

Figure 3-3(a).

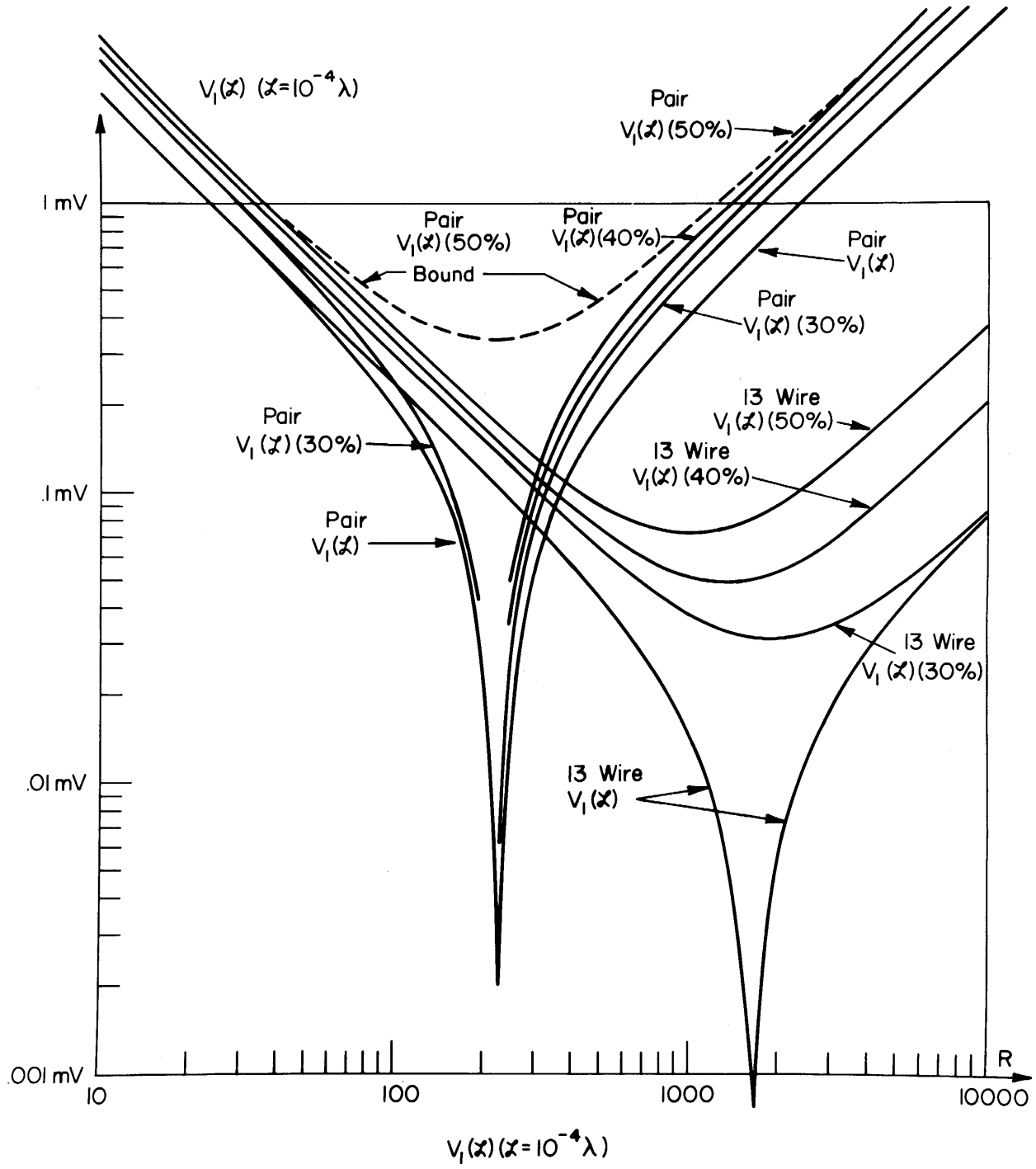
$V_1(\mathcal{X})$ $(\mathcal{X}=10^{-4}\lambda)$
Pair
$V_1(\mathcal{X})$ (50%)
1 mV
Pair
$V_1(\mathcal{X})$ (50%)
Bound
Pair
$V_1(\mathcal{X})$ (40%)
Pair
$V_1(\mathcal{X})$
Pair
$V_1(\mathcal{X})$ (30%)
13 Wire
$V_1(\mathcal{X})$ (50%)
Pair
$V_1(\mathcal{X})$ (30%)
13 Wire
$V_1(\mathcal{X})$ (40%)
.1 mV
Pair
$V_1(\mathcal{X})$
13 Wire
$V_1(\mathcal{X})$ (30%)
.01 mV
13 Wire
$V_1(\mathcal{X})$
.001 mV
10
100
1000
10000
R
$V_1(\mathcal{X})$ $(\mathcal{X}=10^{-4}\lambda)$

Figure 3-3(b).

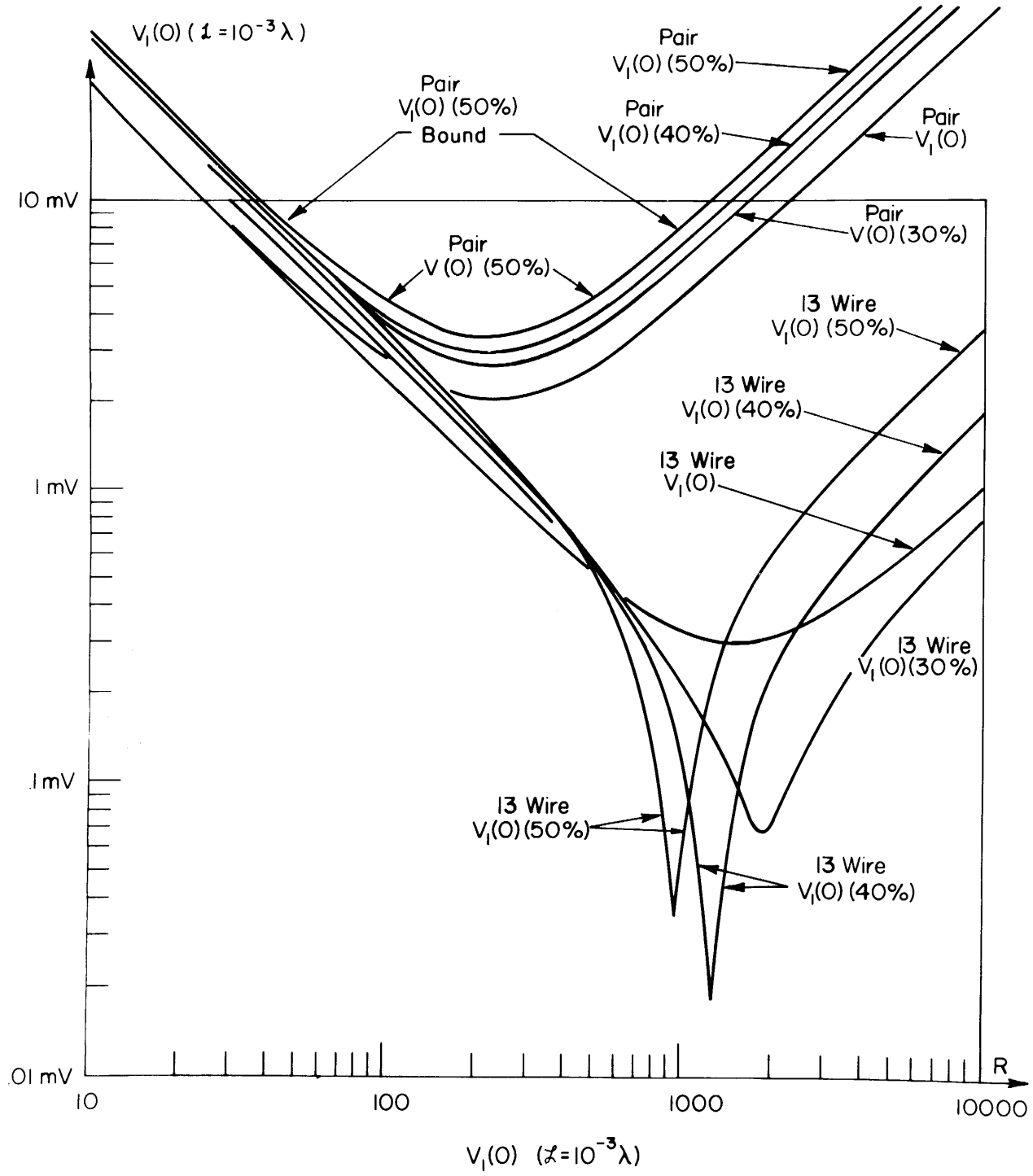
$V_1(0)$ ($\lambda = 10^{-3}\lambda$)
Pair
$V_1(0)$ (50%)
Pair
$V_1(0)$ (50%)
Bound
Pair
$V_1(0)$ (40%)
Pair
$V_1(0)$
10 mV
Pair
V(0) (30%)
Pair
V (0) (50%)
13 Wire
$V_1(0)$ (50%)
13 Wire
$V_1(0)$ (40%)
1 mV
13 Wire
$V_1(0)$
13 Wire
$V_1(0)$ (30%)
.1 mV
13 Wire
$V_1(0)$ (50%)
13 Wire
$V_1(0)$ (40%)
.01 mV
R
10
100
1000
10000
$V_1(0)$ ($\lambda = 10^{-3}\lambda$)

Figure 3-4(a).

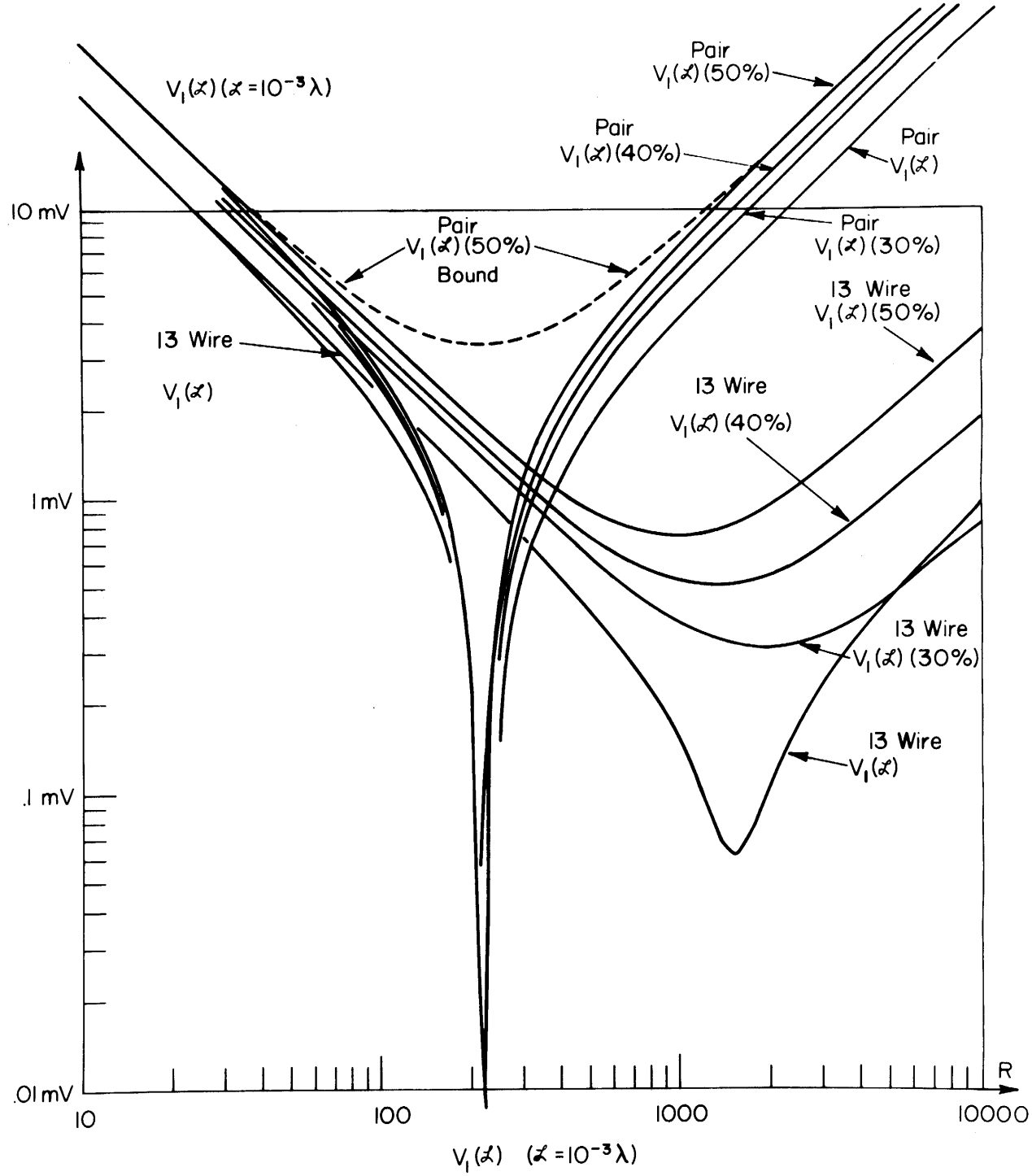
$V_1(\mathcal{L})$ ($\mathcal{L} = 10^{-3}\lambda$)
Pair
$V_1(\mathcal{L})$ (50%)
Pair
$V_1(\mathcal{L})$ (40%)
Pair
$V_1(\mathcal{L})$
10 mV
Pair
$V_1(\mathcal{L})$ (50%)
Bound
Pair
$V_1(\mathcal{L})$ (30%)
13 Wire
$V_1(\mathcal{L})$ (50%)
13 Wire
$V_1(\mathcal{L})$
13 Wire
$V_1(\mathcal{L})$ (40%)
1 mV
13 Wire
$V_1(\mathcal{L})$ (30%)
13 Wire
$V_1(\mathcal{L})$
.1 mV
.01 mV
R
10
100
1000
10000
$V_1(\mathcal{L})$ ($\mathcal{L} = 10^{-3}\lambda$)

Figure 3-4 (b).

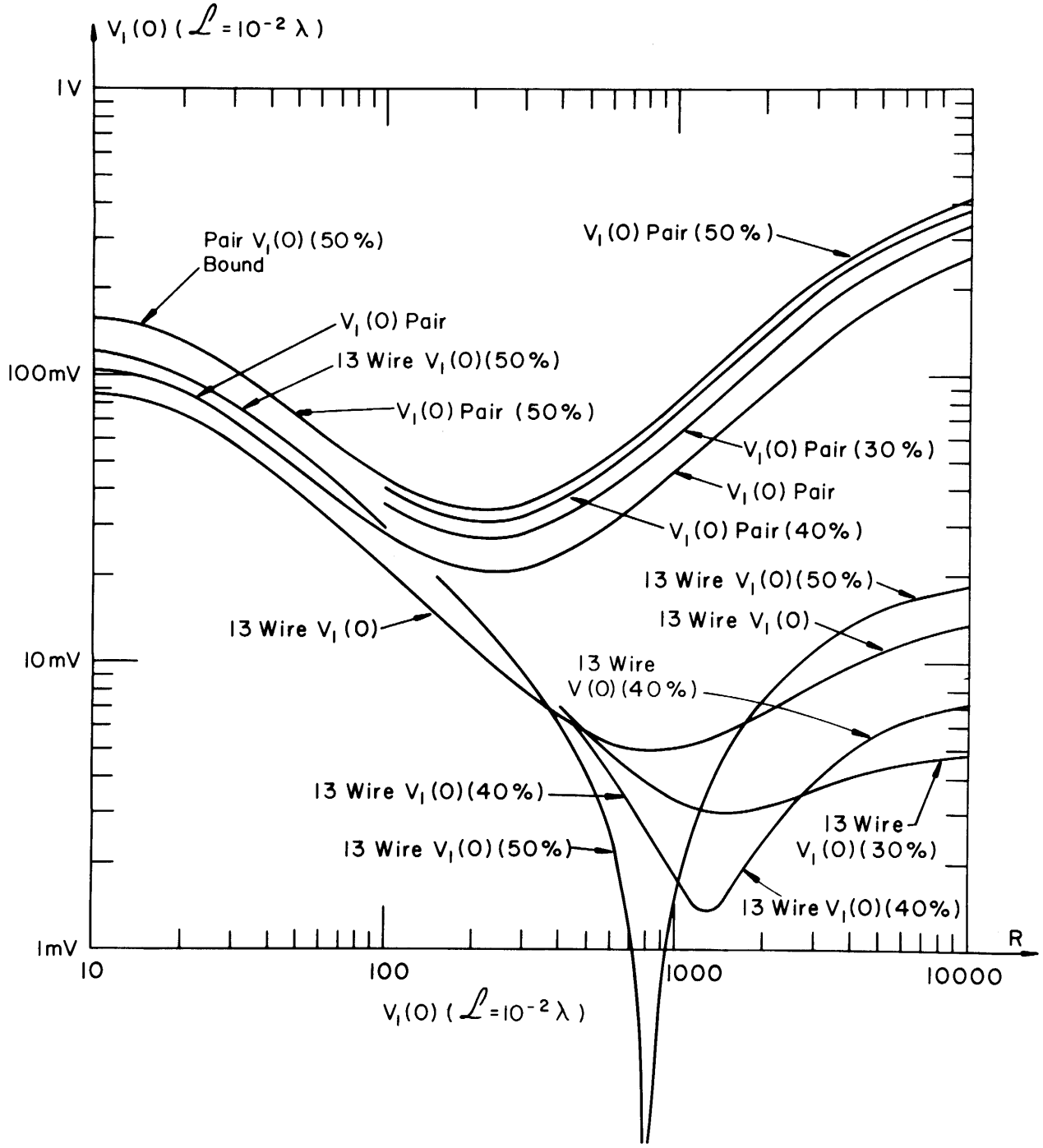
$V_1(0)$ ($\mathcal{L}=10^{-2}\lambda$)
1V
100mV
10mV
1mV
10
100
1000
10000
R
$V_1(0)$ ($\mathcal{L}=10^{-2}\lambda$)
Pair $V_1(0)$ (50%) Bound
$V_1(0)$ Pair
13 Wire $V_1(0)$(50%)
$V_1(0)$ Pair (50%)
$V_1(0)$ Pair (50%)
$V_1(0)$ Pair (30%)
$V_1(0)$ Pair
$V_1(0)$ Pair (40%)
13 Wire $V_1(0)$(50%)
13 Wire $V_1(0)$
13 Wire $V_1(0)$
13 Wire V (0) (40%)
13 Wire $V_1(0)$(40%)
13 Wire $V_1(0)$(50%)
13 Wire $V_1(0)$(30%)
13 Wire $V_1(0)$(40%)

Figure 3-5(a).

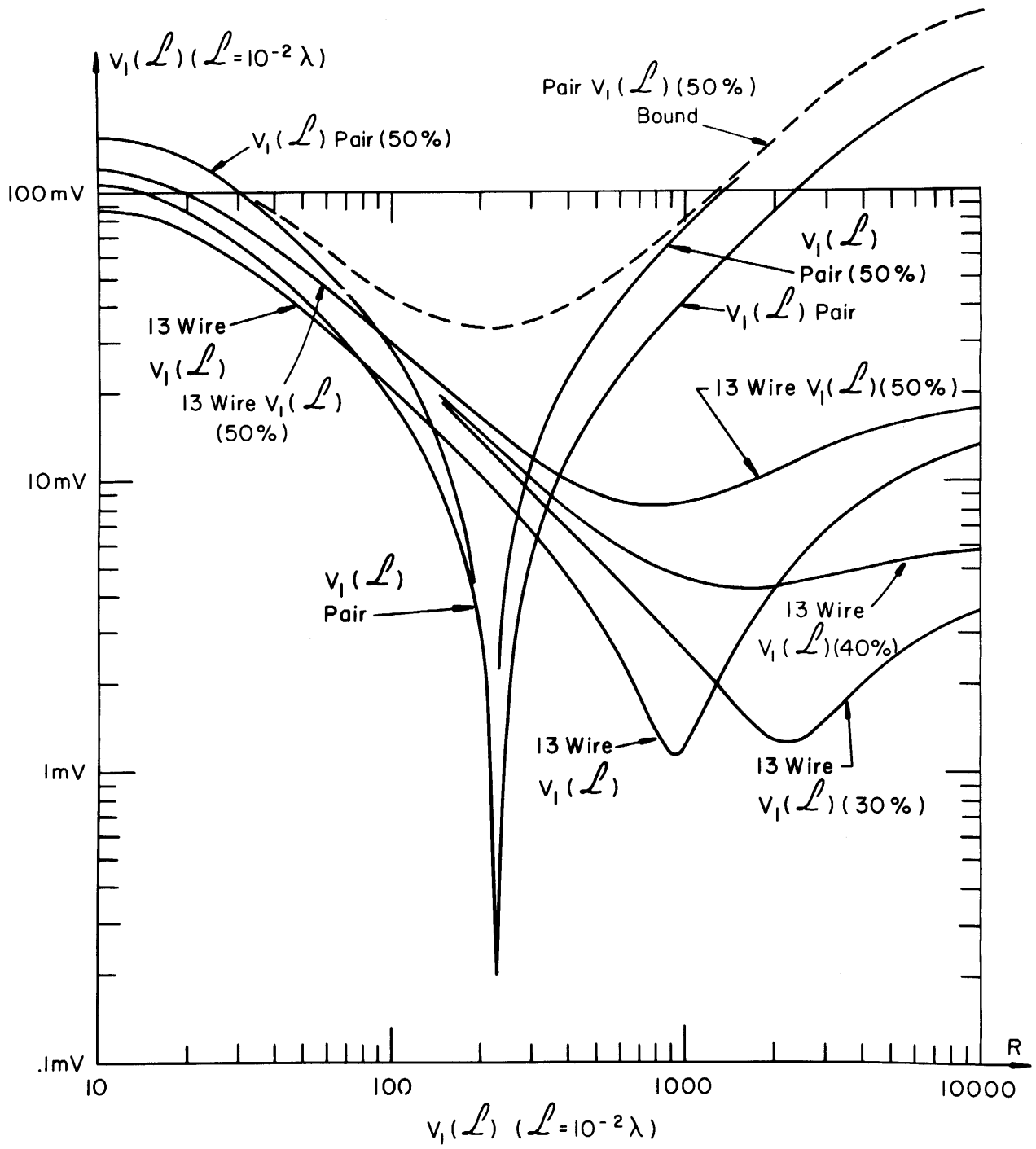
$V_1(\mathcal{L})$ ($\mathcal{L}=10^{-2}\lambda$)
Pair $V_1(\mathcal{L})$ (50%) Bound
$V_1(\mathcal{L})$ Pair (50%)
100mV
$V_1(\mathcal{L})$ Pair (50%)
13 Wire $V_1(\mathcal{L})$ (50%)
$V_1(\mathcal{L})$ Pair
13 Wire $V_1(\mathcal{L})$
13 Wire $V_1(\mathcal{L})$ (50%)
10mV
$V_1(\mathcal{L})$ Pair
13 Wire $V_1(\mathcal{L})$ (40%)
13 Wire $V_1(\mathcal{L})$
13 Wire $V_1(\mathcal{L})$ (30%)
1mV
.1mV
R
10
100
1000
10000
$V_1(\mathcal{L})$ ($\mathcal{L}=10^{-2}\lambda$)

Figure 3-5(b).

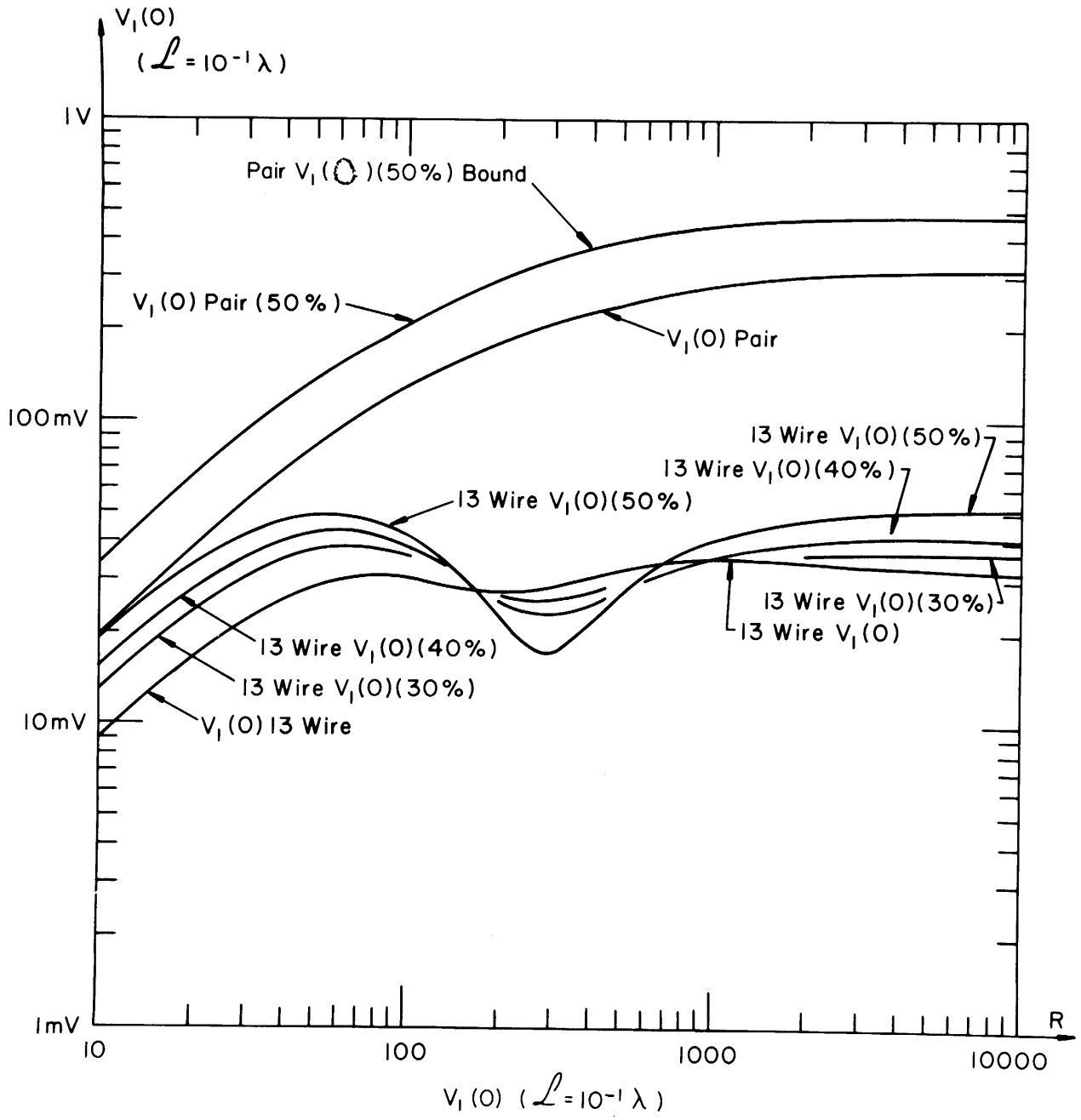
$V_1(0)$
($\ell = 10^{-1}\lambda$)
1V
100mV
10mV
1mV
Pair $V_1(0)$ (50%) Bound
$V_1(0)$ Pair (50%)
$V_1(0)$ Pair
13 Wire $V_1(0)$ (50%)
13 Wire $V_1(0)$ (40%)
13 Wire $V_1(0)$ (50%)
13 Wire $V_1(0)$ (30%)
13 Wire $V_1(0)$
13 Wire $V_1(0)$ (40%)
13 Wire $V_1(0)$ (30%)
$V_1(0)$ 13 Wire
10
100
1000
10000
R
$V_1(0)$ ($\ell = 10^{-1}\lambda$)

Figure 3-6(a).

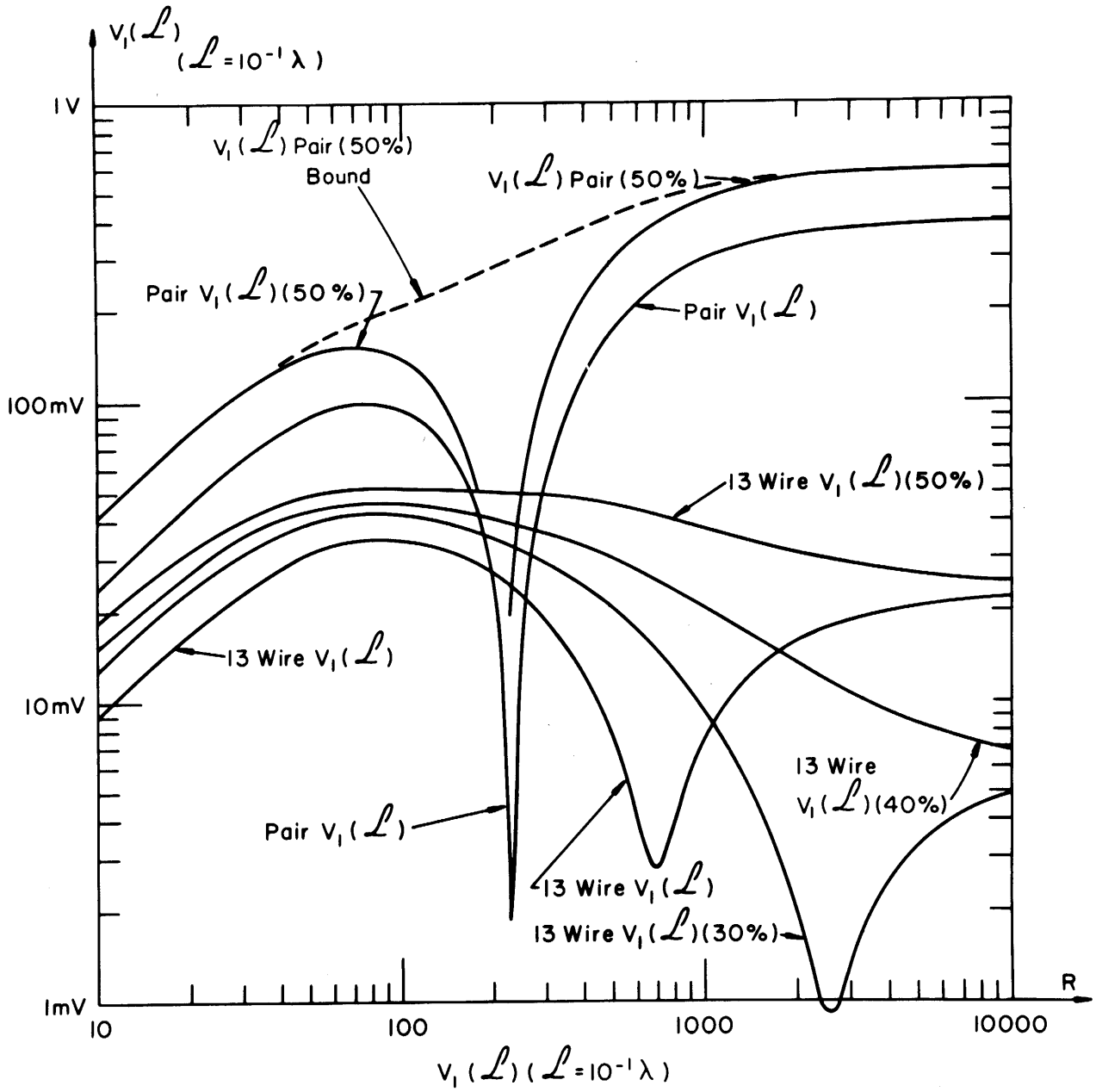
$V_1(\mathcal{L})$
$(\mathcal{L}=10^{-1}\lambda)$
1V
100mV
10mV
1mV
$V_1(\mathcal{L})$ Pair (50%) Bound
$V_1(\mathcal{L})$ Pair (50%)
Pair $V_1(\mathcal{L})$ (50%)
Pair $V_1(\mathcal{L})$
13 Wire $V_1(\mathcal{L})$ (50%)
13 Wire $V_1(\mathcal{L})$
13 Wire
$V_1(\mathcal{L})$ (40%)
Pair $V_1(\mathcal{L})$
13 Wire $V_1(\mathcal{L})$
13 Wire $V_1(\mathcal{L})$ (30%)
R
10
100
1000
10000
$V_1(\mathcal{L})$ $(\mathcal{L}=10^{-1}\lambda)$

Figure 3-6(b).

(13 WIRE, all wires present) of as much as 40dB or more(the null at R = 1200Ω for 13 wire, $V_1(0)$ (40%) is very deep). Thus at this frequency, we have a type of high impedance directional coupler. On the other hand, the PAIR results do not appear to be sensitive to wire position except in the range of R for which the directional coupler effect takes place (around R = 230Ω).

The complete frequency response for $\ell = 10^{-3}\lambda$ to $\ell = \lambda$ for fixed values of R is shown in Figure 3-7 through 3-12. These data show, as frequency is varied, the sensitivities and effects of the parasitic wires uncovered in Figure 3-3 through 3-6. All responses are plotted up to $\ell = .5\lambda$ since the responses repeat this pattern between $.5\lambda$ and λ, λ and 1.5λ, ---, etc.

Note that Figure 3-9 clearly shows that the parasitic wires will nullify the directional coupler effect associated with the isolated generator and receptor circuits.

For low impedance loads, R = 50 Ω, in Figure 3-10, the cable responses clearly are virtually insensitive to wire position. In addition, the parasitic wires have virtually no effect on the coupling between the generator and receptor wires.

In Figure 3-11, we compare $V_1(\ell)$ and $V_{13}(\ell)$, the voltages at the same end of wires #1 and #13. Note in Figure 3-1 that the line structure is physically symmetric about the center of the bundle. If the load structure were symmetric, $V_1(\ell)$ and $V_{13}(\ell)$ would be identical. The load structure on the parasitic wires is not quite symmetric about a vertical line through the midpoint of the wire bundle, wire #7. Note, however, in Figure 3-11 for R = 50Ω (low impedance loads on #1, #7, #13) that $V_1(\ell)$ and $V_{13}(\ell)$ are almost identical. This again shows that for low impedance loads on the

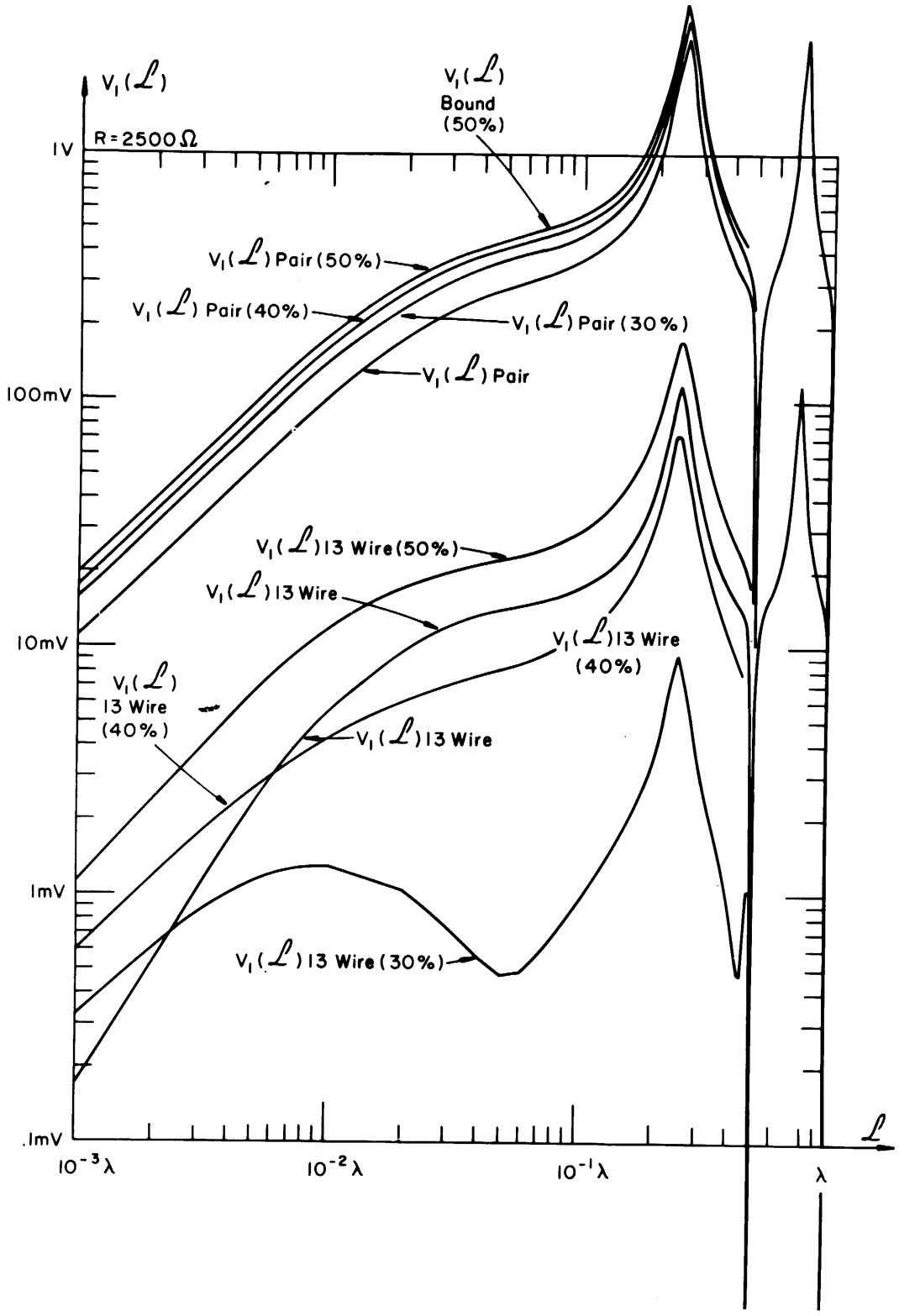
$V_1(\ell)$
R = 2500 Ω
1V
100mV
10mV
1mV
.1mV
$V_1(\ell)$ Bound (50%)
$V_1(\ell)$ Pair (50%)
$V_1(\ell)$ Pair (40%)
$V_1(\ell)$ Pair (30%)
$V_1(\ell)$ Pair
$V_1(\ell)$ 13 Wire (50%)
$V_1(\ell)$ 13 Wire
$V_1(\ell)$ 13 Wire (40%)
$V_1(\ell)$ 13 Wire (40%)
$V_1(\ell)$ 13 Wire
$V_1(\ell)$ 13 Wire (30%)
$10^{-3}\lambda$
$10^{-2}\lambda$
$10^{-1}\lambda$
λ
ℓ

Figure 3-7.

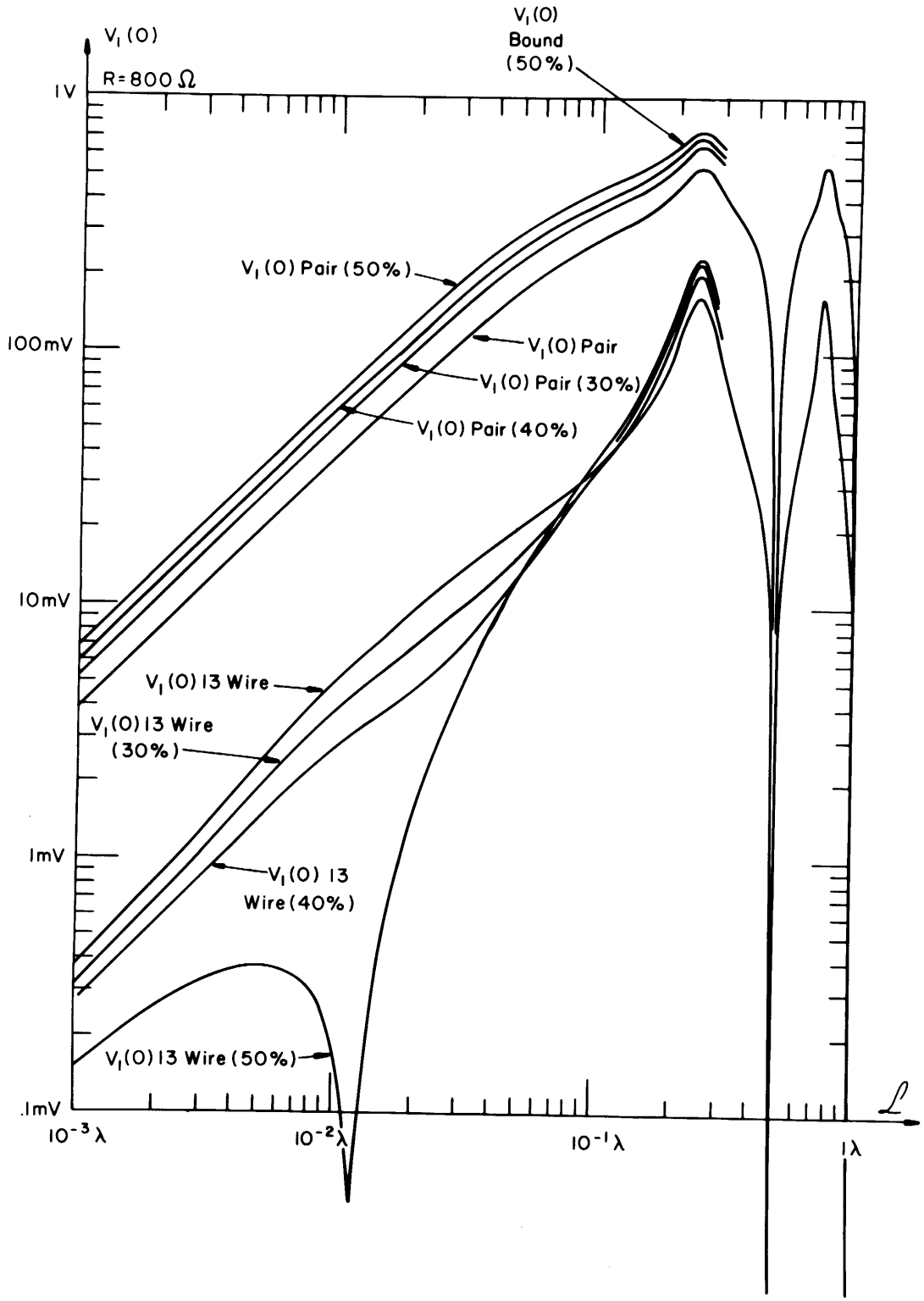
$V_1(0)$
R=800 Ω
1V
100mV
10mV
1mV
.1mV
$V_1(0)$ Bound (50%)
$V_1(0)$ Pair (50%)
$V_1(0)$ Pair
$V_1(0)$ Pair (30%)
$V_1(0)$ Pair (40%)
$V_1(0)$ 13 Wire
$V_1(0)$ 13 Wire (30%)
$V_1(0)$ 13 Wire (40%)
$V_1(0)$ 13 Wire (50%)
$10^{-3}\lambda$
$10^{-2}\lambda$
$10^{-1}\lambda$
1λ
ℓ

Figure 3-8.

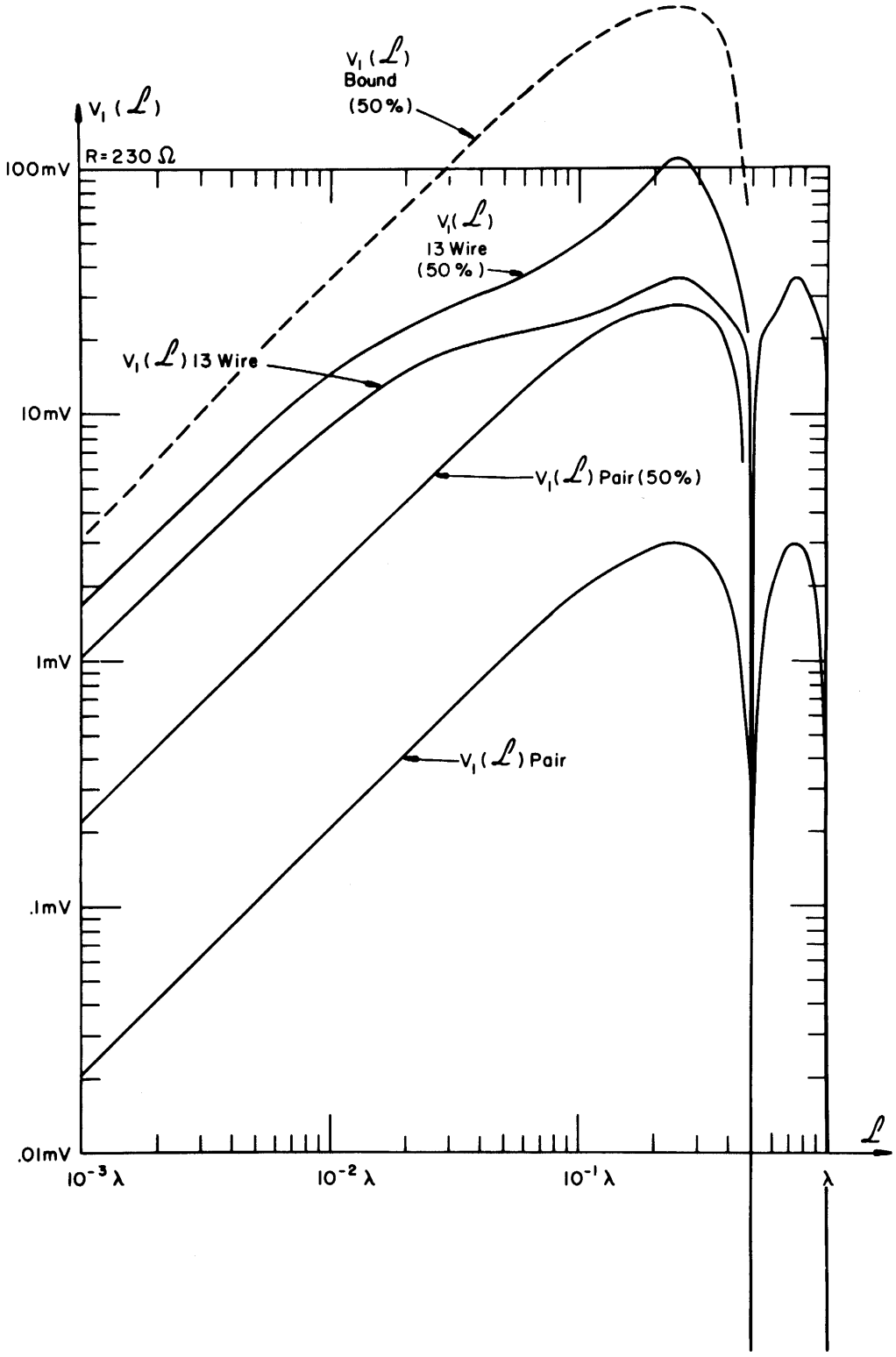
$V_1(\ell)$ Bound (50%)
$V_1(\ell)$
R = 230 Ω
100mV
$V_1(\ell)$ 13 Wire (50%)
$V_1(\ell)$ 13 Wire
10mV
$V_1(\ell)$ Pair (50%)
1mV
$V_1(\ell)$ Pair
.1mV
.01mV
$10^{-3}\lambda$
$10^{-2}\lambda$
$10^{-1}\lambda$
λ
ℓ

Figure 3-9.

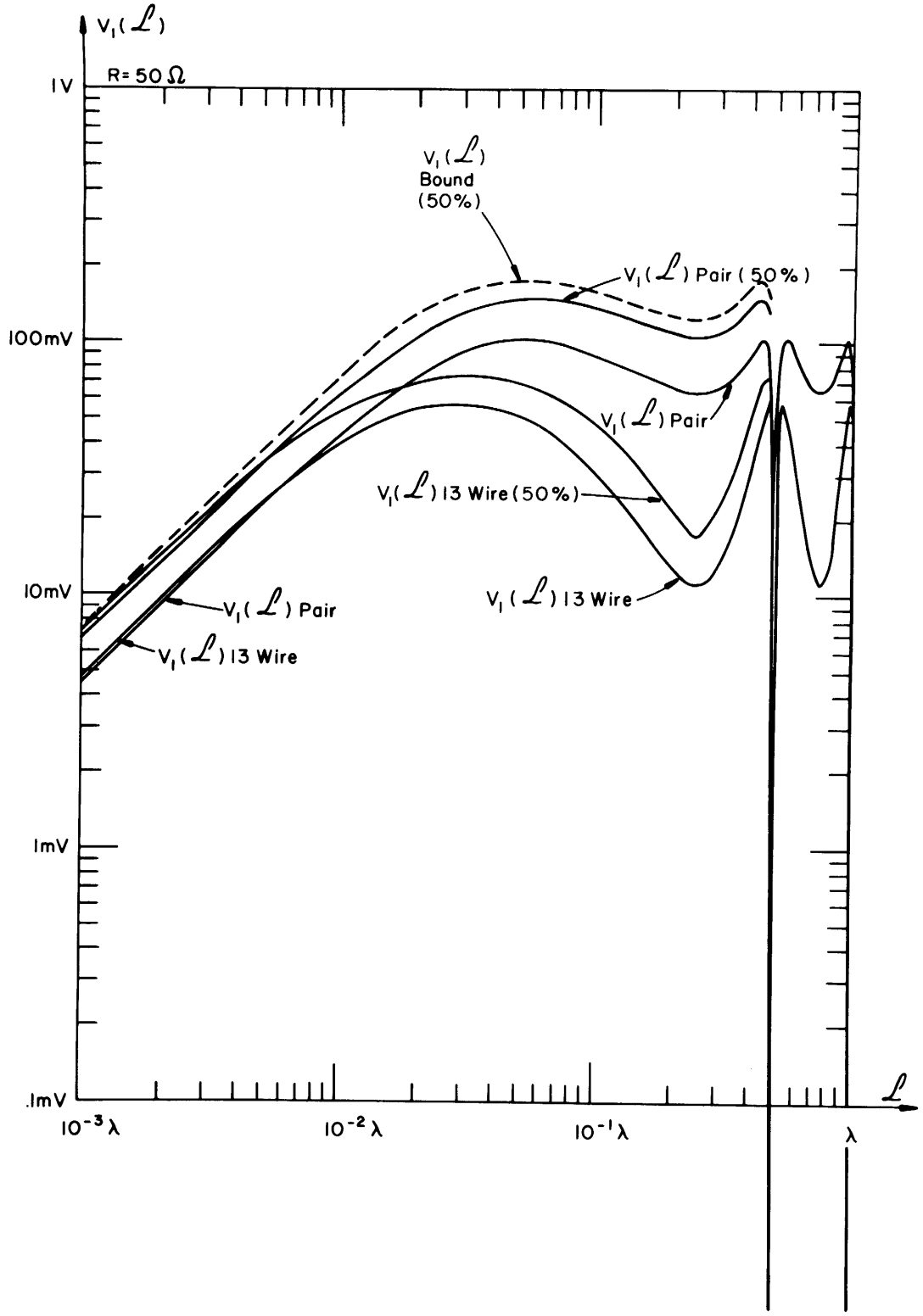
$V_1(\ell)$
R= 50 Ω
1V
100mV
10mV
1mV
.1mV
$V_1(\ell)$ Bound (50%)
$V_1(\ell)$ Pair (50%)
$V_1(\ell)$ Pair
$V_1(\ell)$ 13 Wire (50%)
$V_1(\ell)$ 13 Wire
$V_1(\ell)$ Pair
$V_1(\ell)$ 13 Wire
$10^{-3}\lambda$
$10^{-2}\lambda$
$10^{-1}\lambda$
λ
ℓ

Figure 3-10.

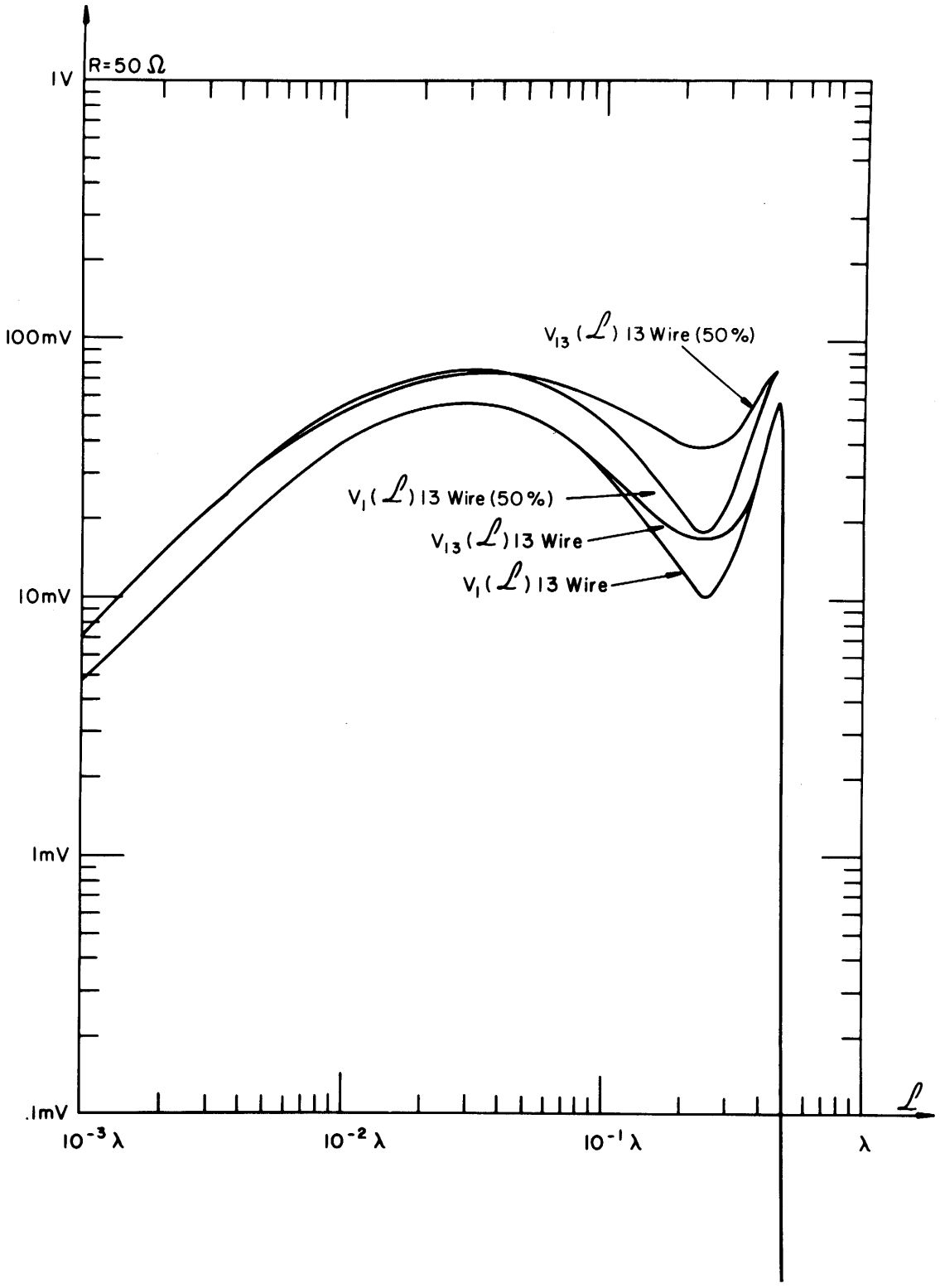
R=50 Ω
1V
100mV
10mV
1mV
.1mV
$V_{13}(\ell)$ 13 Wire (50%)
$V_1(\ell)$ 13 Wire (50%)
$V_{13}(\ell)$ 13 Wire
$V_1(\ell)$ 13 Wire
$10^{-3}\lambda$
$10^{-2}\lambda$
$10^{-1}\lambda$
λ
ℓ

Figure 3-11.

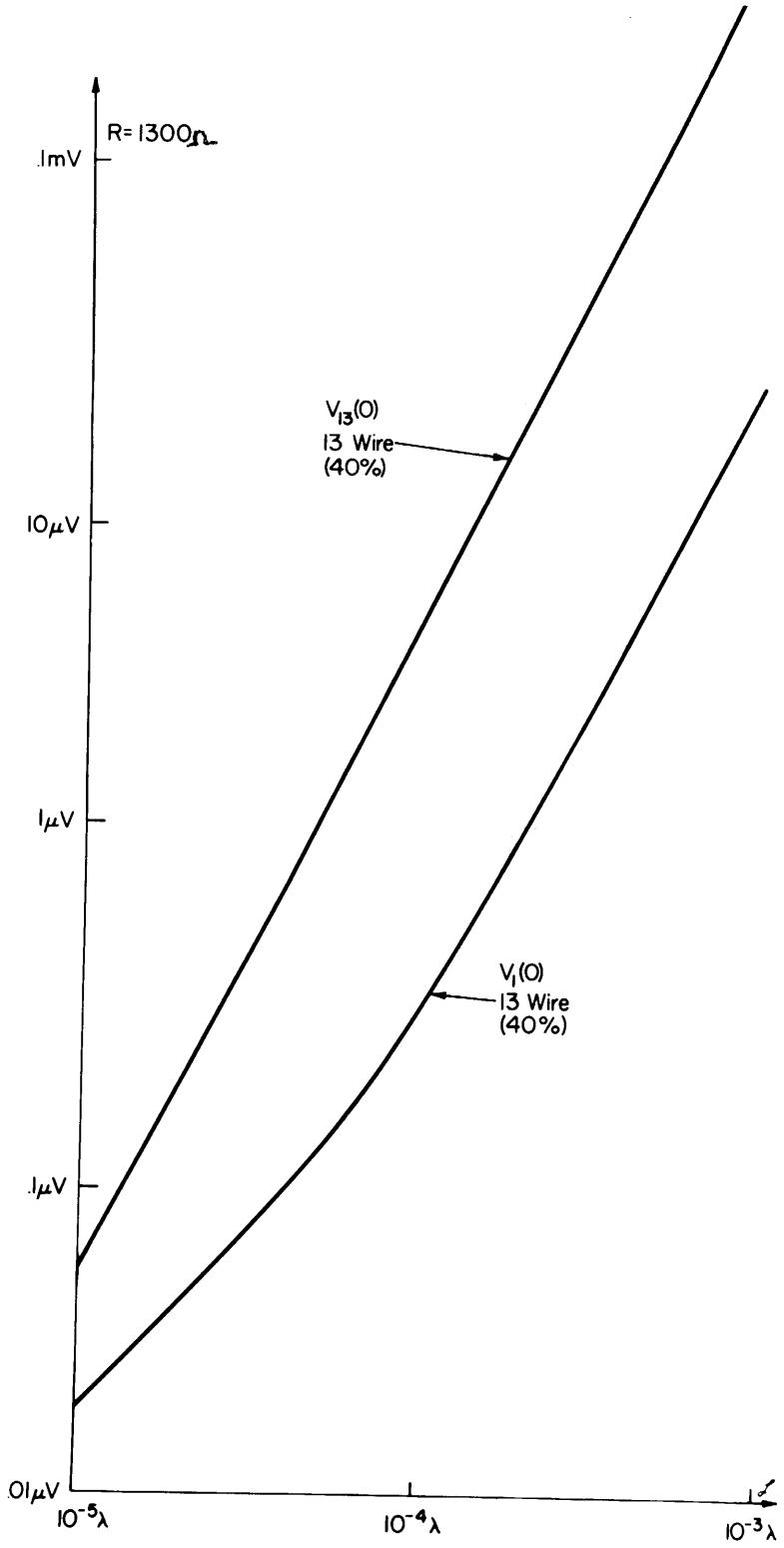
R= 1300Ω
.1mV
10μV
1μV
.1μV
.01μV
$V_{13}(0)$
13 Wire
(40%)
$V_1(0)$
13 Wire
(40%)
$10^{-5}\lambda$
$10^{-4}\lambda$
$10^{-3}\lambda$

Figure 3-12.

generator and receptor wires, the parasitic wires have virtually no effect on the coupling between the generator and receptor wires. For high impedance loads (R = 1300 Ω), $V_1(0)$ and $V_{13}(0)$ differ by as much as 25dB as shown in Figure 3-12. This asymmetry is clearly due to the asymmetric load structure on the parasitic wires since the cable bundle has physical symmetry about a vertical line through its center (wire #7).

These computed results clearly show (for this cable) that for high impedance loads, R, on the generator and receptor wires, the cable responses can be extremely sensitive to wire position and the effect of the parasitic wires on the coupling between the generator and receptor wires can be quite large. For low impedance loads, R, on the generator and receptor wires, the cable responses are insensitive to wire position and the parasitic wires have virtually no effect on the coupling between the generator and receptor wires.

IV. EXPERIMENTAL VERIFICATION OF THE SENSITIVITY OF CABLE RESPONSES TO VARIATIONS IN WIRE POSITION

The sensitivity of cable responses to variations in wire position and the effect of parasitic wires in the cable on the coupling between a generator circuit and a receptor circuit were investigated in Chapter III by using the distributed parameter, multiconductor transmission line (MTL) model. The wires were assumed to be bare,i.e., dielectric insulations around the wires were not considered, when in practice, wires in cable bundles must be insulated from each other. The primary reason for the exclusion of dielectric insulations from the MTL model used in Chapter III was that the addition of dielectric insulations increases the required computation time for the MTL model considerably [1]. Furthermore, reasonable approximations to the per-unit-length parameters in the MTL model are quite simple to determine for bare wires whereas the inclusion of dielectric insulations complicates the determination of these parameters considerably [1]. In this Chapter, however, the cable bundle which was investigated in Chapter III will be constructed of dielectric-insulated wires and the cable responses will be investigated experimentally. The MTL model predictions as well as the BOUND model predictions will also be compared to the experimental results. The MTL predictions were obtained using the XTALK computer program described in Volume VII of this series [7].

The cable bundle in Figure 3-1 and Figure 3-2 was constructed of #20 gauge solid wires having polyvinyl chloride insulations 17 mils in thickness. The cable length was 12 feet (ℓ = 12 feet in Figure 3-2) and the cable was mounted on a 5 foot by 12 foot aluminum ground plane 1/8 inch in thickness as shown in Figure 4-1 and Figure 4-2. The resistors R which terminate both

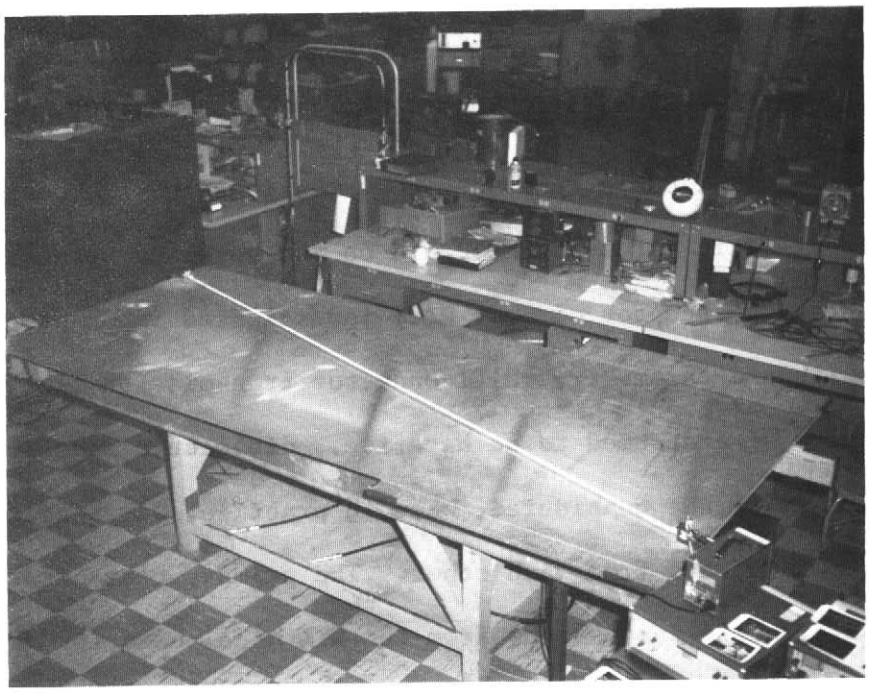

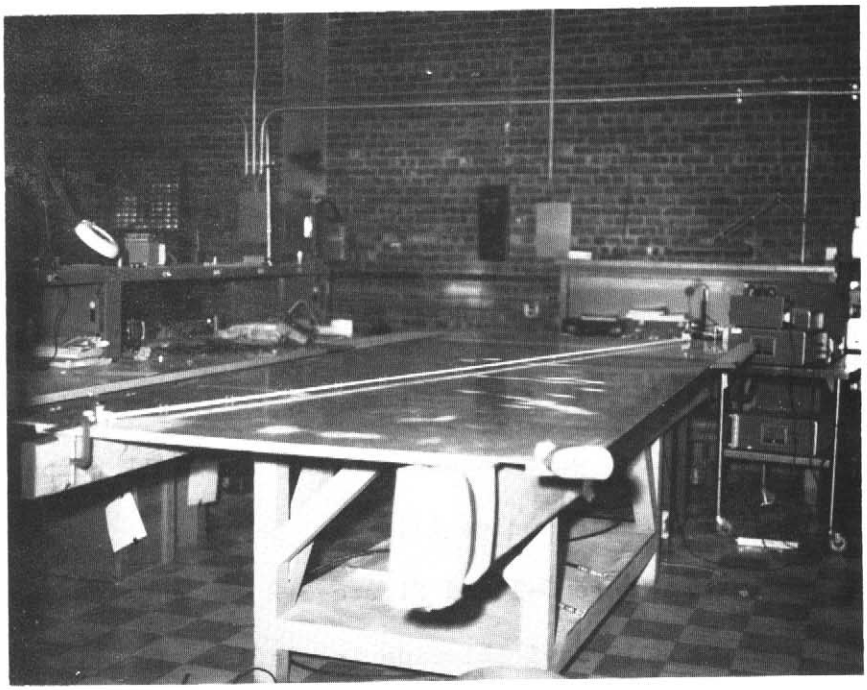

Figure 4-1. The experimental configuration (cont.).

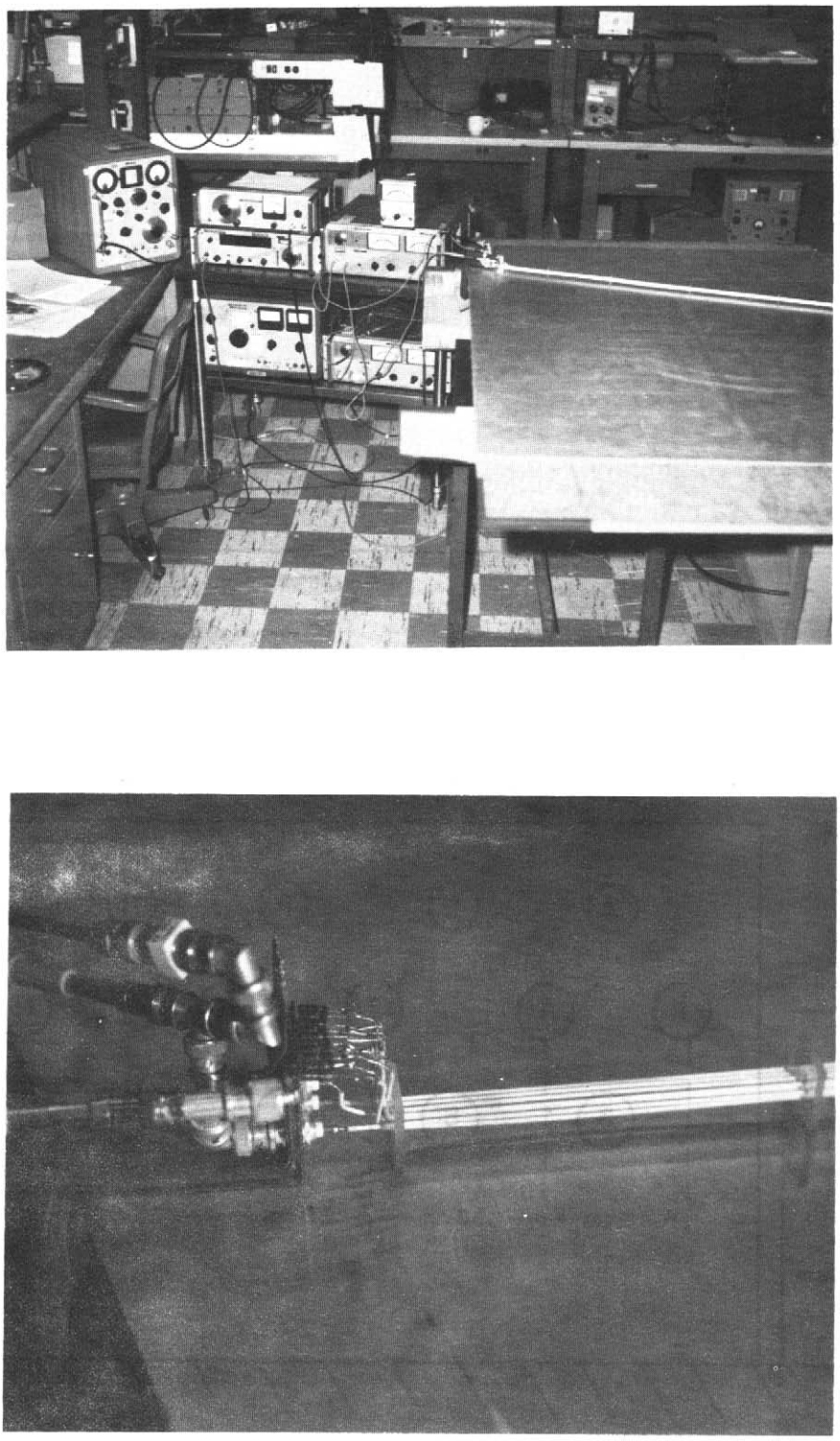

Figure 4-1. The experimental configuration.

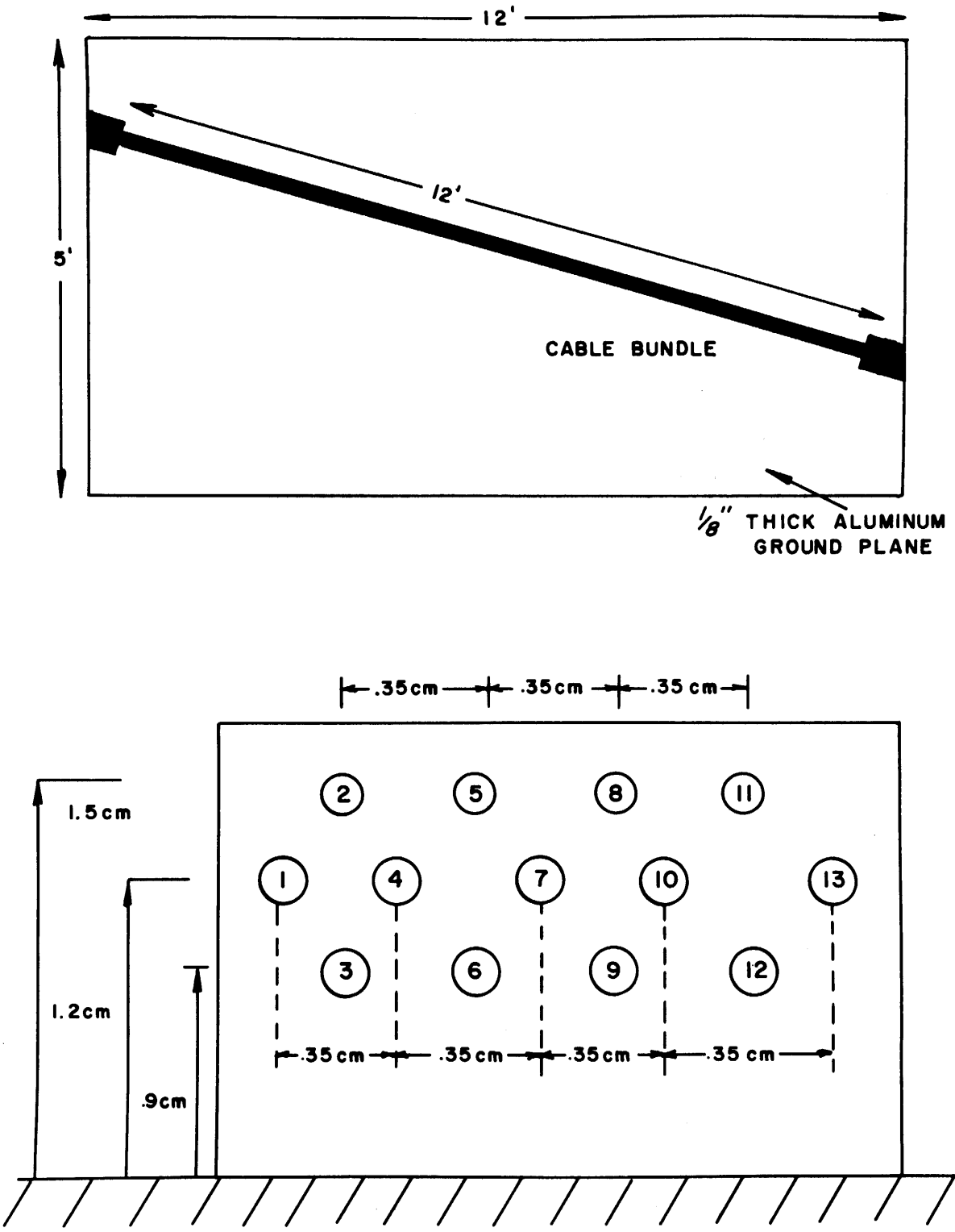

Figure 4-2. The experimental configuration.

ends of wires #1 and #13(the receptor wires) and one end of wire #7 (the generator wire) as shown in Figure 3-2 were constructed by inserting small resistors into BNC connectors so that they may be easily removed from the cable and different values of R (R = 50 Ω, R = 1KΩ, and R = 10KΩ) are used to terminate wires #1, #7, #13. This construction of these resistors resulted in approximately 10pF of capacitance in parallel with R which will be included in all computed predictions with the MTL model. These capacitances are not included in the BOUND model. The resistors terminating both ends of the parasitic wires (50Ω or 10KΩ) shown in Figure 3-2 are unchanged throughout the experiment.

Two wire separation configurations will be investigated. In the CONTROLLED SEPARATION configuration, plastic spacers were constructed to control the wire separations at the initial spacings used in Chapter III (h = 1.2 cm, Δh = .3 cm, Δd = .175 cm) as shown in Figure 4-2(b). These spacers were placed along the line and controlled the wire separations. In the RANDOM BUNDLE configuration, the plastic spacers were removed; the wires were taped together, and the bundle was supported by small styrofoam blocks at an average height of 1.2 cm above the ground plane.

The experimental data were taken from 10KHz to 100 MHz. The cable is one wavelength long at approximately 82 MHz (computed assuming free space propagation). Thus this frequency range will allow an investigation of the cable responses for electrically short to electrically long cable lengths (ℓ = .00123λ to ℓ = 1.23λ). Measurements were taken at discrete frequencies: 10 KHz, 20 KHz, 30 KHz, ---, 90 KHz, 100 KHz, 200 KHz, ---, 900 MHz, 1 MHz, ---, 9 MHz, 10 MHz, ---, 100 MHz. These data points are connected by straight lines on the graph to facilitate the interpretation of the results.

The apparatus used for measurement and excitation of the line are:

		FREQUENCY RANGE
(1)	HP 8405A Vector Voltmeter	1 MHz → 100 MHz
(2)	HP 3400A RMS Voltmeter	10 KHz → 1 MHz
(3)	HP 651A Oscillator	10 KHz → 10 MHz
(4)	HP 608D Oscillator	10 MHz → 100 MHz
(5)	HP 5245L Counter	10 KHz → 100 MHz

A frequency counter was used to control the frequency output of the oscillator to within approximately .1% of the desired frequency. The input to the generator wire (# 7) at x = 0 in Figure 3-2 is a one volt sinusoidal source (zero source impedance). This was accomplished in the experiment by monitoring the input voltage to wire #7 at x = 0 and adjusting the oscillator output to provide one volt at this point. For a one volt input voltage, the received voltage represents the voltage transfer ratio. Although the re - ceived voltages are phasors with a magnitude and phase angle relative to the source, only the magnitudes will be plotted.

The various notations on the plotted data are:

EXP - Experimental Results

13 WIRE - All wires present (see Figure 3-1(a))

PAIR - Only wires #1 and #7 present and the remaining wires removed (see Figure 3-1(b))

DIST - The distributed parameter, multiconductor transmission line (MTL) model. (PAIR, DIST denotes the model applied to a configuration consisting of only wires #1 and #7 (see Figure 3-1(a)). 13 WIRE, DIST denotes the model applied to the configuration consisting of all 13 wires (see Figure 3-1(b))).

BOUND - The BOUND model described in Section 2.2 and given in equations (2-48). For this model, the generator wire is wire #7 and the receptor wire is wire #1. The 10 pF of capacitance introduced by the BNC connectors into which the resistors R are inserted is not included in the results of this model.

4.1 Effects of Parasitic Wires

In this section, the effect of parasitic wires on the coupling between a generator circuit and a receptor circuit will be investigated. In order to insure that valid comparisons can be made, i.e., the positions of the generator and receptor wires must remain the same with and without the other wires present, the CONTROLLED SEPARATION configuration is used.

The received voltage at the $x = \ell$ end of wire #1, $V_1(\ell)$, (see Figure 3-2) is plotted for R = 50Ω in Figure 4-3, R = 1KΩ in Figure 4-4 and R = 10KΩ in Figure 4-5. Note that for R = 50Ω (low impedance loads), the parasitic wires have virtually no effect on the coupling between wire #7 and wire #1 until the line becomes electrically long, $\ell > 1/100\lambda$. Yet even then the effect is on the order of only 6 - 10dB. However for high impedance loads, R = 1KΩ and R = 10KΩ , the parasitic wires dramatically affect the PAIR results. As much as 35-40 dB reduction in coupling is attributable to the presence of the parasitic wires for R = 1KΩ and R = 10KΩ even though the line is very short, electrically. In the RANDOM CABLE configuration, however, where the wires are closer together, it will be found that the PAIR and 13 WIRE results are much closer in value.

4.2 Prediction Accuracies of the MTL Model for PAIR Results

In this section, the distributed parameter, transmission line model will be investigated to determine its ability to predict the coupling between

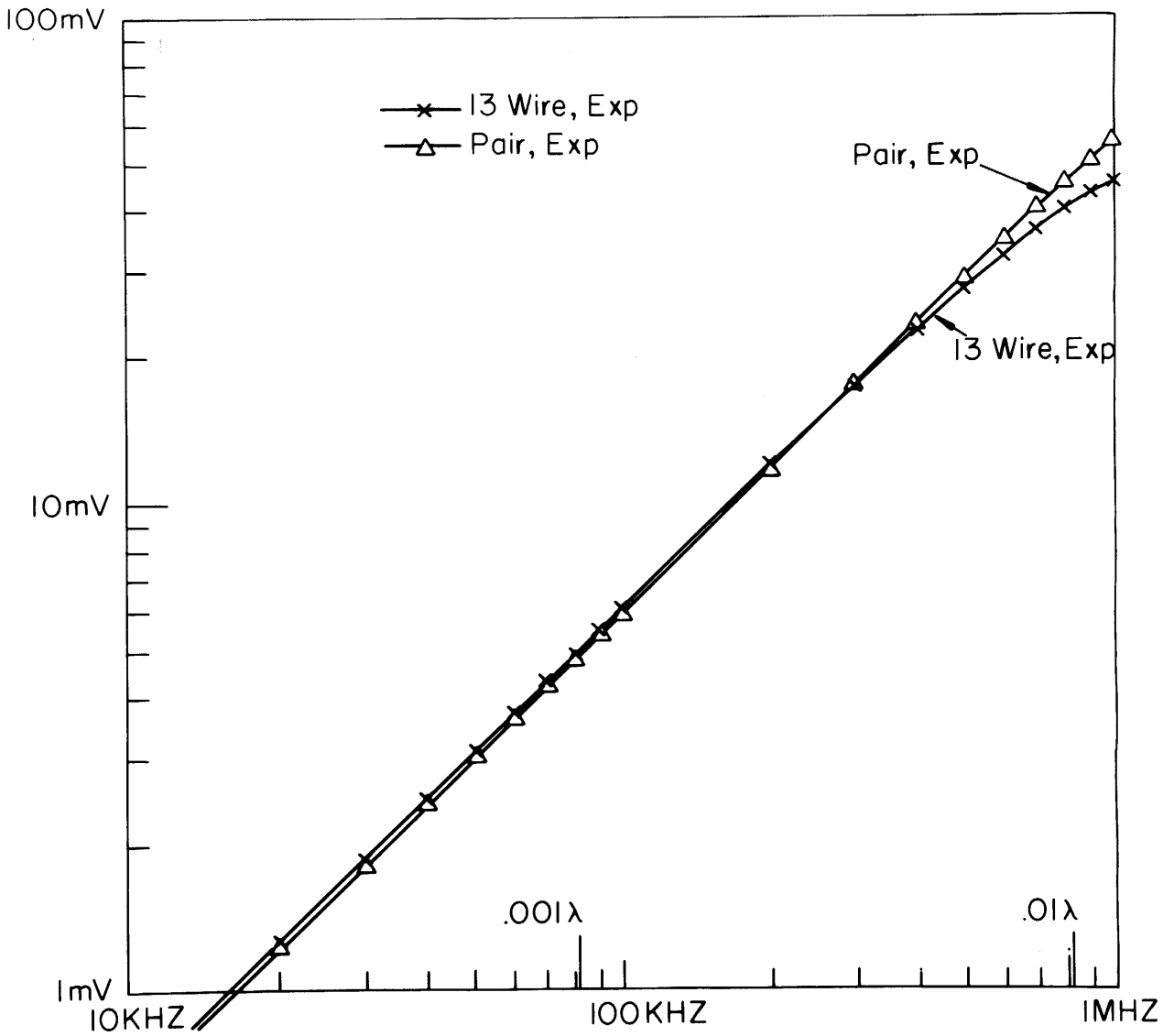

$V_1(f)$ $R = 50\,\Omega$

Controlled Separation

Figure 4-3(a).

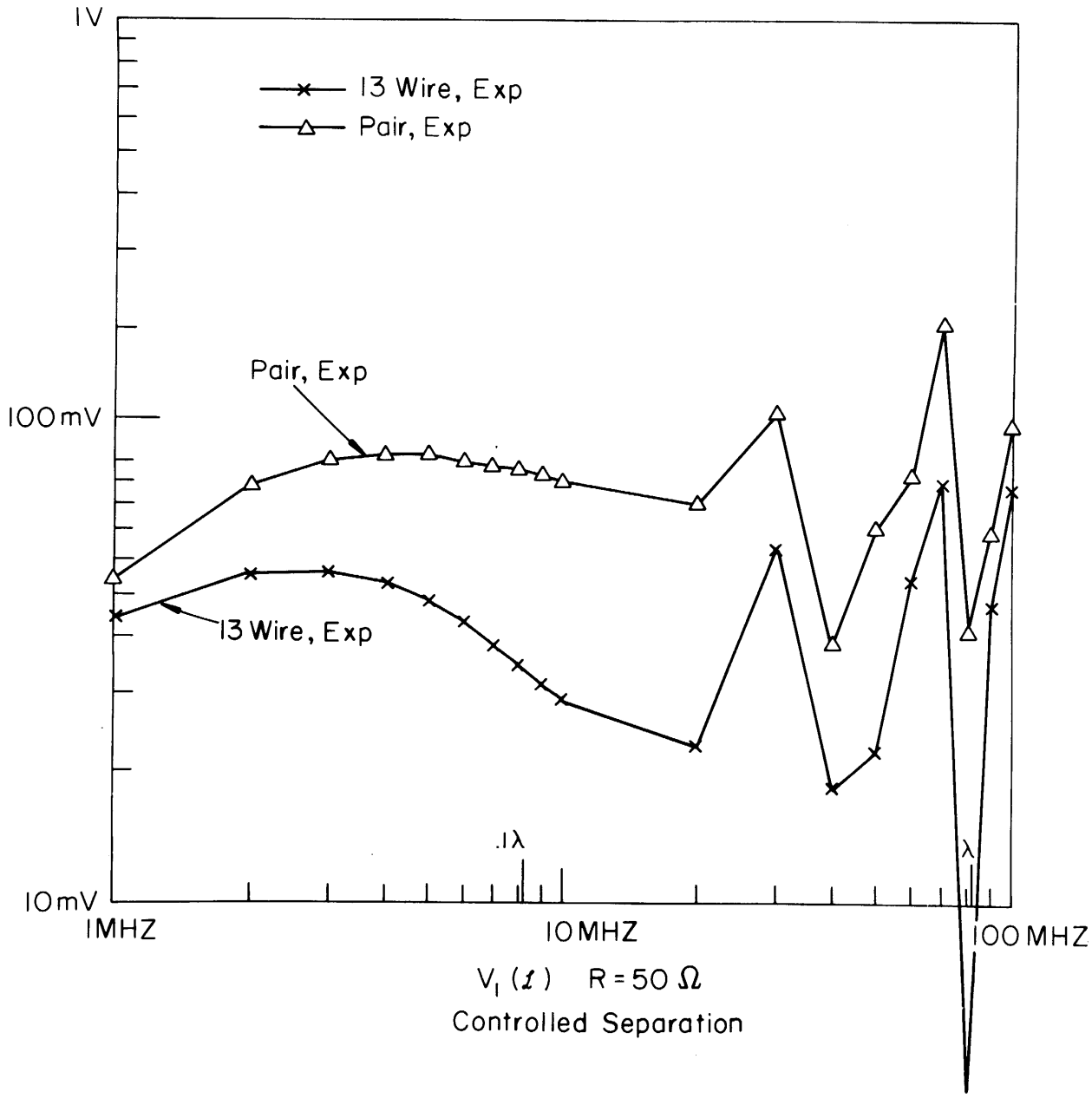
1V
13 Wire, Exp
Pair, Exp
Pair, Exp
100mV
13 Wire, Exp
10mV
.1λ
λ
1MHZ
10MHZ
100MHZ
$V_1(t)$ R = 50 Ω
Controlled Separation

Figure 4-3(b).

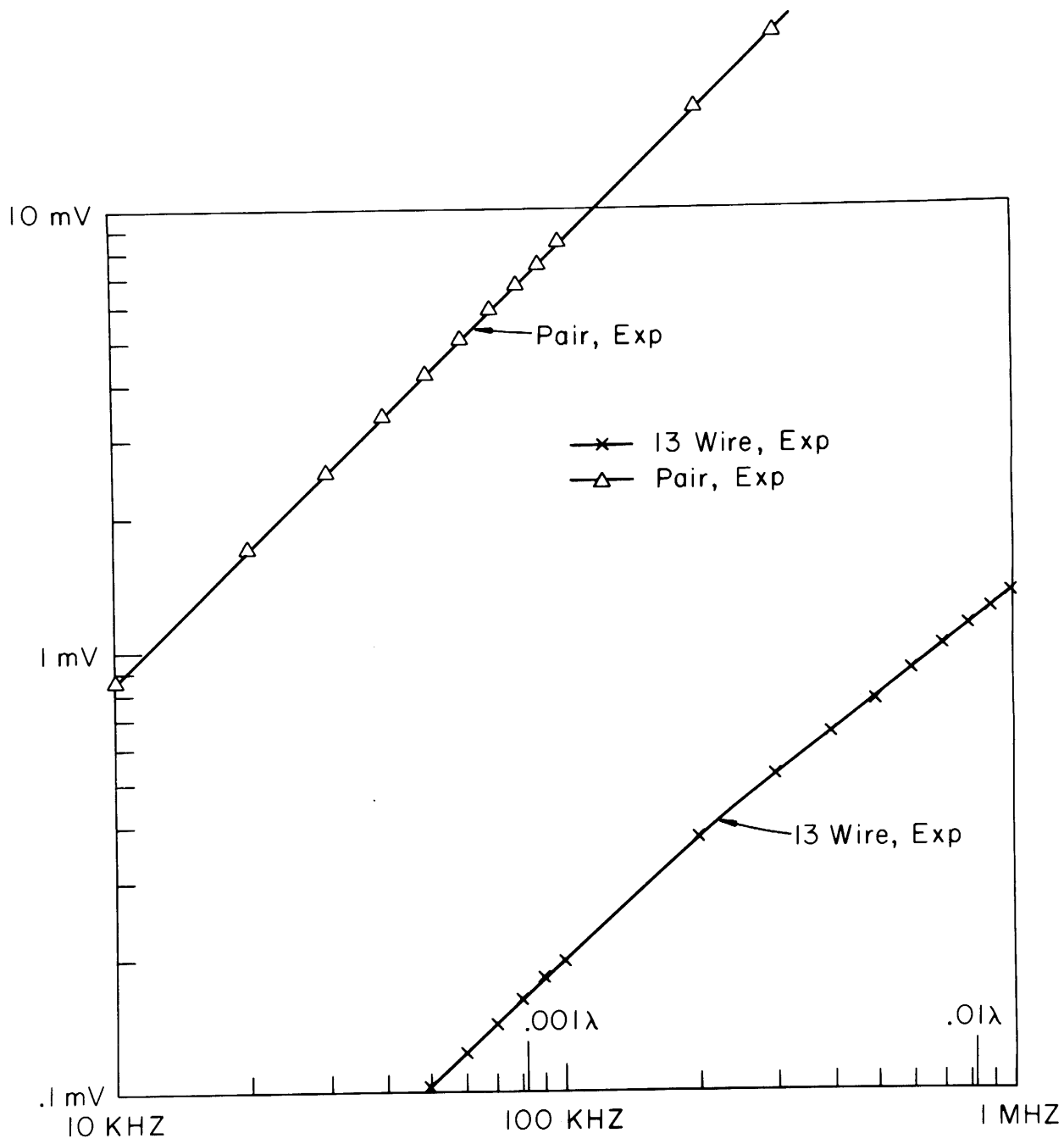

$V_1(\ell)$ R = 1 KΩ
Controlled Separation

Figure 4-4(a).

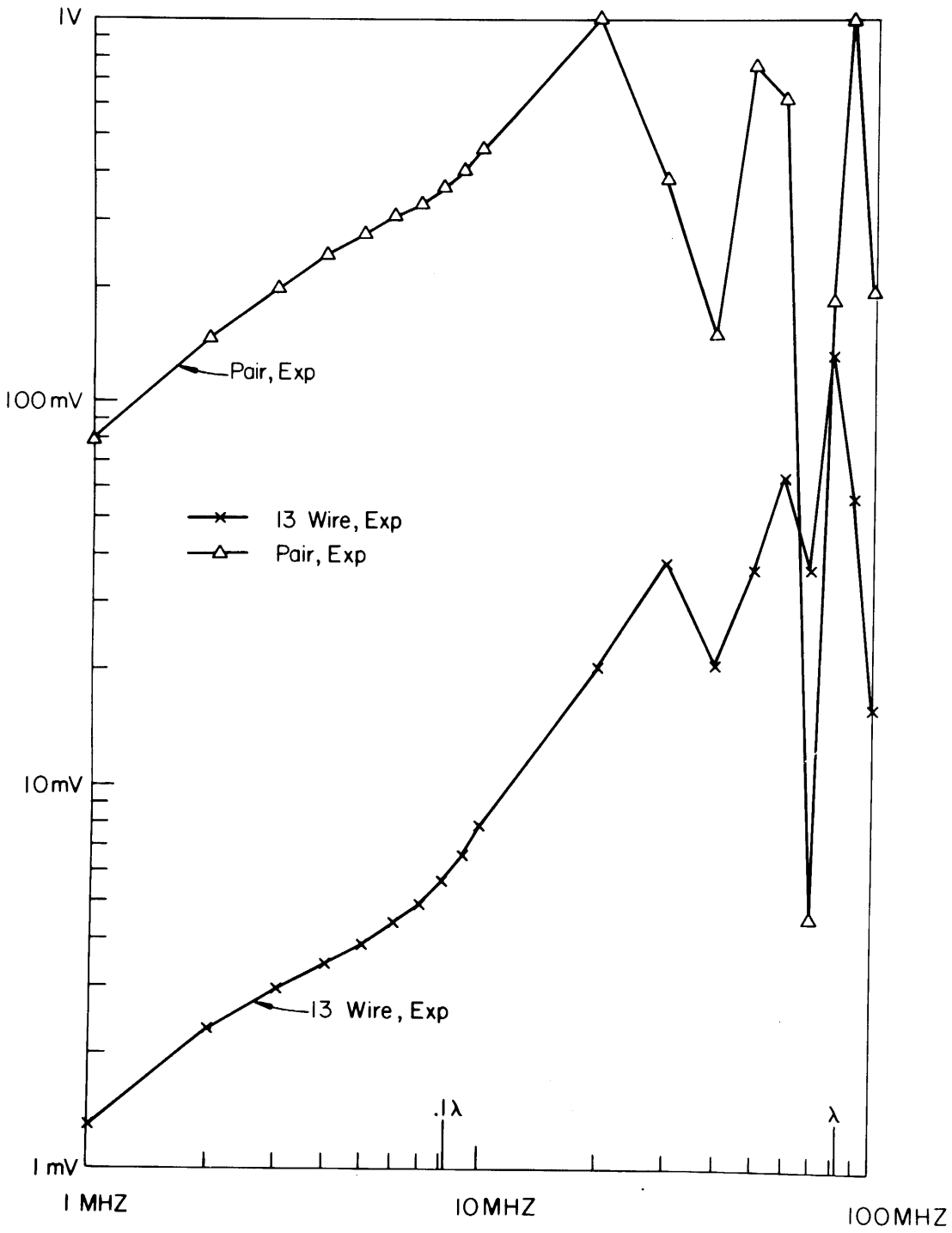

$V_1(\ell)$ R= 1KΩ

Controlled Separation

Figure 4-4(b).

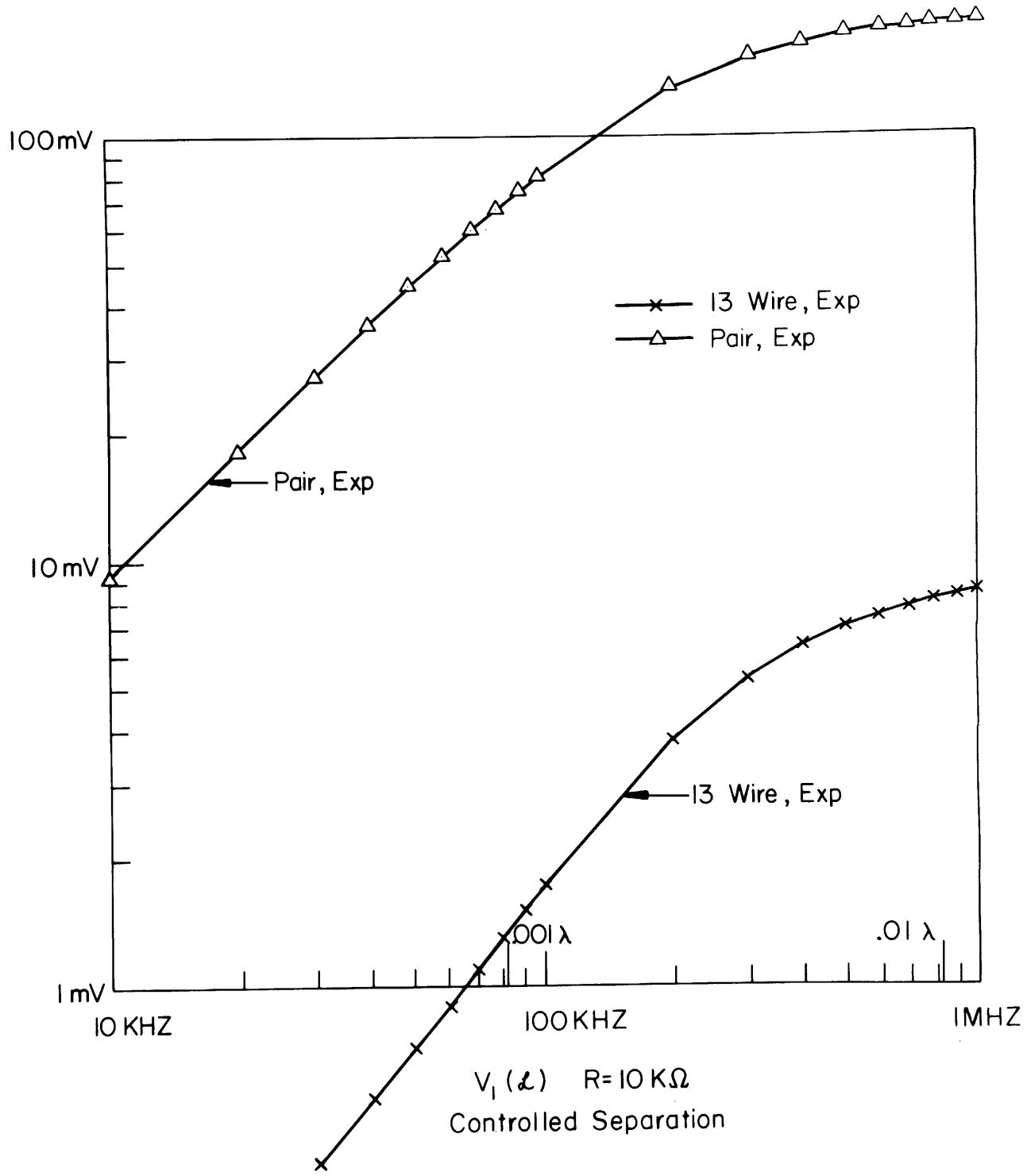
100mV
10mV
1mV
13 Wire, Exp
Pair, Exp
Pair, Exp
13 Wire, Exp
.001 λ
.01 λ
10 KHZ
100 KHZ
1MHZ
$V_1(\ell)$ R=10 KΩ
Controlled Separation

Figure 4-5(a).

a generator circuit (wire #7) and receptor circuit (wire #1) with all other wires removed (PAIR). The results are shown for R = 50Ω in Figure 4-6, R = 1KΩ in Figure 4-7 and R = 10KΩ in Figure 4-8. The predictions of the distributed parameter, transmission line model (DIST) are shown with and without dielectric insulations included in the calculation of the per-unit-length parameters. The per-unit-length capacitances with wire insulations included (ε_r = 3.0) were determined in Volume I of this series [1] pp. 116 - 122.

In Figure 4-6, for R = 50Ω, the transmission line model provides prediction accuracies within 1dB except in the "standing wave region", i.e., for $\ell > .1\lambda$. Similar results are obtained for R = 1KΩ in Figure 4-7 and R = 10KΩ in Figure 4-8. Note, however, that for these cases the wire dielectric affects the results somewhat (on the order of 3-6dB).

4.3 Prediction Accuracies of the MTL Model for 13 WIRE Results

In this section, the distributed parameter, transmission line model will be investigated to determine its ability to predict the coupling between the generator circuit (wire #7) and the receptor circuit (wire #1) when all 13 wires are present (13 WIRE). The results are shown for R = 50Ω in Figure 4-9, R = 1KΩ in Figure 4-10 and R = 10KΩ in Figure 4-11.

For R = 50Ω in Figure 4-9, the MTL model provides prediction accuracies within 1dB up to the standing wave region ($\ell < .1\lambda$). In the standing wave region ($\ell > .1\lambda$) the prediction accuracies are considerably poorer.

For R = 1KΩ and R = 10KΩ in Figure 4-10 and Figure 4-11, prediction accuracies are within 1-2dB for $\ell < .1\lambda$ and for $\ell > .1\lambda$ the accuracies are poorer although the model predicts the trend in the experimental results quite well.

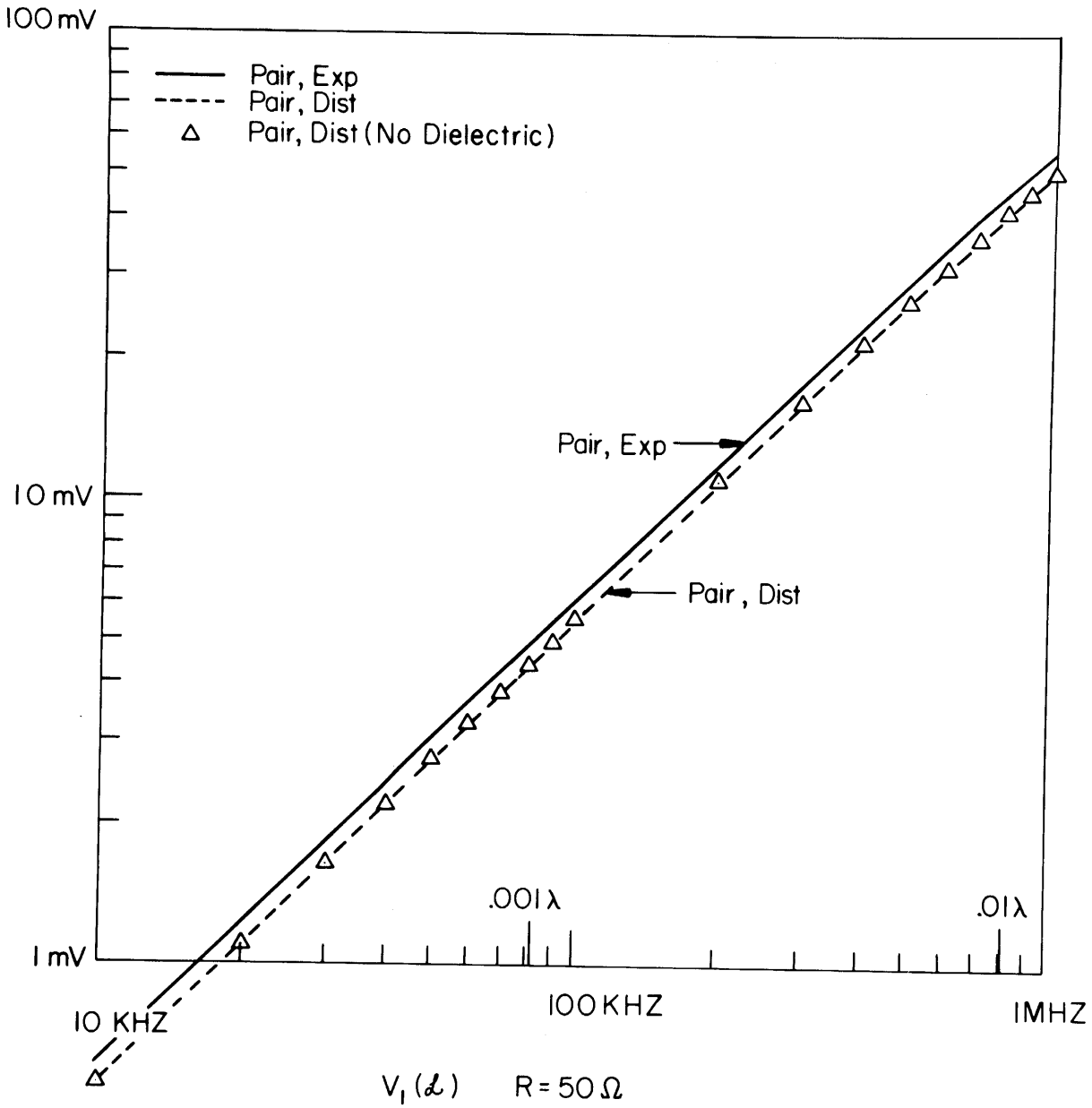
100 mV
10 mV
1 mV
Pair, Exp
Pair, Dist
Pair, Dist (No Dielectric)
Pair, Exp
Pair , Dist
.001λ
.01λ
10 KHZ
100 KHZ
1MHZ
$V_1(\ell)$ R = 50 Ω
Controlled Separation

Figure 4-6(a).

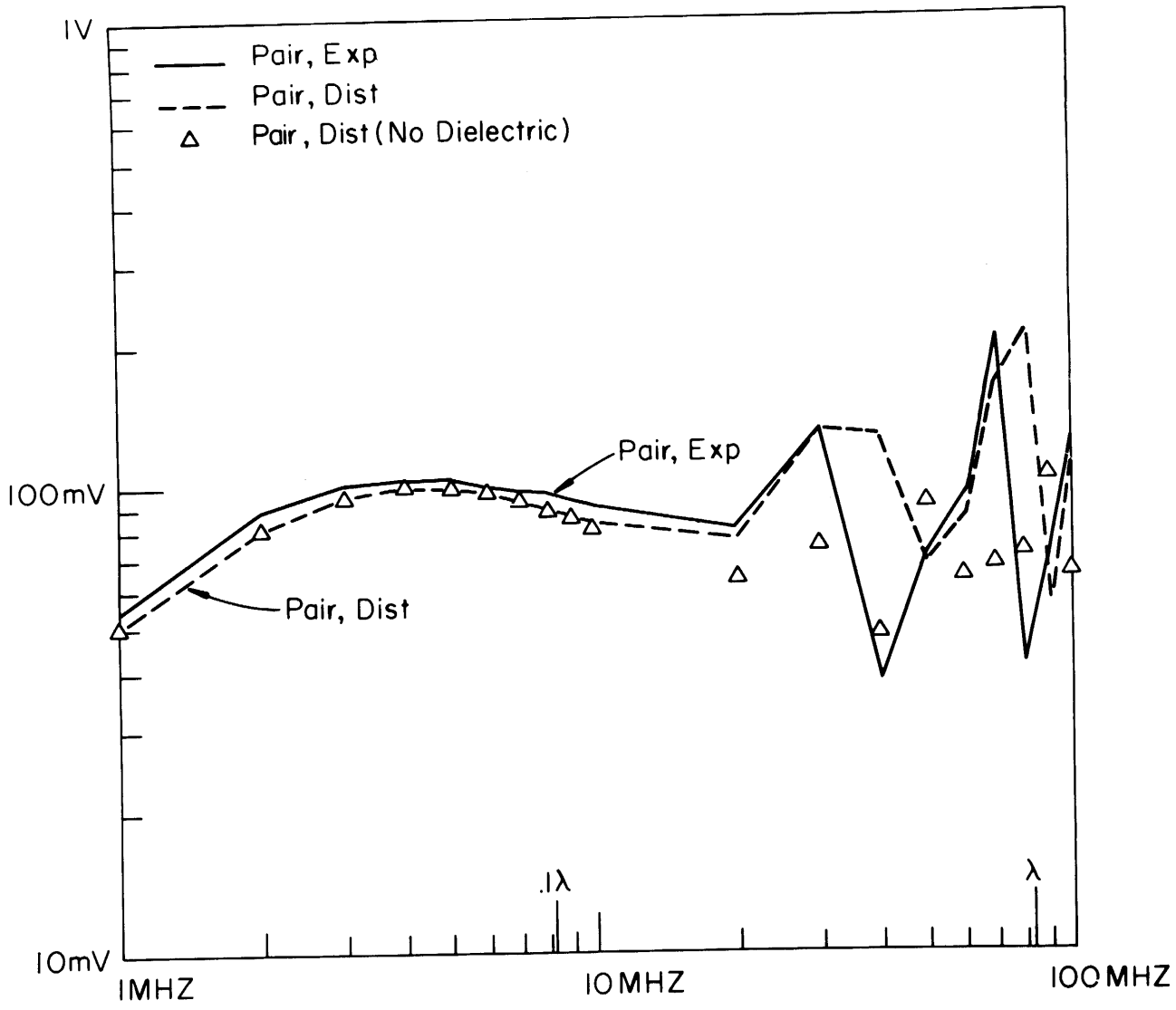

$V_1(t)$ $R = 50\,\Omega$

Controlled Separation

Figure 4-6(b).

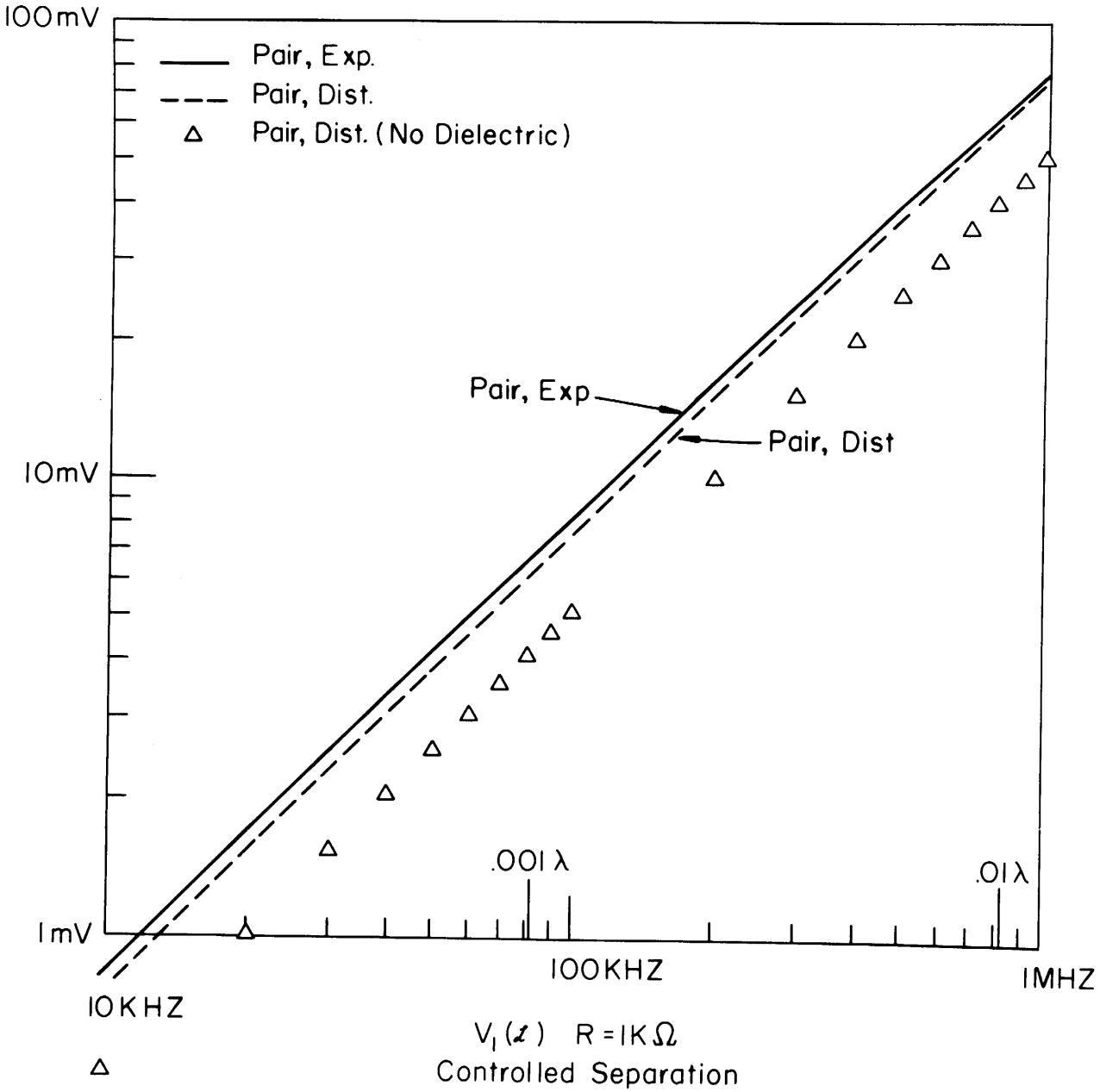
100mV
Pair, Exp.
Pair, Dist.
Pair, Dist. (No Dielectric)
Pair, Exp
Pair, Dist
10mV
1mV
.001λ
.01λ
10KHZ
100KHZ
1MHZ
$V_1(\ell)$ R = 1KΩ
Controlled Separation

Figure 4-7(a).

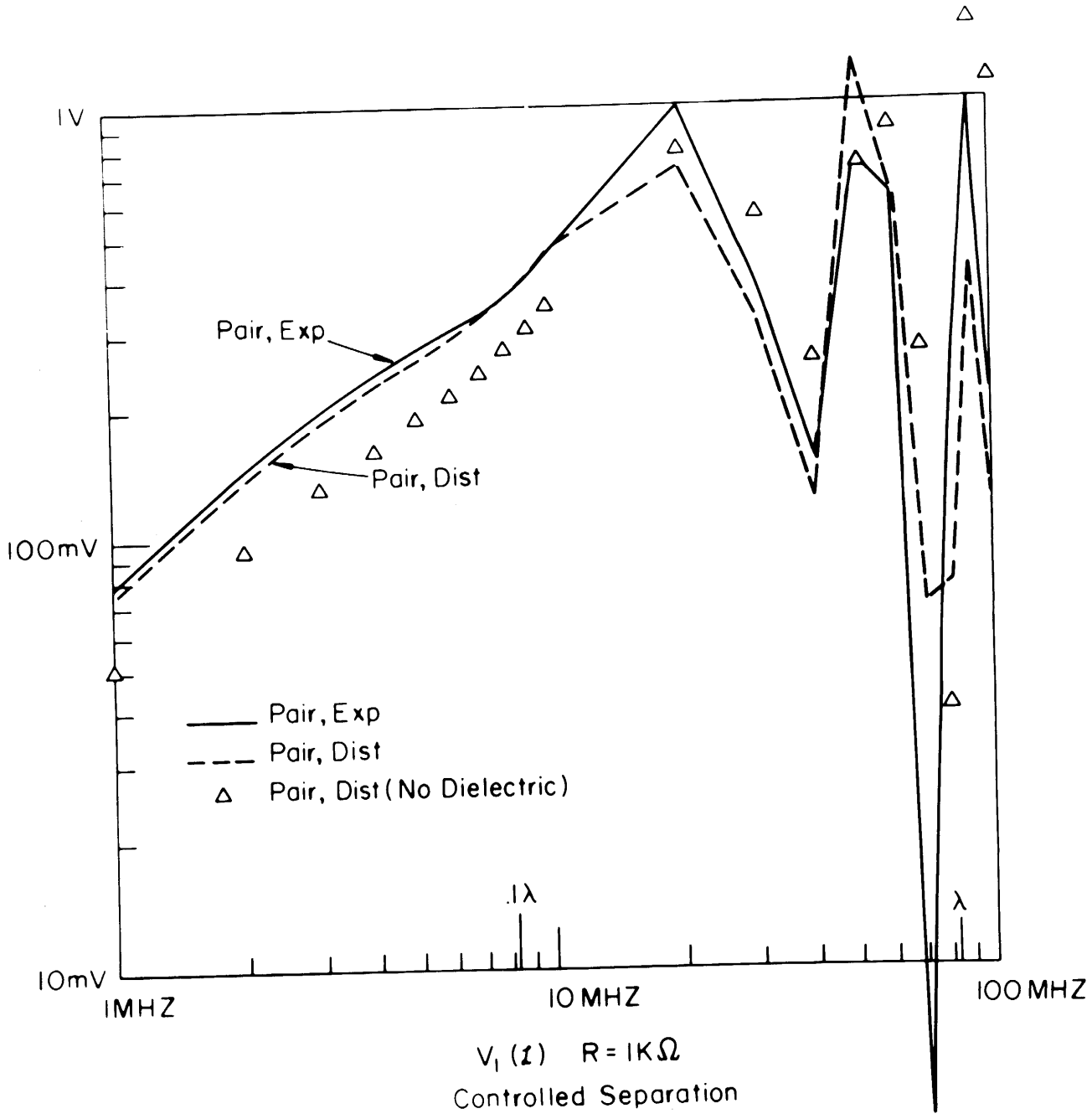
1V
100mV
10mV
1MHZ
10 MHZ
100 MHZ
.1λ
λ
Pair, Exp
Pair, Dist
Pair, Exp
Pair, Dist
Pair, Dist (No Dielectric)
V1 (1) R = 1KΩ
Controlled Separation

Figure 4-7(b).

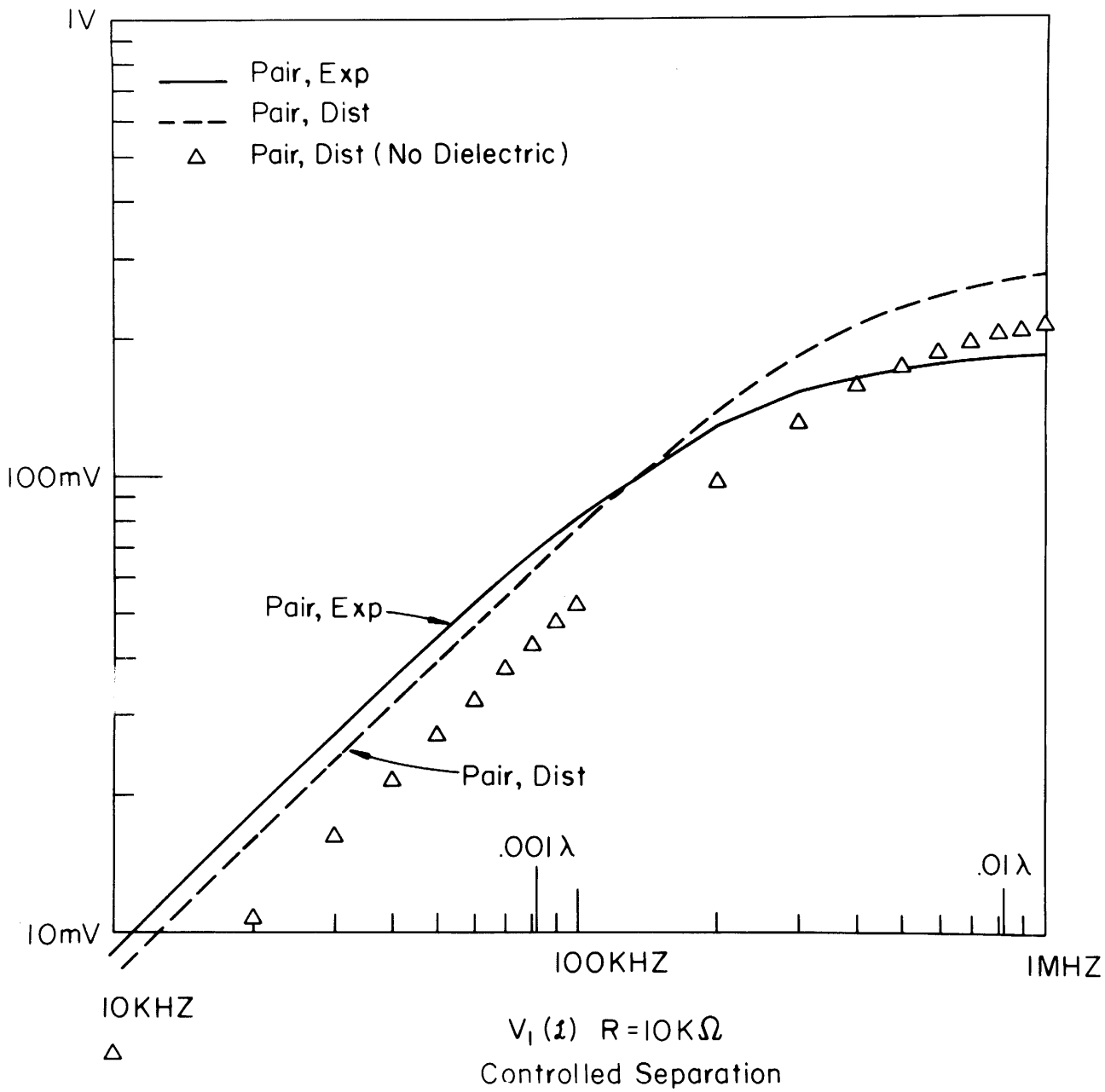
1V
Pair, Exp
Pair, Dist
Pair, Dist (No Dielectric)
100mV
10mV
Pair, Exp
Pair, Dist
.001λ
.01λ
10KHZ
100KHZ
1MHZ
V1 (1) R=10KΩ
Controlled Separation

Figure 4-8(a).

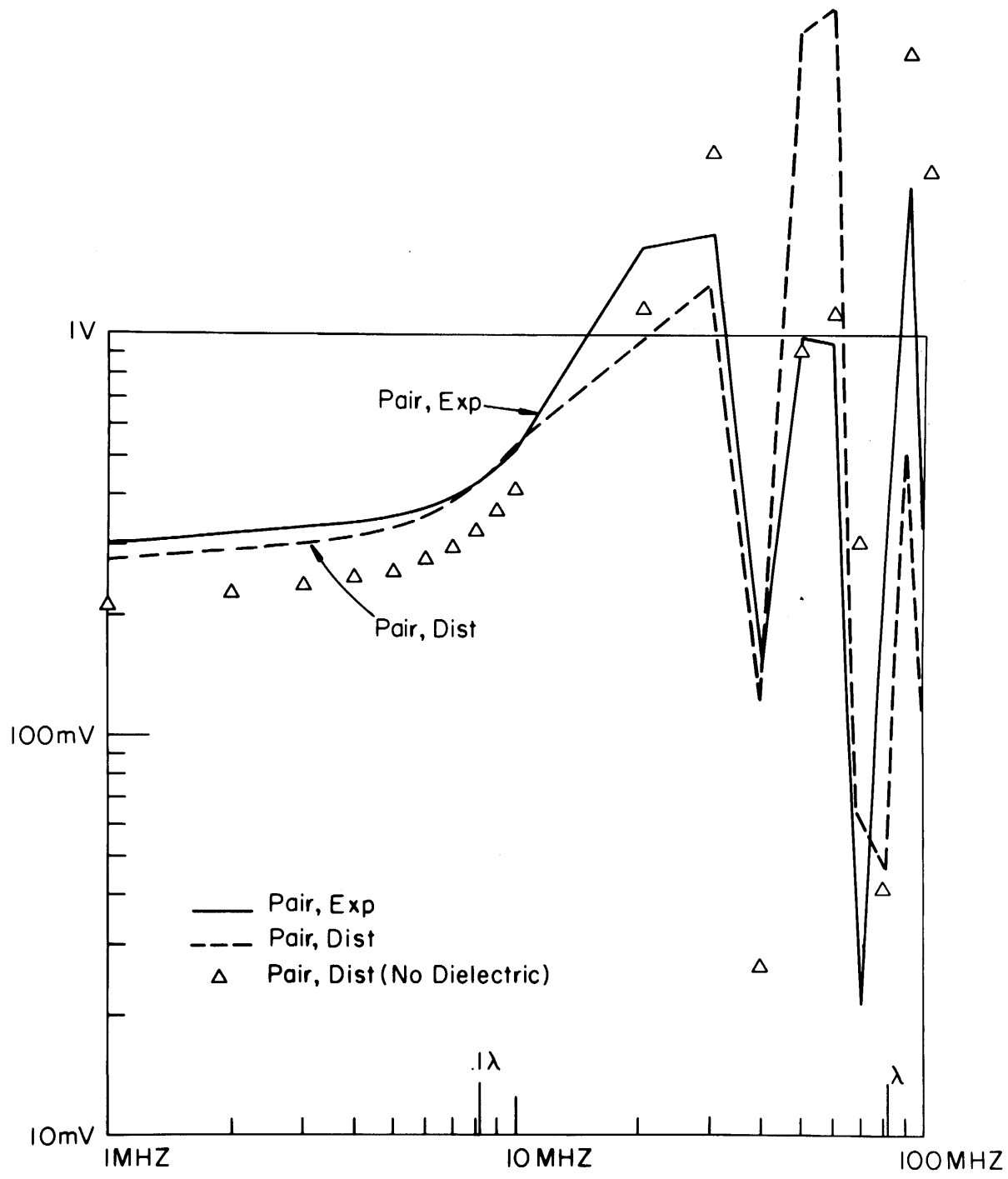

V_1 (ℓ) R = 10KΩ
Controlled Separation

Figure 4-8(b).

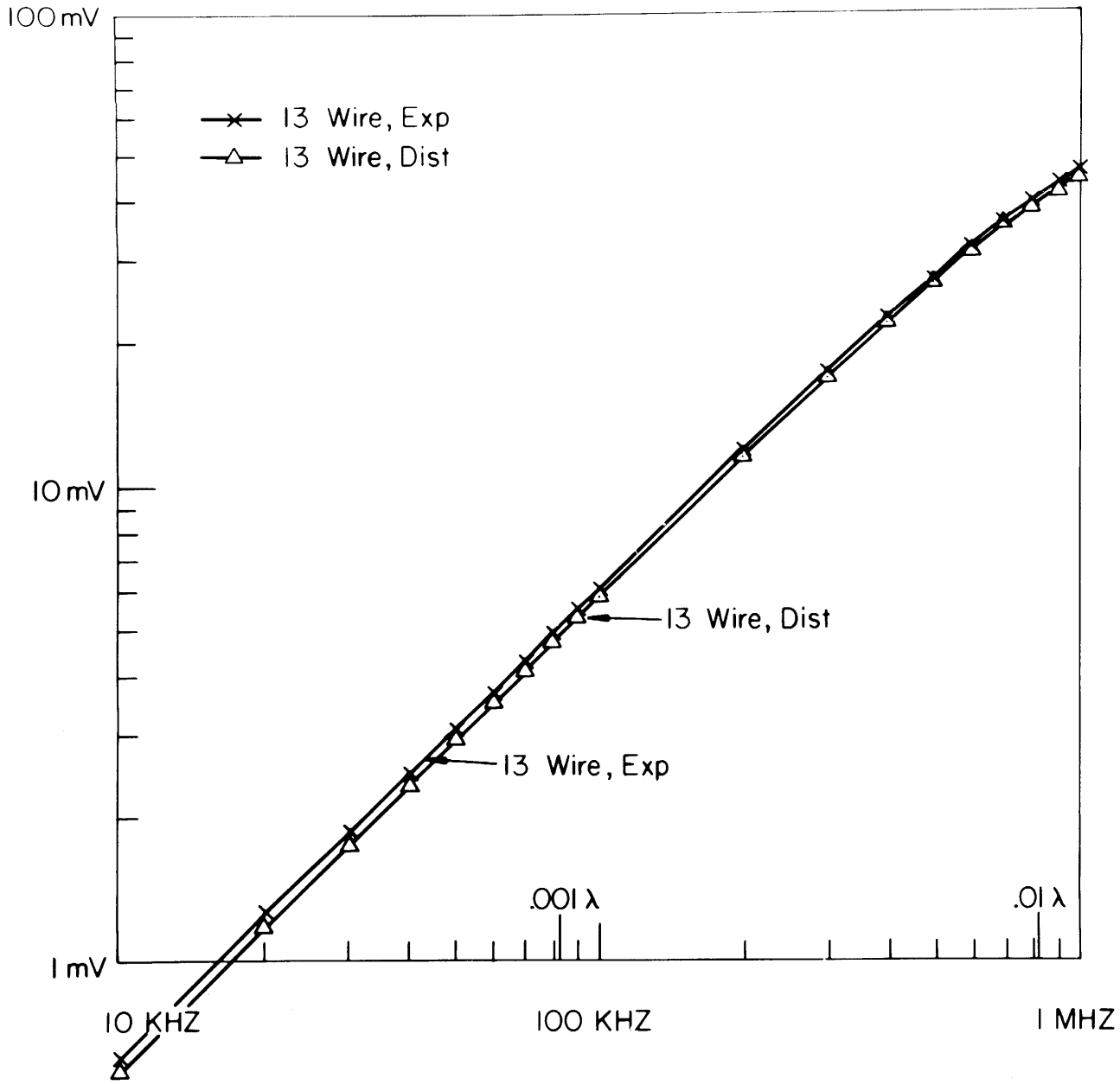
100 mV
13 Wire, Exp
13 Wire, Dist
10 mV
13 Wire, Dist
13 Wire, Exp
.001 λ
.01 λ
1 mV
10 KHZ
100 KHZ
1 MHZ
$V_1(\ell)$ R=50 Ω
Controlled Separation

Figure 4-9(a).

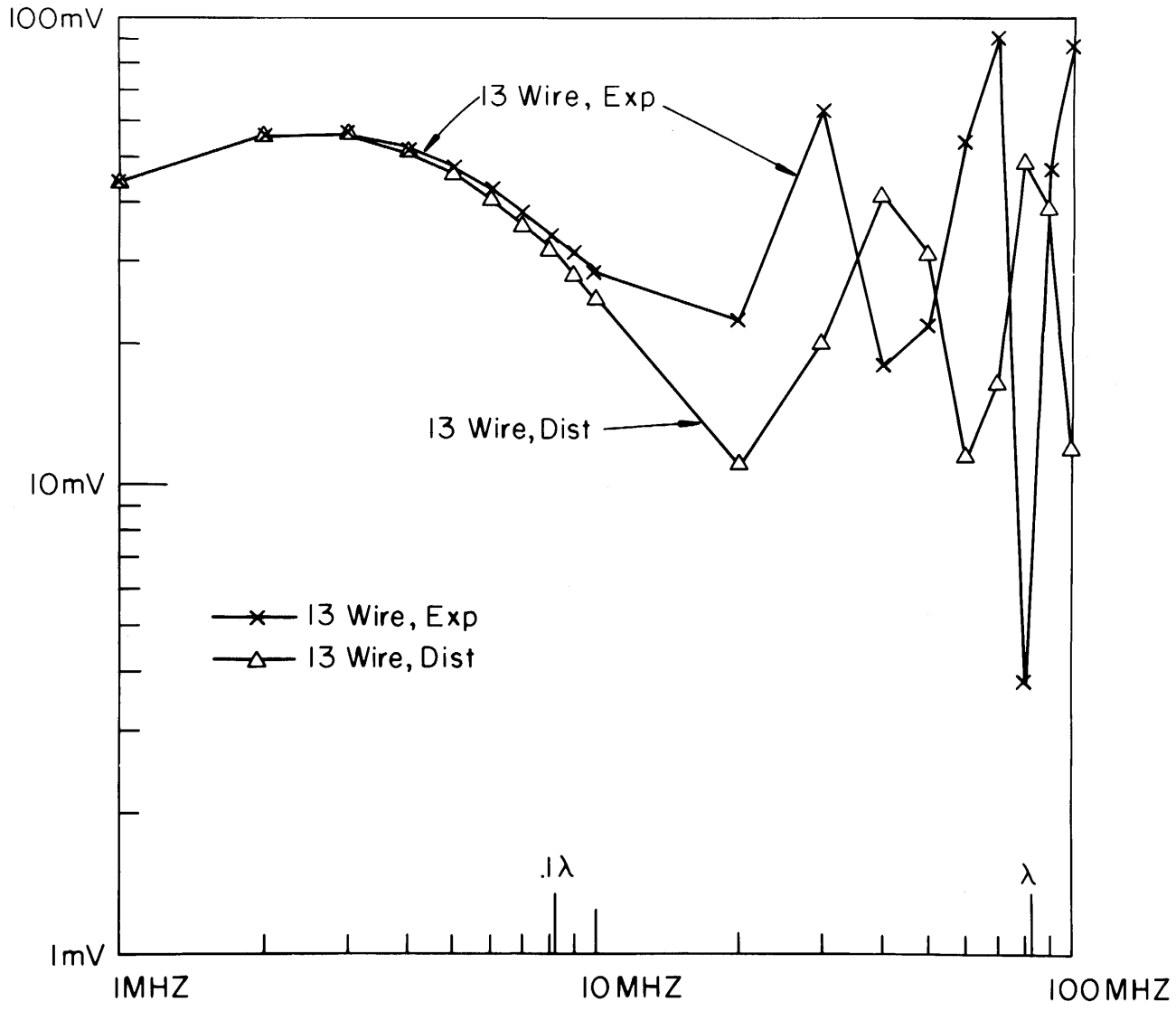

$V_1(\ell)$ R=50Ω
Controlled Separation

Figure 4-9(b).

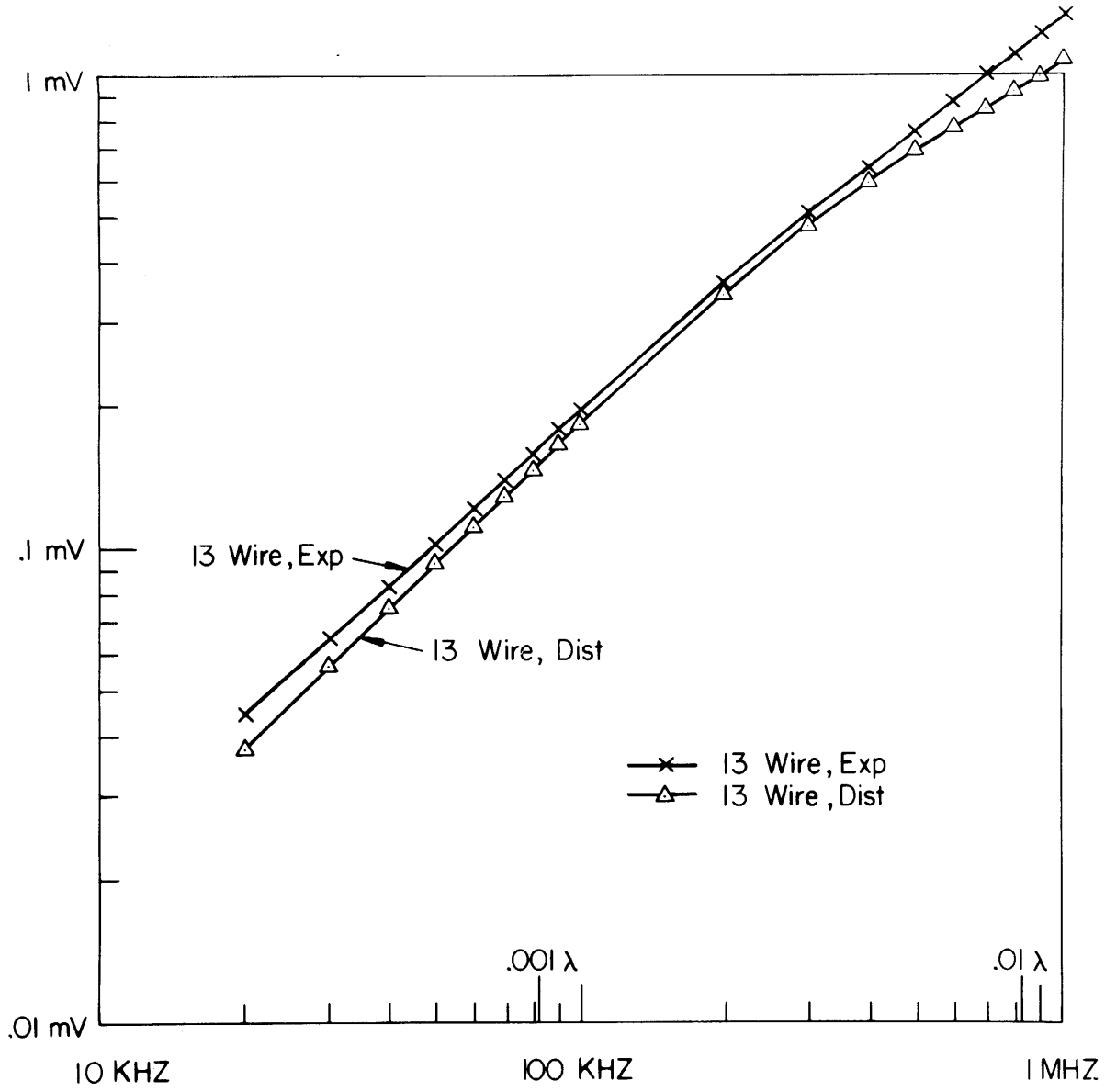

V_1 (ℓ) R = 1KΩ
Controlled Separation

Figure 4-10(a).

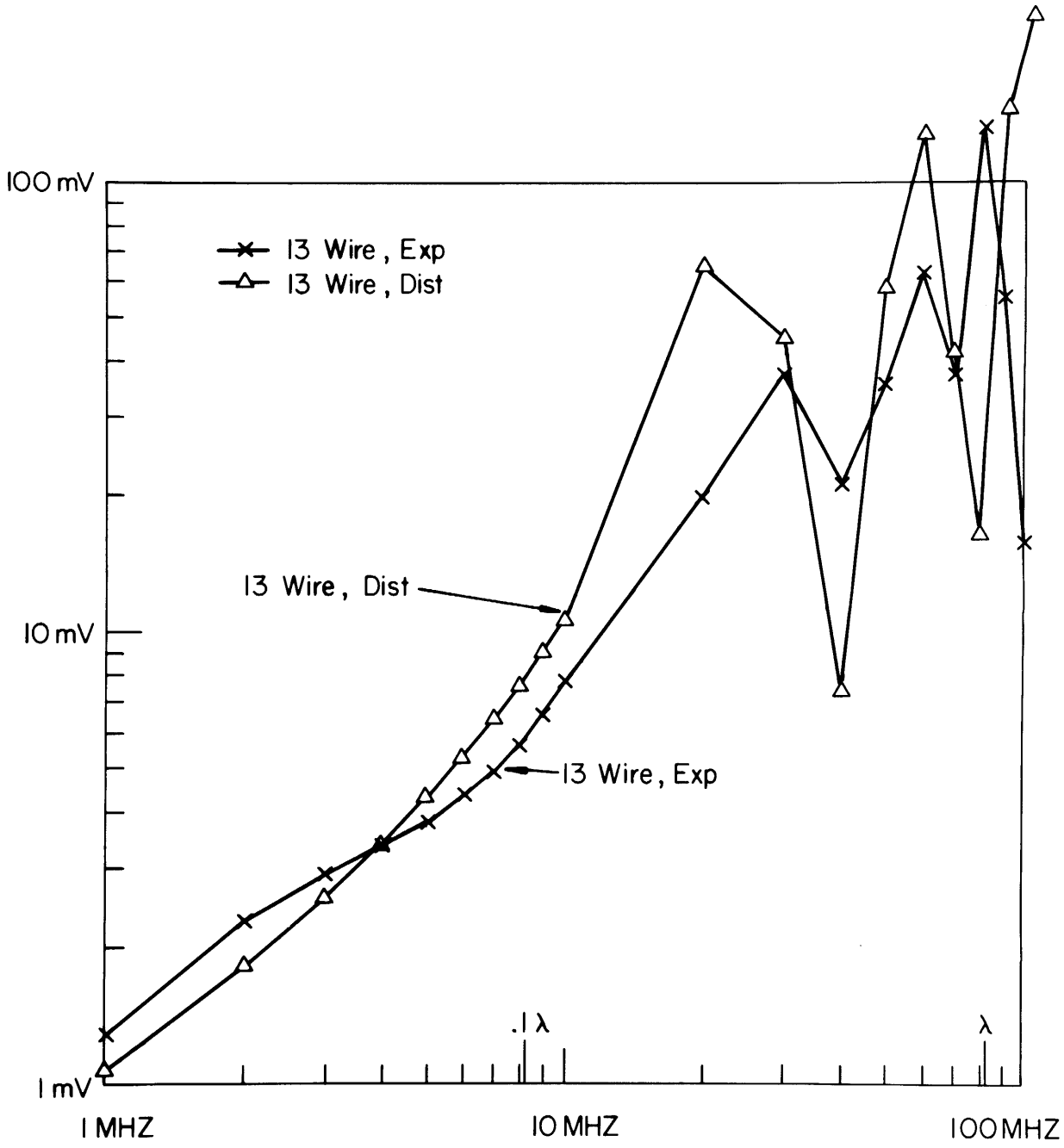

$V_1(\ell)$ R=1 KΩ
Controlled Separation

Figure 4-10(b).

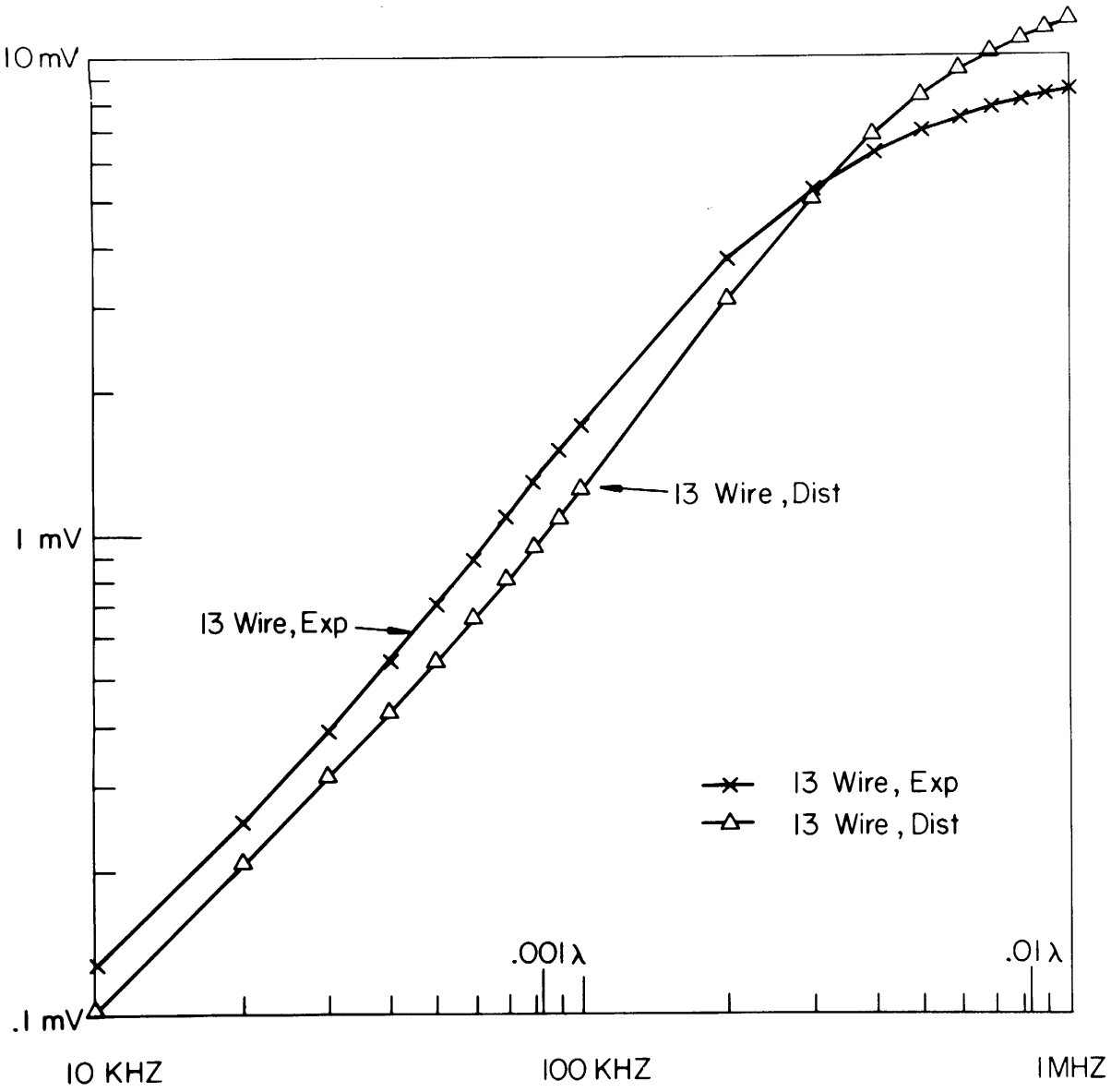

V_1 (ℓ) R=10KΩ
Controlled Separation

Figure 4-11(a).

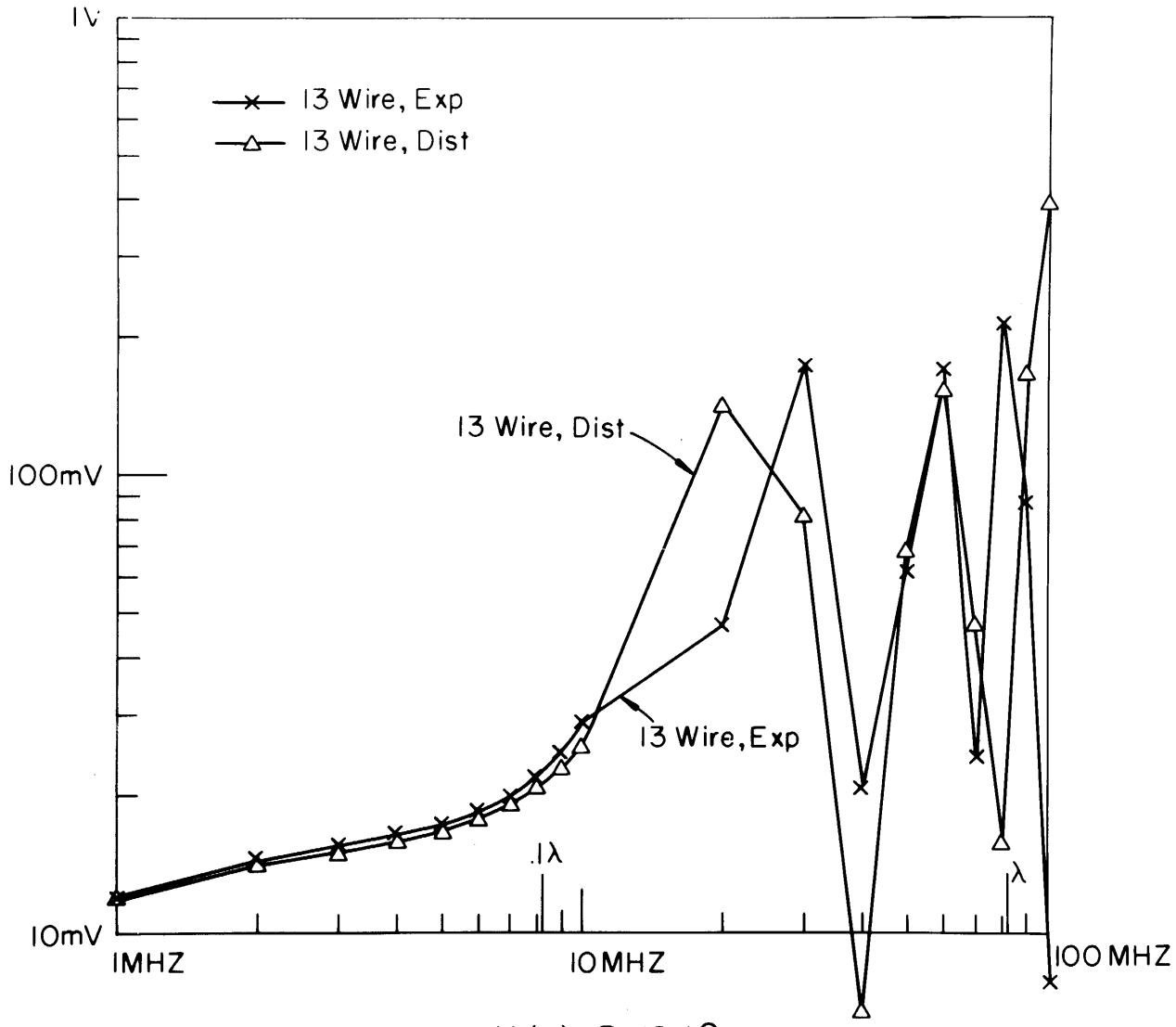

$V_1(\mathcal{I})$ R = 10KΩ
Controlled Separation

Figure 4-11(b).

4.4 Sensitivity of Cable Responses to Variations in Wire Position

In random cables, relative wire position is unknown and varies in some uncontrolled fashion along the cable length. To investigate the sensitivity of the cable responses to wire position, the RANDOM BUNDLE configuration is used. The plastic spacers used to control wire separation in the CONTROLLED SEPARATION configuration are removed and the 13 wires are taped together randomly. This random bundle is supported above the ground plane by small styrofoam blocks at an average height of 1.2 cm.

The sensitivity to wire position is investigated in the following manner. Four sets of data on the frequency response of $V_1(\mathcal{L})$ are obtained. The random bundle is initially constructed and the frequency response for $V_1(\mathcal{L})$ is obtained for R = 50Ω, R = 1KΩ, R = 10KΩ. This is denoted as Data (1) on the graphs. The tape is then removed from the cable; the wires are allowed to lie on the ground plane; the wires are then gathered together; the tape is replaced; the styrofoam blocks are inserted again, and the frequency response for $V_1(\mathcal{L})$ is obtained for R = 50Ω, R = 1KΩand R = 10KΩ. This is designated as Data (2). This process is repeated to obtain Data (3) and Data (4). Thus the ONLY difference between the experiments used to obtain the four sets of data are that the relative wire positions have been changed in some unknown fashion by removing the tape holding the wires together and then taping the wires together again. No attempt was made to reposition wires as they lay on the ground plane. They were simply gathered together and the bundle retaped together in the same fashion as random bundles are constructed for the same type of aircraft on a production line. Clearly, these data should indicate the sensitivity of the cable responses to variations in wire position.

Note that for R = 50Ω in Figure 4-12, the cable responses

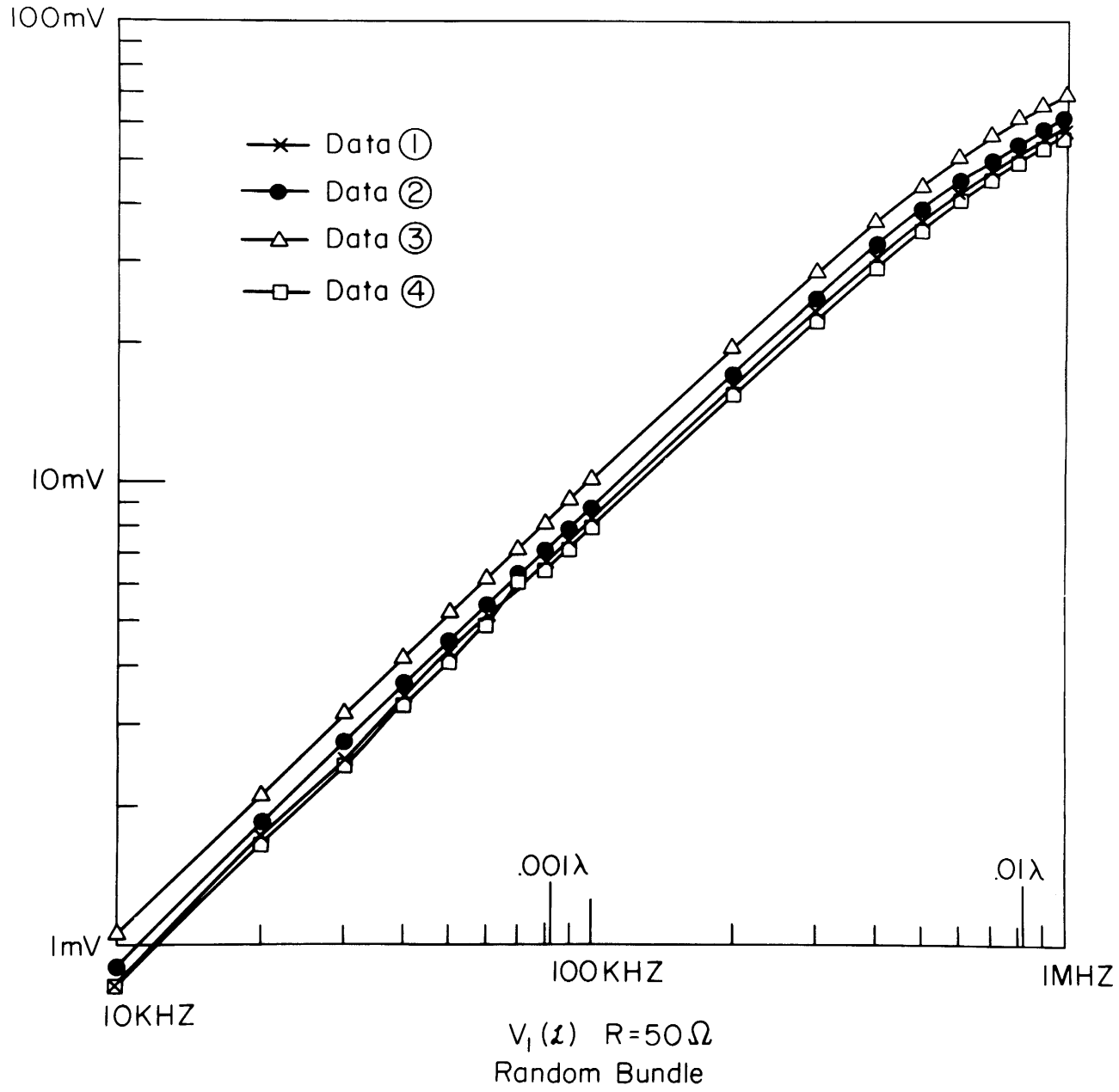
100mV
10mV
1mV
Data ①
Data ②
Data ③
Data ④
.001λ
.01λ
10KHZ
100KHZ
1MHZ
$V_1(\ell)$ R=50Ω
Random Bundle

Figure 4-12(a).

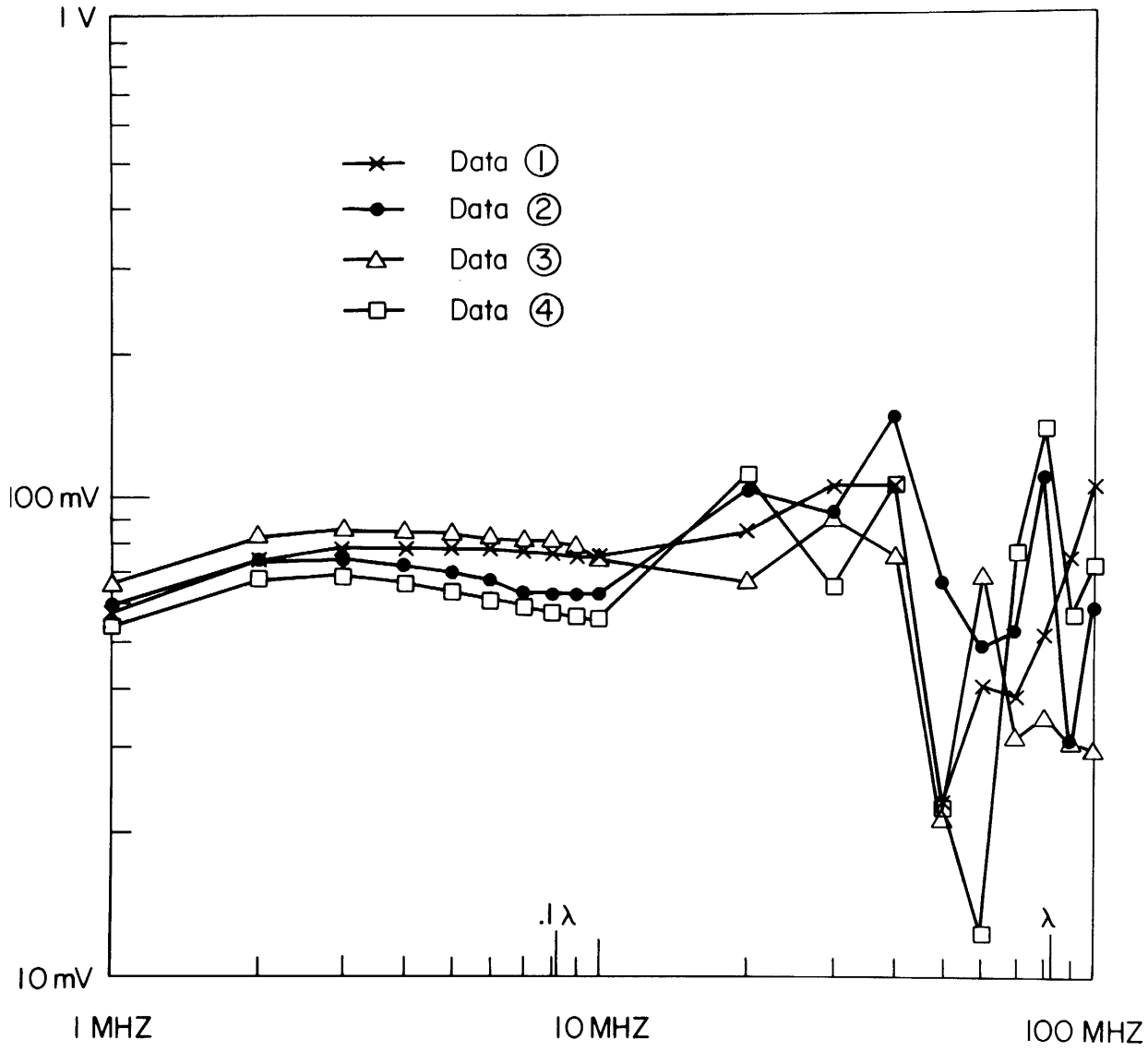

$V_1(\ell)$ R=50Ω
Random Bundle

Figure 4-12(b).

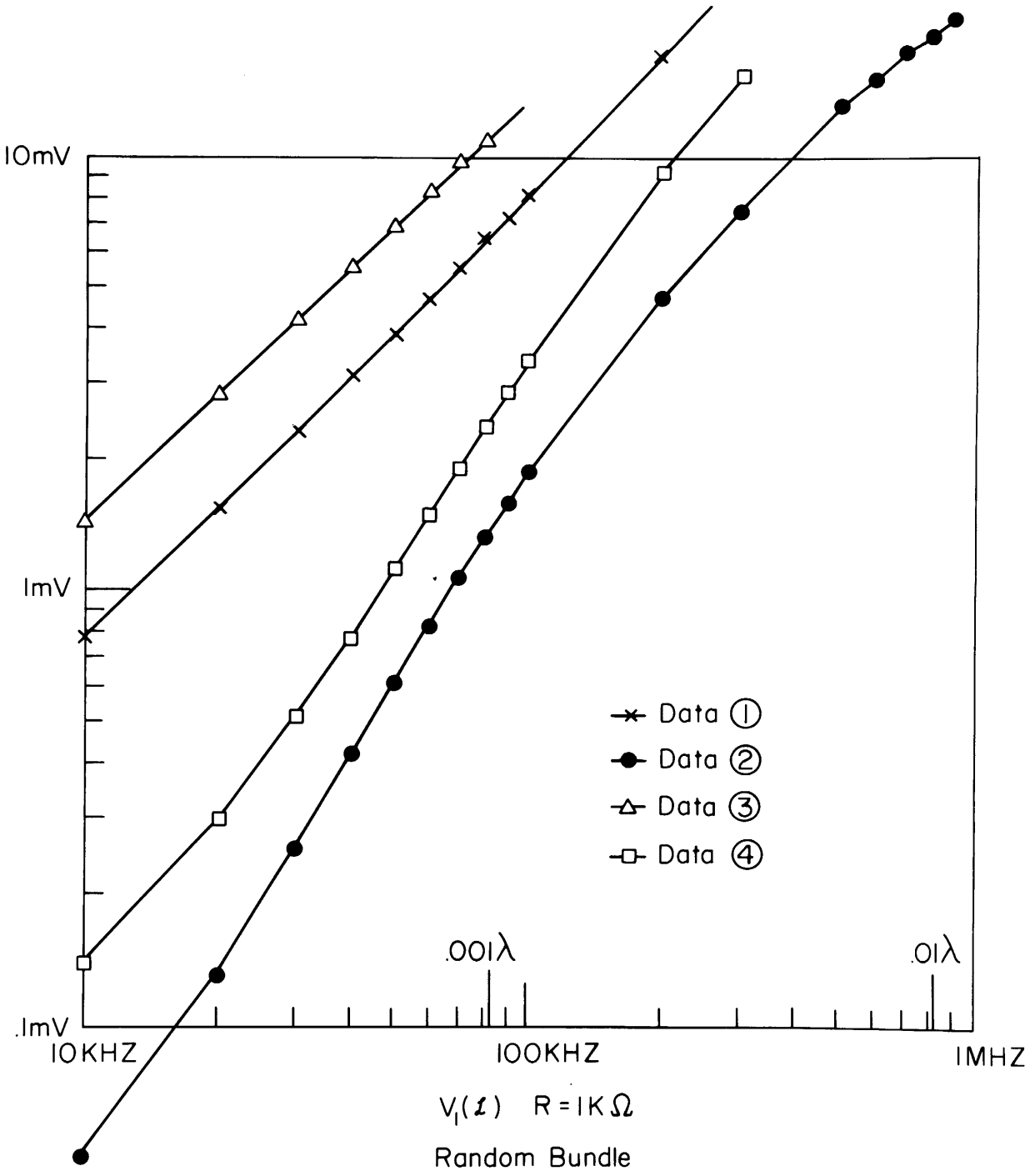
10mV
1mV
.1mV
10KHZ
100KHZ
1MHZ
.001λ
.01λ
Data ①
Data ②
Data ③
Data ④
V1(1) R = 1KΩ
Random Bundle

Figure 4-13(a).

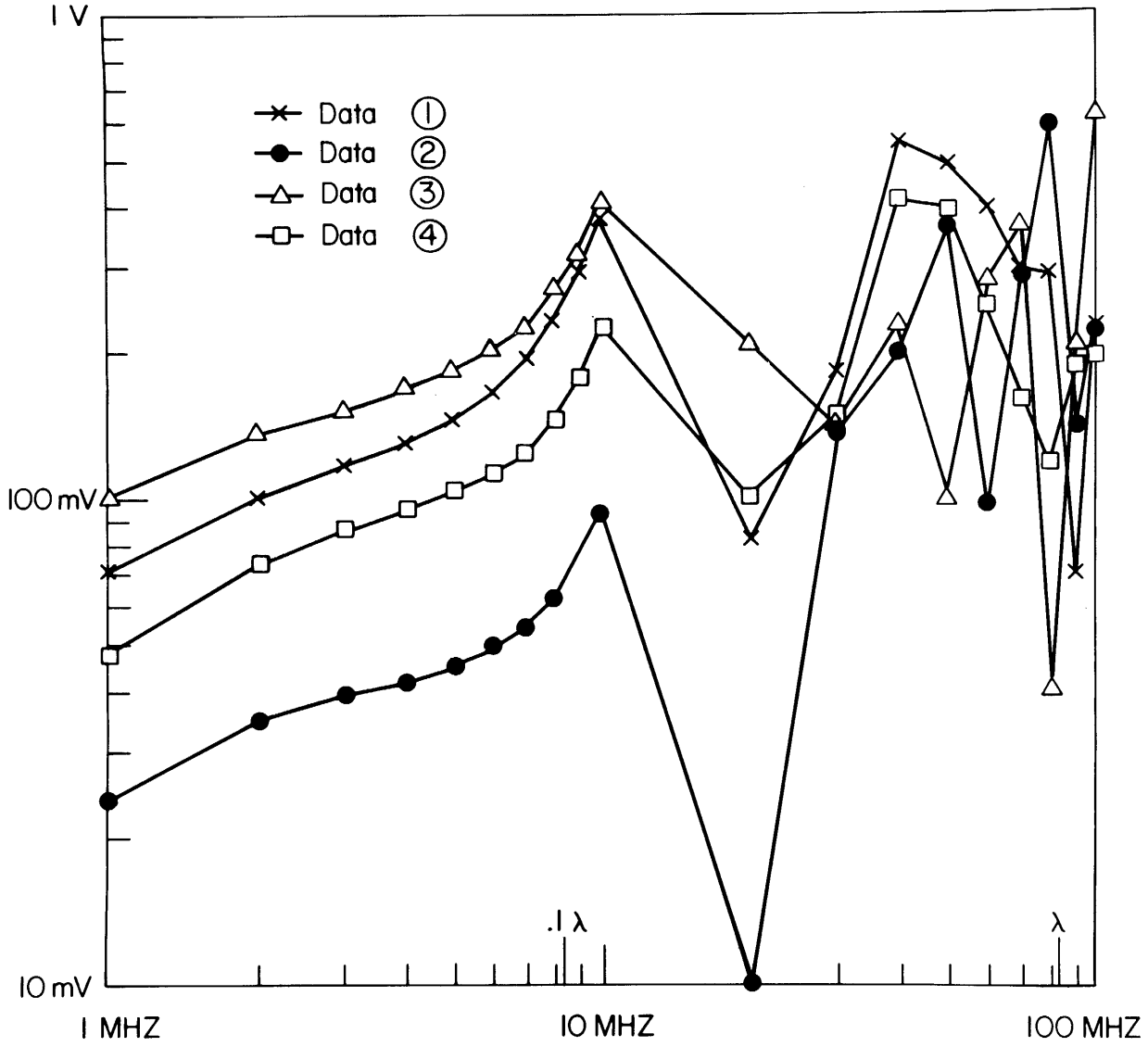

$V_1(\ell)$ R=1KΩ
Random Bundle

Figure 4-13(b).

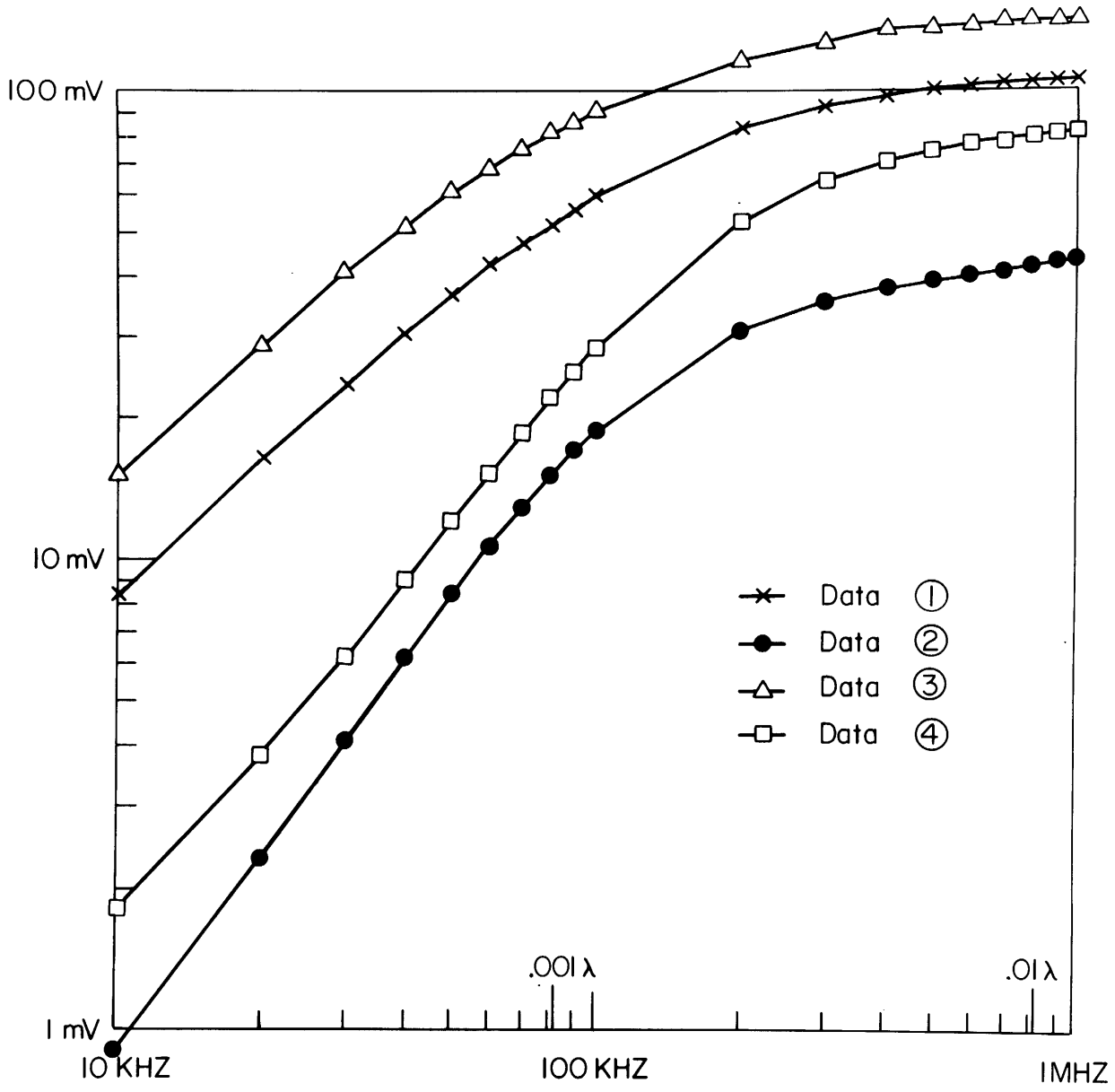

V_1 (ℓ) R=10 KΩ
Random Bundle

Figure 4-14(a).

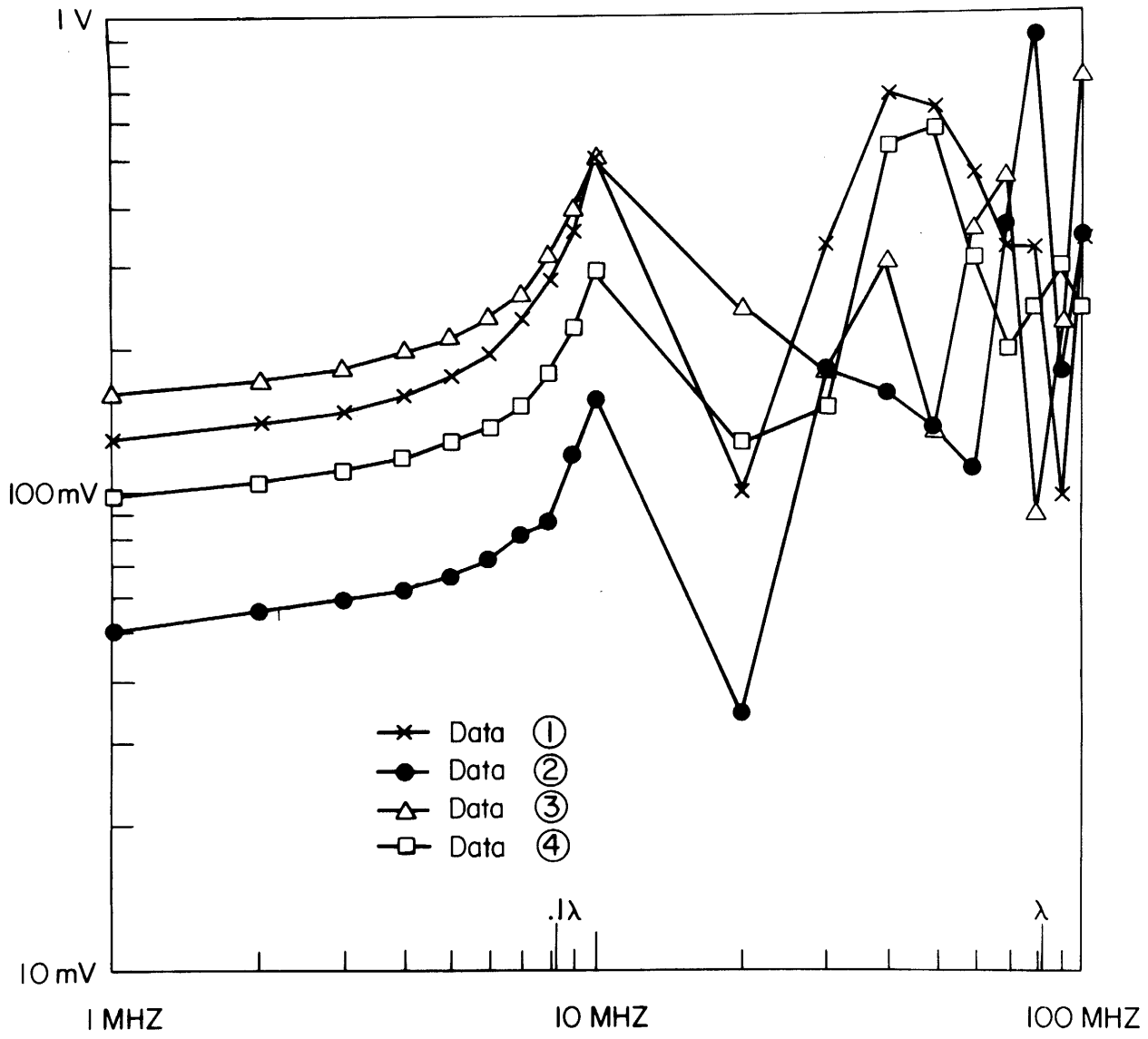

$V_1(\ell)$ R=10KΩ
Random Bundle

Figure 4-14(b).

are virtually insensitive to wire position. However for R = 1KΩ in Figure 4-13 and R = 10KΩ in Figure 4-14, the minor changes in wire position result in an extreme sensitivity of the response ($V_1(\ell)$). For example, in Figure 4-13(a) for R = 1KΩ, there is as much as 35dB change in the response even when ℓ = .00123λ, i.e., the cable is very short electrically, which is caused solely by slight changes in wire position due to untaping and then retaping the wires together!

Clearly then, the sensitivity of cable responses to wire position can be extraordinarily large. For low impedance loads (R = 50Ω), the responses are virtually insensitive to wire position. For high impedance loads (R = 1KΩ and R = 10KΩ) the sensitivities are extraordinarily large. Obviously, these data show that in some cases, it is impossible to predict cable responses accurately for random cable bundles. Therefore, for random cable bundles, it appears that a more reasonable approach would be to estimate the cable responses. Thus the ability of the BOUND model to estimate the cable responses will be the next objective of the investigation.

The predictions of the BOUND model for the random cable data are shown for R = 50Ω in Figure 4-15, R = 1KΩ in Figure 4-16 and R = 10KΩ in Figure 4-17. Recall that the BOUND model neglects the effects of all other wires in the bundle when predicting the coupling between a generator and a receptor circuit. However, a separation between the generator wire and the receptor wire needs to be determined in using this model. Obviously the separation between wire #1 and wire #7 is unknown. Furthermore the wires are probably not separated by a constant distance along the bundle. Therefore we have chosen a wire separation to be used in the BOUND model to be 1/2 of the bundle diameter. This choice is, of course, arbitrary. The

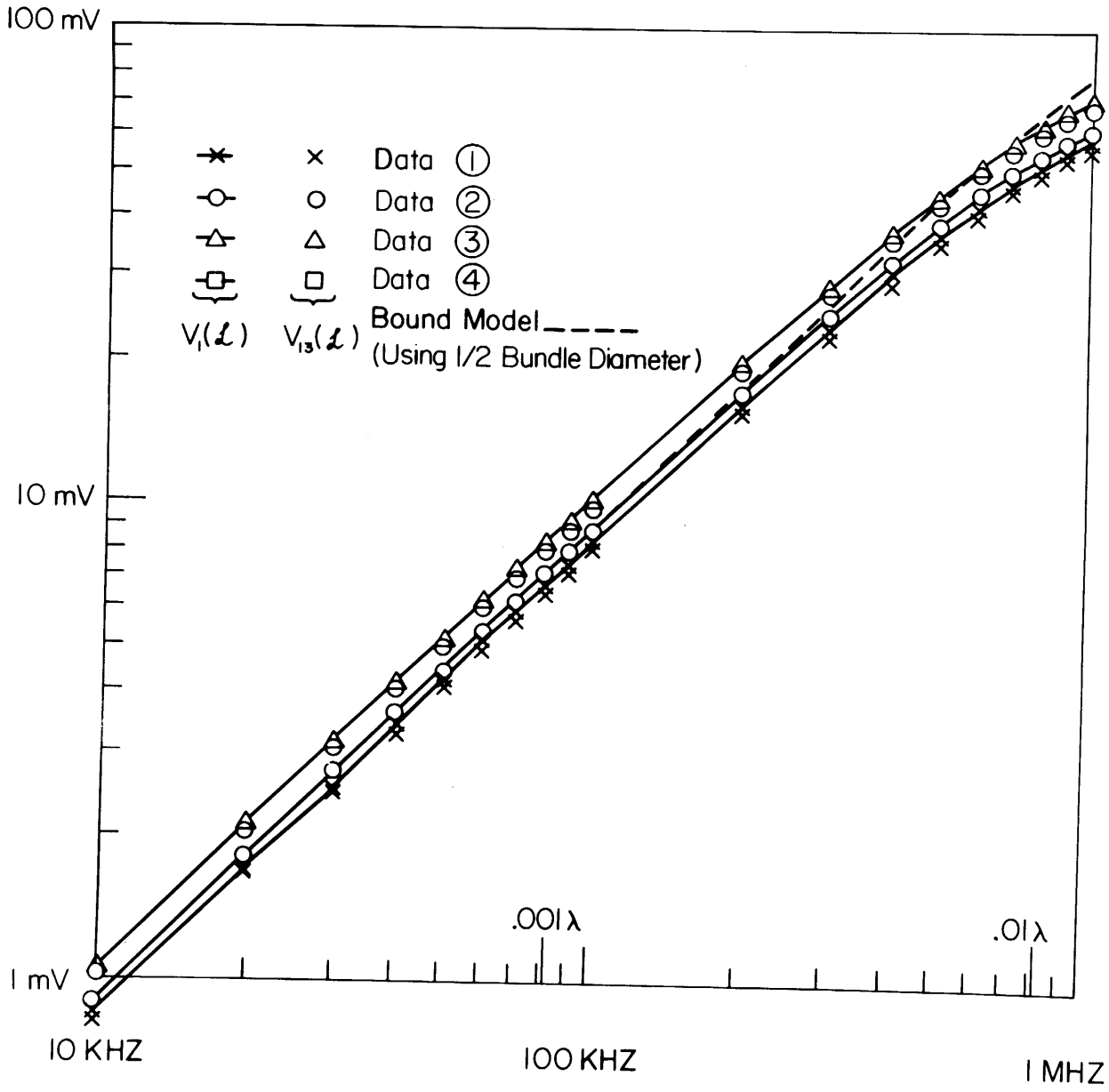

$V_1(\ell)$ vs. $V_{13}(\ell)$ $R=50\Omega$

Random Bundle

Figure 4-15(a).

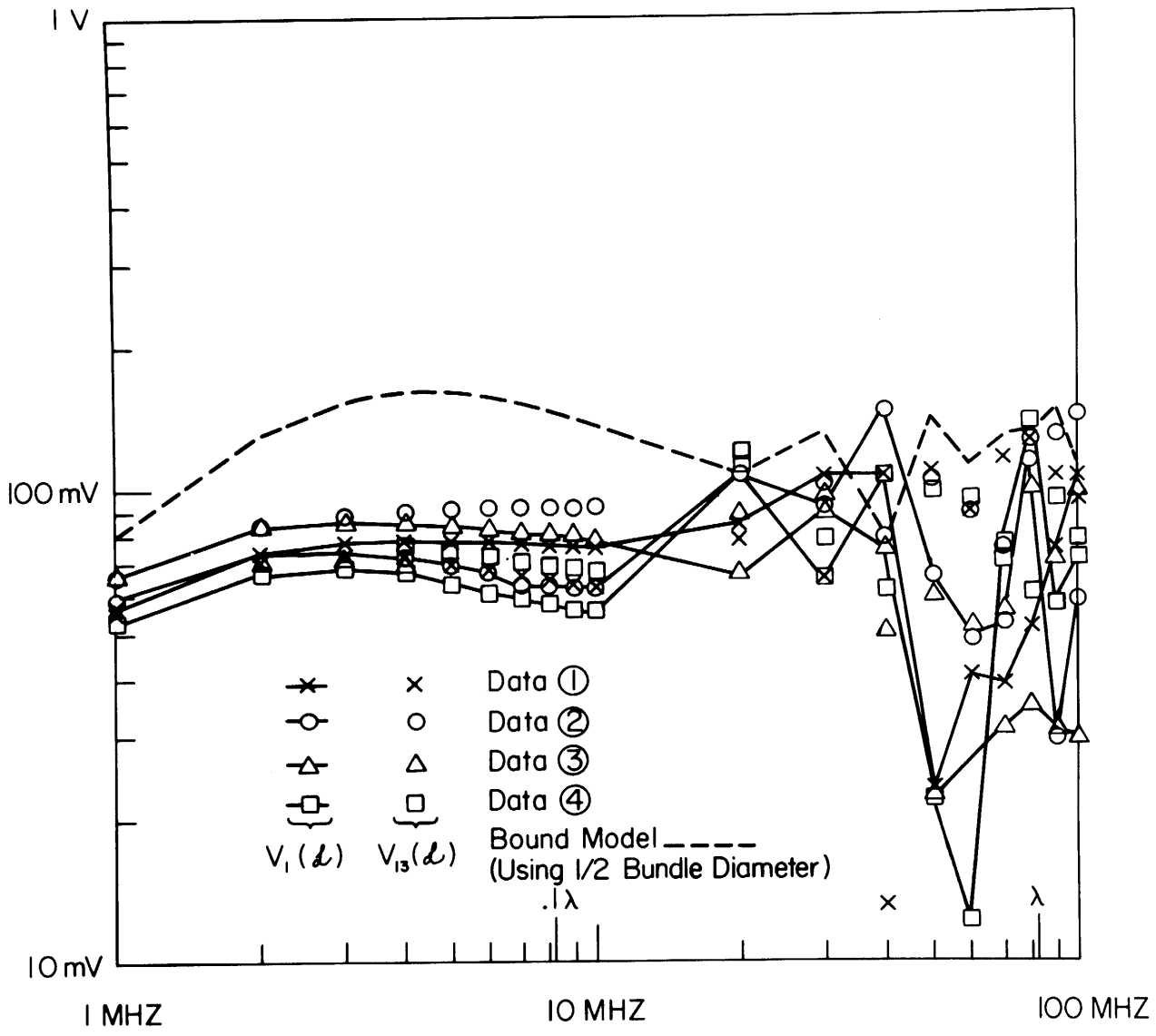

$V_1(\ell)$ vs. $V_{13}(\ell)$ $R = 50\Omega$

Random Bundle

Figure 4-15(b).

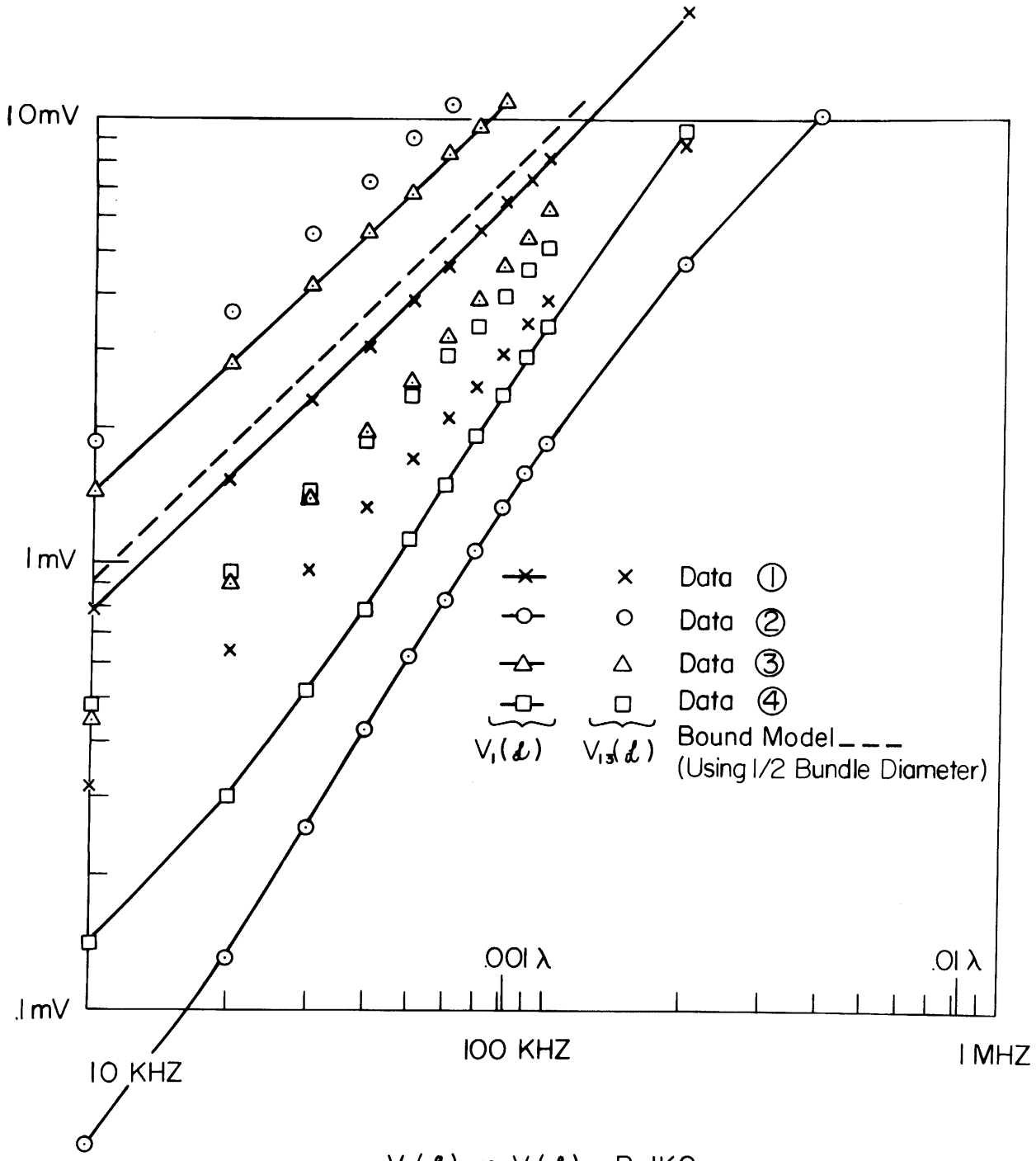

$V_1(\ell)$ vs. $V_{13}(\ell)$ R=1KΩ

Random Bundle

Figure 4-16(a).

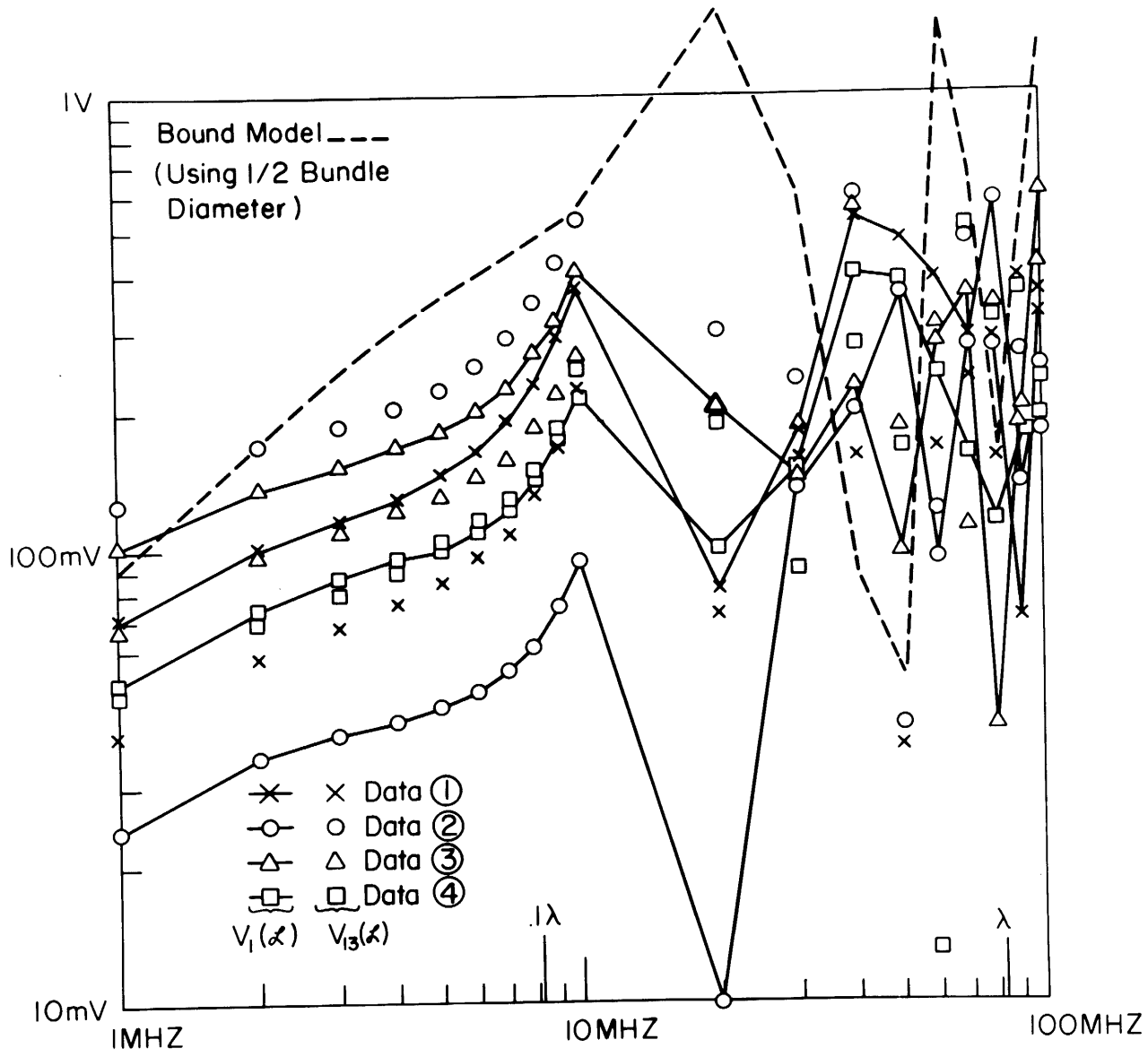

$V_1(\ell)$ vs $V_{13}(\ell)$ R=1KΩ
Random Bundle

Figure 4-16(b).

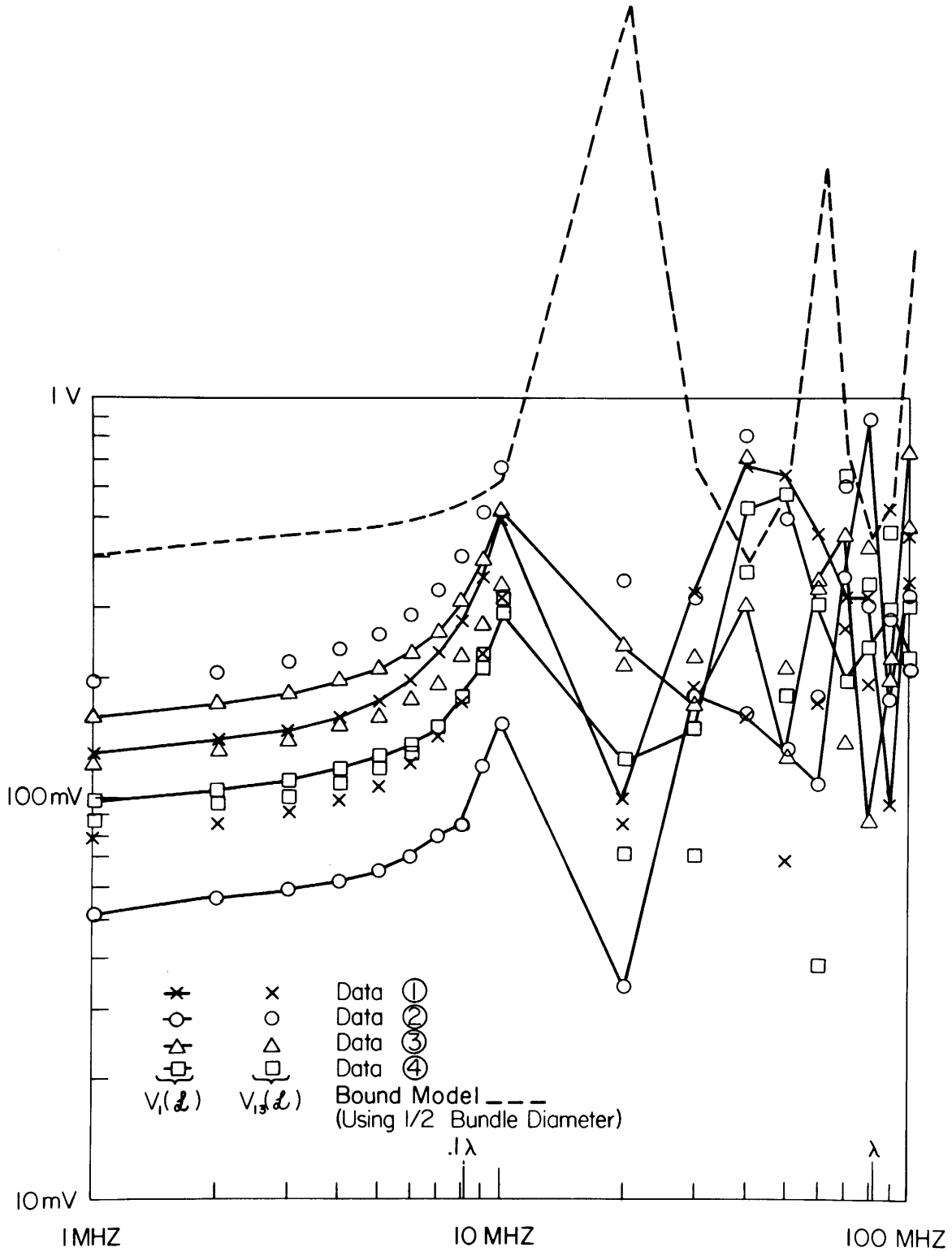

$V_1(\ell)$ vs. $V_{13}(\ell)$ R=10KΩ

Random Bundle

Figure 4-17(b).

bundle diameter is approximately .8 cm. Therefore the wire separation in the BOUND model is chosen to be .4 cm. The wire heights are chosen to be the average bundle height, 1.2 cm.

The responses of wire #1, $V_1(\ell)$, and wire #13, $V_{13}(\ell)$, are shown in the data of Figure 4-15, Figure 4-16 and Figure 4-17. This comparison is relevant since the load structure on wire #1 and on wire #13 is identical (R on both ends of each wire). Therefore in this closely coupled bundle, these circuits are virtually indistinguishable from each other. Of interest here is any difference between $V_1(\ell)$ and $V_{13}(\ell)$. Such differences provide an additional indication of the sensitivity of the cable responses to wire position as well as the effect of parasitic wires in the bundle.

For R = 50Ω in Figure 4-15, the responses for all data sets for $V_1(\ell)$ and $V_{13}(\ell)$ are virtually identical up to the standing wave region. The BOUND model provides prediction accuracies within 3dB up to $\ell = .025\lambda$. Above this, the model tracks the envelope of the responses quite well.

For R = 1KΩ in Figure 4-16 and R = 10KΩ in Figure 4-17, there is a considerable variation between the data sets even when the cable is very short electrically. The BOUND model, however, provides a reasonable estimate of these very sensitive responses. In the standing wave region, $\ell > .1\lambda$, the model tracks the envelope of the responses to some degree although there is a considerable variation at certain frequencies. This is to be expected in this frequency range where the cable is very short, electrically.

V. SUMMARY AND CONCLUSIONS

The predominant method of maintaining wires connecting electronic systems in compact groups is the use of random cable bundles. In these types of bundles, relative wire position is unknown and varies in some uncontrolled fashion along the cable length. Wire-coupled interference (crosstalk) occurring within these compact bundles can be an important contributor to the degradation of system performance. The prediction of this crosstalk is therefore of considerable importance in determining overall system electromagnetic compatibility. This report has been directed toward an investigation of the prediction of wire-coupled interference in random cable bundles.

A particular 13 wire cable above a ground plane was chosen for investigation. It was found that, depending upon the values of the impedances terminating the generator and receptor circuits, the sensitivity of the cable responses to variations in relative wire position can be extraordinarily large. For low impedance loads on the generator and receptor circuits (values less than the"characteristic impedance" of either circuit in the presence of the other circuit), the cable responses were virtually insensitive to wire position. For high impedance loads on the generator and receptor circuits, the cable responses were very sensitive to variations in wire position. For low impedance loads on the generator and receptor circuits, the coupling between the generator and receptor circuits was virtually unaffected by the presence of other wires in the bundle. For high impedance loads on the generator and receptor circuits, the coupling between the generator and receptor circuits was affected considerably by the presence of other wires in the bundle.

Although these conclusions were obtained for a specific cable bundle

with specific loads on the parasitic wires, they have the following impact on crosstalk predictions for other random cables. A specific case was shown for which the prediction of crosstalk in a random cable bundle was impossible. There seems to be no reason to consider this bundle as some special case. Thus one would reasonably expect that there exist other types of random cable bundles to which this observation applies.

Obviously, random cable bundle responses either are sensitive to wire position or they are not (to what degree they may be sensitive is subject to interpretation). In cases where the cable responses are sensitive to wire position and wire position is unknown and varies along the cable, attempting to achieve "accurate" predictions could be an exercise in futility.

The BOUND model seems to provide a reasonable estimate of the random cable bundle responses. It should again be pointed out that the BOUND model only considers the generator circuit and the receptor circuit. The effect of all other wires in the cable bundle on the coupling between the generator and receptor circuits is disregarded in the BOUND model. Since a simple model (see equations (2-48) and (2-33)) is used to model the coupling between the generator circuit and the receptor circuit with the effects all other wires in the bundle disregarded, the BOUND model may be programmed on a digital computer with a trivial amount of difficulty. The per-frequency computation time is also virtually trivial. For the case investigated in this report, the computation time per frequency was .00092 seconds on an IBM 370/165 computer.

The distributed parameter, multiconductor transmission line model entails considerably more programming complexity and per-frequency computation time when the effects of all wires in the bundle on the coupling between the

generator and receptor circuits are considered [1]. A minimum of n simultaneous, complex equations must be solved at each frequency for an n wire cable [1]. For the 13 wire cable investigated in this report, the MTL model required .27 seconds computation time at each frequency on an IBM 370/165 digital computer; about three hundred times that required for the BOUND model. When the response is desired at many frequencies (as it usually is), this difference in computation times becomes an even more important consideration. The computation time for the MTL model also increases as the number of wires in the cable increases. This increase is on the order of n^3 where n is the number of wires in the cable. Although the large per-frequency computation times required by the MTL model are a serious consideration, the main reason for not using this model for random cable bundle predictions is that in cases where the cable responses are sensitive to relative wire position, accurate predictions cannot generally be achieved.

Therefore, the preferred alternative would seem to be the use of simpler, approximate prediction models which tend to estimate the cable responses. One specific model, the BOUND model, which seems to meet these criteria was used in this report. There exist other variations of this model which are intended to meet these criteria [4,5], and these have evidently been used with much success in the estimation of random cable bundle responses.

This, of course, is not meant to imply that the distributed parameter, multiconductor transmission line model should be completely disregarded. Experimental results were shown in this report where accurate predictions can be made for multiconductor cables when the relative wire positions are known and well controlled. The effects of parasitic wires on the coupling between two wires in a cable bundle which were uncovered were shown to be

quite significant even when the wire positions are well controlled. These cases virtually demand an exact treatment of the cable with the MTL model which includes the effects of the parasitic wires. There exist certain cables in which wire position is well controlled, e.g., controlled lay cables and ribbon or flat pack cables [1]. For these types of cables, it should be possible to obtain accurate predictions with the MTL model. This subject will be addressed in Volume IV of this series. The results of this report apply to bundles of single wires above a ground plane. Individually shielded wires and twisted pairs will be considered in future publications.

REFERENCES

[1] C. R. Paul, Applications of Multiconductor Transmission Line Theory to the Prediction of Cable Coupling,Volume I,Multiconductor Transmission Line Theory, Technical Report, Rome Air Development Center, Griffiss AFB, NY, RADC-TR-76-101, Volume I, April 1976, (A025028).

[2] C. R. Paul, "Useful Matrix Chain Parameter Identities for the Analysis of Multiconductor Transmission Lines", IEEE Trans. on Microwave Theory and Techniques, Volume MTT-23, No. 9, pp. 756-760, September 1975.

[3] R. E. Matick, Transmission Lines for Digital and Communication Networks. New York: McGraw-Hill, 1969.

[4] W. R. Johnson, A. K. Thomas, et.al., Development of a Space Vehicle Electromagnetic Interference/Compatibility Specification, NASA Contract Number 9-7305, The TRW Company 08900-6001-T000, June 1968.

[5] J. L. Bogdanor, R. A. Pearlman and M. D. Siegel, Intrasystem Electromagnetic Compatibility Analysis Program, Technical Report, RADC-TR-74-342, Vols I -III, (A008526), (A008527), (A008528), Rome Air Development Center, Griffiss AFB, N.Y., December 1974.

[6] C. R. Paul, "Sensitivity of Multiconductor Cable Coupling to Parameter Variations", 1974 IEEE Symposium on Electromagnetic Compatibility, San Francisco, CA, July 1974.

[7] C. R. Paul, Applications of Multiconductor Transmission Line Theory to the Prediction of Cable Coupling, Volume VII, Digital Computer Programs for the Analysis of Multiconductor Transmission Lines, Technical Report, Rome Air Development Center, Griffiss AFB, N.Y., to appear.

METRIC SYSTEM

BASE UNITS:

Quantity	Unit	SI Symbol	Formula
length	metre	m	...
mass	kilogram	kg	...
time	second	s	...
electric current	ampere	A	...
thermodynamic temperature	kelvin	K	...
amount of substance	mole	mol	...
luminous intensity	candela	cd	...

SUPPLEMENTARY UNITS:

plane angle	radian	rad	...
solid angle	steradian	sr	...

DERIVED UNITS:

Acceleration	metre per second squared	...	m/s
activity (of a radioactive source)	disintegration per second	...	(disintegration)/s
angular acceleration	radian per second squared	...	rad/s
angular velocity	radian per second	...	rad/s
area	square metre	...	m
density	kilogram per cubic metre	...	kg/m
electric capacitance	farad	F	A·s/V
electrical conductance	siemens	S	A/V
electric field strength	volt per metre	...	V/m
electric inductance	henry	H	V·s/A
electric potential difference	volt	V	W/A
electric resistance	ohm		V/A
electromotive force	volt	V	W/A
energy	joule	J	N·m
entropy	joule per kelvin	...	J/K
force	newton	N	kg·m/s
frequency	hertz	Hz	(cycle)/s
illuminance	lux	lx	lm/m
luminance	candela per square metre	...	cd/m
luminous flux	lumen	lm	cd·sr
magnetic field strength	ampere per metre	...	A/m
magnetic flux	weber	Wb	V·s
magnetic flux density	tesla	T	Wb/m
magnetomotive force	ampere	A	...
power	watt	W	J/s
pressure	pascal	Pa	N/m
quantity of electricity	coulomb	C	A·s
quantity of heat	joule	J	N·m
radiant intensity	watt per steradian	...	W/sr
specific heat	joule per kilogram-kelvin	...	J/kg·K
stress	pascal	Pa	N/m
thermal conductivity	watt per metre-kelvin	...	W/m·K
velocity	metre per second	...	m/s
viscosity, dynamic	pascal-second	...	Pa·s
viscosity, kinematic	square metre per second	...	m/s
voltage	volt	V	W/A
volume	cubic metre	...	m
wavenumber	reciprocal metre	...	(wave)/m
work	joule	J	N·m

SI PREFIXES:

Multiplication Factors	Prefix	SI Symbol
$1\,000\,000\,000\,000 = 10^{12}$	tera	T
$1\,000\,000\,000 = 10^{9}$	giga	G
$1\,000\,000 = 10^{6}$	mega	M
$1\,000 = 10^{3}$	kilo	k
$100 = 10^{2}$	hecto*	h
$10 = 10^{1}$	deka*	da
$0.1 = 10^{-1}$	deci*	d
$0.01 = 10^{-2}$	centi*	c
$0.001 = 10^{-3}$	milli	m
$0.000\,001 = 10^{-6}$	micro	μ
$0.000\,000\,001 = 10^{-9}$	nano	n
$0.000\,000\,000\,001 = 10^{-12}$	pico	p
$0.000\,000\,000\,000\,001 = 10^{-15}$	femto	f
$0.000\,000\,000\,000\,000\,001 = 10^{-18}$	atto	a

* To be avoided where possible.